PROCESS INTEGRATION OF CELL DISRUPTION AND FLUIDISED BED ADSORPTION OF MICROBIAL ENZYMES: APPLICATION TO THE RETRO-DESIGN OF THE PURIFICATION OF L-ASPARAGINASE

by

HORST BIERAU

A thesis submitted to
The University of Birmingham
for the degree of
DOCTOR OF PHILOSOPHY

School of Chemical Engineering
The University of Birmingham
November 2000

ABSTRACT

The practical feasibility and generic applicability of the direct integration in the same time frame of cell disruption by bead milling with the capture of intracellular products by fluidised bed adsorption has been demonstrated. Pilot-scale purification of the enzyme L-asparaginase from unclarified *Erwinia chrysanthemi* disruptates exploiting this novel approach yielded an interim product which rivalled or bettered that produced by the current commercial process employing discrete operations of alkaline lysis, centrifugal clarification and batch adsorption. In addition to improved yield and quality of product, the process time during primary stages of purification was greatly diminished.

Two cation exchange adsorbents, CM HyperD LS (Biosepra/Life Technologies) and SP UpFront (custom made SP form of a prototype stainless steel/agarose matrix, UpFront Chromatography) were physically and biochemically evaluated for such direct product sequestration. Differences in performance with regard to product capacity and adsorption/desorption kinetics were demonstrated and are discussed with respect to the design of adsorbents for specific applications.

In any purification of L-asparaginase (pI=8.6), product-debris interactions commonly diminish the recovery of available product. It was demonstrated herein, that immediate disruptate exposure to a fluidised bed adsorbent promoted concomitant reduction of product in the liquid phase, which clearly counter-acted the product-debris interactions to the benefit of overall product yield.

”Anyone who has never made a mistake has never tried anything new.”

ALBERT EINSTEIN

I would like to dedicate this work to my mother ANNEMARIE and my late father HEINRICH for their support and for having faith in my success.

Acknowledgements

First of all I would like to express my gratitude to Professor Andrew Lyddiatt for inviting me to become a member of the Biochemical Recovery Group (BRG), for his supervision, guidance and friendship.

This studentship was funded by The Centre for Applied Microbiology and Research (CAMR, Porton Down, Salisbury). Many thanks to Roger Hinton, Chris Nwoguh, Peter Hambleton, Ross Cameron, Derek Rutherford and Gary Stevens, for providing the cell paste, for their support, advice and discussion.

Thanks are due also to past and present member of the BRG (especially Deirdre, Grant, Ian, Zhang, Ling, Sharon, Ade, Maurice, Frank, Eric, and Simon) for a warm welcome, their support, valuable discussions, friendship and an invaluable cultural experience.

I would also like to gratefully acknowledge Biosepra and UpFront Chromatography for providing adsorbent materials.

TABLE OF CONTENTS

LIST OF TABLES

LIST OF FIGURES

DEFINITIONS AND ABBREVIATIONS

Bo	Bodenstein number
BSA	bovine serum albumin
buffer A	*Erwinia* experiments: citric acid / tri-sodium citrate, 20 mM (pH 5.5 if not stated otherwise)
	yeast experiments: 10 mM Tris/HCl, pH 7.5 containing 1 mM EDTA
buffer B	citric acid / tri-sodium citrate, 20 mM containing 1 M NaCl (pH 5.5 if not stated otherwise)
CIP	cleaning-in-place
d	internal diameter of a contactor (fixed or fluidised bed)
DEAE	diethyl aminoethyl, weak anion exchange ligand
DPS	direct product sequestration
DSP	downstream processing
E	molar extinction coefficient
EDTA	ethylenediamine tetra-acetic acid
FBA	Fluidised Bed Adsorption
G3PDH	glyceraldehyde 3-phosphate dehydrogenase
H	height of a fluidised bed
H_0	settled bed height of an adsorbent bed (= SBH)
HETP	Height equivalent to a theoretical plate
HIC	hydrophobic interaction chromatography
HPH	high-pressure homogeniser
i.d.	internal diameter
IU	unit of enzyme activity (G3PDH), designated as the number of µmoles of NADH produced per minute at 25 °C
IMAC	immobilised metal affinity chromatography
K_D	Dissociation constant (Langmuir adsorption isotherm)
KSCN	potassium thiocyanate
MRT	mean residence time
MSFB	magnetically stabilised fluidised bed
MU	Mega units (10^6 U)

MWCO	molecular weight cut-off
N	Number of theoretical plates
NAD	nicotinamide adenine dinucleotide
NAG	N-acetylglucosamin
NAM	N-actetylmuramic acid
LPS	lipopolysaccharids
pI	isoelectric point
RTD	residence time distribution
SBH	settled bed height of an adsorbent bed (= H_0)
SDS	sodium docecyl sulphate
SDS-PAGE	sodium dodecyl sulphate polyacrylamide gel electrophoresis
SP	sulphopropyl, strong cation exchange ligand
Tris	Tris(hydroxymethyl-)-aminomethane
u	superficial / linear flow velocity
U	unit of enzyme activity. One unit of L-asparaginase activity is defined as the amount of enzyme which catalyses the liberation of 1.0 µmol of NH_3 per minute at 37°C.
U_{mf}	minimum fluidisation velocity. The flow velocity at which a bed of adsorbent particles becomes suspended in an upward stream of liquid
U_t	terminal velocity. The flow velocity at which a particle of a definite size and density is elutriated from a fluidised bed.
ww/v	wet weight per volume (original concentration of biomass before cell disruption)

1 INTRODUCTION

1.1 Downstream processing in biotechnology

In recent decades, advances in biotechnology have increased the potential usage of protein products and the emergence of new and promising research activities in molecular biology and immunology is continuously expanding the number of proteins that need to be purified and characterized. A wide variety of proteins is used as pharmaceuticals and diagnostic reagents such as vaccines, monoclonal antibodies, enzymes, and regulatory factors. In addition, protein products are also found in industrial and domestic applications (Bristow, 1990; Harris, 1989). Traditionally, the source would have been extracted animal tissue, serum or other natural materials. However, with the advent of recombinant DNA techniques, sources now include cultured microorganisms (both prokaryotic and eukaryotic expression systems) and mammalian cells.

The unit operations employed for the purification of protein products can be collectively described by the term "downstream processing", commonly abbreviated to DSP (Wheelwright, 1987). The objective is to find a sequence of operations that will transfer the starting material to a state defined by the specification of the desired end-product. Individual steps should be based on molecular-based knowledge of how the individual target molecule, as well as impurities such as proteins, lipids, DNA, and lipopolysaccharides, will behave during purification in order to establish an efficient and economic process which achieves the purity and specification of the end product required.

Processes suitable for the purification of proteins differ from conventional methods of DSP generally employed in chemical technology owing to their sensitivity to temperature, interfacial contact and any agent affecting their three-dimensional structure and dynamic

conformation. Although individual steps during a purification process are product specific and selected in order to exploit specific molecular properties of the target molecule, a general approach has evolved which is depicted in Figure 1.1.

In the case of an intracellular product, cell disruption is the first step in the sequence following the harvest of the cells (e.g. by centrifugation or tangential flow filtration, TFF). Here, the envelope of the cell is permeabilised, punctured or disintegrated in order to release the product into the surrounding medium. Cell disruption can be achieved by mechanical methods, e.g. homogenisation and bead milling, or non-mechanical methods such as chemical or enzymatic treatments (Harrison, 1991; Kula and Schütte, 1987; Middelberg, 1995; Asenjo and Patrick, 1990). A review of different cell disruption methods is given in Chapter 2. The disruptate, or the supernatant of a clarified fermentation, contains a large variety of dissolved compounds characterised by a variety of molecular characters and the target molecule is often only a minor component in this mixture. Subsequent purification is commonly achieved by chromatographic adsorption based upon selected molecular characteristics (Harris, 1989). Ion exchange (IEXC) and hydrophobic interaction chromatography (HIC) are effective tools for product capture and primary purification. For a subsequent final purification, unit operations of affinity adsorption and/or gel filtration are often exploited. A survey conducted by Bonnerjea *et al.* (1986) revealed that IEXC was used in 75% and affinity adsorption in 60% of the reviewed purification schemes. Since chromatographic processes are conventionally performed in packed beds, preliminary clarification by solid-liquid separation of the feedstock is required. If this is not undertaken, particulate material becomes trapped in the voids of the bed leading to the formation of a plug which distorts or obstructs the liquid flow through the bed. Similar constraints apply to the operation of batch adsorption / desorption processes.

Figure 1.1. Conventional downstream processing for protein purification.

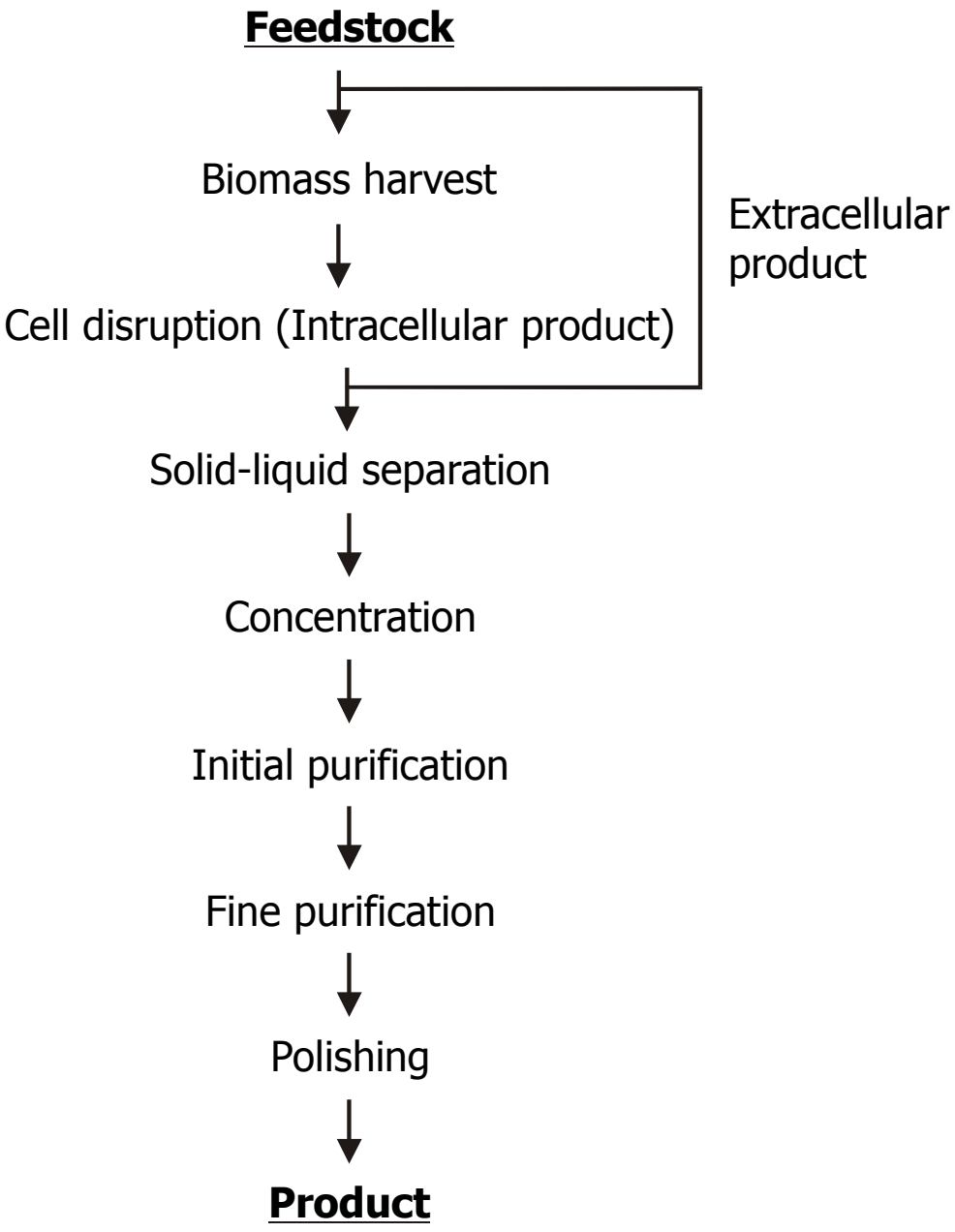

1.2 General problems involved with conventional downstream processing procedures

From an economic point of view, the number of sequential operations necessary to achieve the desired purity of a protein product contributes significantly to the overall cost of the downstream process. This is due to the capital investment and amount of consumables needed for each step as well as the individual time required for each operation. Additionally, the overall yield of the purification is reduced with each additional process step as a result of inherent handling losses of product and/or product activity. It has been estimated that in the production of recombinant proteins, 45% of the equipment costs are associated with product recovery while only 14% can be attributed to the fermentation process (Fish and Lilly, 1984). The overall downstream process may account for more than 80% of the total production costs (Datar *et al.*, 1993) which clearly reflects the necessity for process optimisation (Spalding, 1991).

Traditional techniques employed both for harvesting biomass and feedstock clarification are centrifugation and filtration (Kroner *et al.*, 1984; Lee, 1989; van Reis *et al.*, 1991). The expense and the effectiveness of such methods are highly dependent on the physical nature of the particulate material to be removed, e.g. particle size, density difference between particulates and the bulk fluid, and the compressibility of the sedimented solids (Asenjo and Patrick, 1990). Particles of submicron size, when suspended in a viscous liquid (as when cells are disrupted by mechanical procedures) are particularly difficult to remove. Although centrifugation and filtration are regarded as standard unit operations in the biotechnology industry, they suffer from some drawbacks particularly at a large scale. For example, the degree of clarification in industrial centrifuges is usually in the range of 99 –

99.9% in terms of cell clearance (Datar and Rosen, 1996). Thus, centrifugation is commonly operated in tandem with a depth or microfiltration step to ensure a particle free solution which can be fractionised by conventional packed bed chromatography (Berthold and Kempken, 1994). Although microfiltration yields cell-free solutions, in many cases the flux rate of liquid per unit membrane area is dramatically decreased during the filtration process due to fouling of the membranes, e.g. by small particles, lipids, nucleic acids (Gilbert *et al.*, 1986; Göklen *et al.*, 1994). In addition, combined centrifugation and filtration operations often result in long processing times. A rapid method of product capture of the target protein is therefore preferred since the time taken to remove particulates can promote denaturation due to process conditions detrimental to structural integrity, e.g. the action of proteases, carbohydrases, or oxidising conditions. Thus, novel solutions for the rapid clarification of biological feedstocks and isolation of products are highly desirable.

1.3 Integrative protein recovery

As a consequence of the problems associated with conventional downstream processing, integrative operations, which on the one hand simplify solid-liquid separation and on the other hand combine originally independent steps to formulate new unit operations, now promise to streamline and condense protein production schemes. Such operations should tolerate particle-containing suspensions as initial feedstocks and deliver a clarified product concentrate compatible with subsequent purification steps. Ideally, a preliminary sequestration of the target protein from bulk impurities should be achieved simultaneously, combining clarification, concentration and capture in a single process step operated in a common time frame.

The criteria mentioned above are met by three approaches reported in the literature. Firstly, liquid-liquid extraction based on aqueous two-phase systems allows processing of

biomass-containing feedstocks at high biomass loads. Here, the solid-liquid separation in a centrifugal separator is replaced by a thermodynamically controlled partitioning of particulate material and dissolved protein product between two different aqueous phases (Huddleston *et al.*, 1992; Kula, 1990). In addition, an initial fractionation of protein mixtures may be achieved by choosing suitable phase compositions. Another approach is the introduction of protein binding ligands to crossflow microfiltration membranes which allows the combination of filtration and protein adsorption (for example see Langlotz and Kroner, 1992). The third approach is based on the adsorption of proteins to particulate adsorbents in the presence of biomass which can be achieved by different modes of operation. Batch adsorption is performed by contacting adsorbent particles with unclarified suspension in stirred tanks (Thiele *et al.*, 1985; Roe, 1987). After product capture, the adsorbent is separated from the broth by decantation washing and thereupon the product is eluted. Batch adsorption is a process which is characterised by a single equilibrium stage and thus lacks high resolution in comparison with classical frontal chromatography. In addition, the problem of separating the protein-loaded adsorbent from the biomass has to be solved. A recently reported approach to facilitate the recovery of the loaded adsorbent exploited magnetic supports which are captured from the suspending fluid by a magnetic field in a custom designed filter chamber (Hubbuch *et al.*, 2000). The most common method of whole broth adsorption with particulate matrices is by fluidising the matrix particles to form an expanded bed, i.e. a bed of adsorbent particles with a reduced local mobility. In such stable fluidised beds, which are exploited for chromatographic separations, a minimisation of particle movement is anticipated in order to mimic the flow characteristics and the resolution achieved by packed bed chromatographic processes. By way of contrast, in conventional gas-fluidised beds a high degree of mixing is

desirable for maximum heat and/or mass transfer rates (Levenspiel, 1972). The fundamentals and characteristics of liquid fluidised beds will be discussed in more detail in the next section.

1.4 Fluidised bed adsorption

Fluidised bed adsorption (FBA) has emerged as an efficient recovery method proven to have significant advantages over conventional procedural sequences, e.g. discrete feedstock clarification followed by fixed bed adsorption of the product. In fluidised beds, liquid is pumped upwards through a bed of adsorbent beads which, in contrast to a packed bed, is not constrained by an upper flow adapter. Thus, the bed can expand and spaces open up between the adsorbent beads. The increased voidage of the bed allows particulates in the feed to pass freely through the spaces without entrapment (see Figure 1.2). Thus, the need for prior removal of cells and/or debris is eliminated. After the adsorption stage, the remaining feedstock and particulates are washed from the adsorbent bed and product is subsequently eluted either in fluidised or packed bed mode. As a consequence, clarification, concentration and initial fractionation is combined in one unit operation and thus fluidised beds exhibit great potential for simplifying downstream processes with concomitant savings in capital and operating costs.

Fluidised beds have been used previously for the industrial scale recovery of the antibiotics streptomycin (Barthels *et al.*, 1958) and novobiocin (Belter *et al.*, 1973). However, more recently, considerably interest has been shown in the use of fluidised beds for the direct extraction of proteins from whole fermentation broths (Chase, 1994; Gailliot *et al.*, 1990; Wells and Lyddiatt, 1987; Gibson and Lyddiatt, 1990).

Figure 1.2. Adsorbent particles in a packed and a fluidised bed

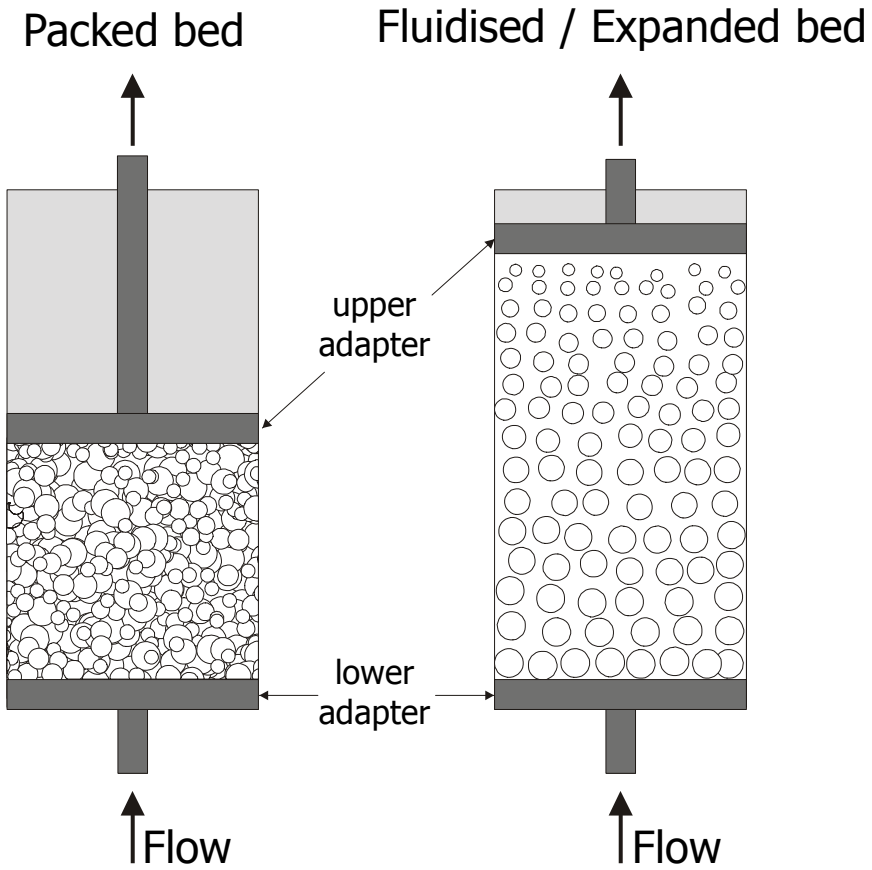

In a packed bed, the adsorbent particles are packed between the lower and upper adapter. The voidage, i.e. the inter-particle space, is minimal and thus, feedstock clarification is mandatory to avoid clogging of the bed. In a fluidised / expanded bed, the adsorbent bed is allowed to expand by irrigation with feedstock. Bed voidage is increased allowing the passage of particulates in the feed. The diameters of the adsorbent beads are exaggerated for illustrative clarity.

1.4.1 Mixing behaviour in fluidised / expanded beds

The conventional chemical-engineering view of a fluidised bed is one in which there is a significant degree of mixing, both of the solid and the fluid phase, e.g. in gas-fluidised systems (Levenspiel, 1972). In many applications, mixing of the solid phase is desirable, for example in order to obtain high rates of heat transfer and a uniform temperature within the bed. Gas fluidised beds are characterised by an *'aggregative'* behaviour in which bubbles of gas pass through a bed of particles which are just fluidised resulting in considerable mixing of the solid phase as well as distinct bypassing of the gas phase. In general, mixing in liquid fluidised systems is not as severe as in gas fluidised systems. Here, the density difference between the solid and the fluid phase are comparatively small and, thus, the bed shows a *'particulate'* behaviour in which the bed retains a uniform character (Chase, 1994).

In a packed bed, the adsorbent beads are stationary and liquid flow through the bed approximates plug flow. Thus, the number of theoretical equilibrium stages (referred to as plates) is maximised which results in good adsorption and chromatographic performance. As a consequence of the absence of plug flow in the liquid phase, compounded by the mixing of the adsorbent, a well-mixed fluidised bed would be expected to show an inferior adsorption performance compared with that of a packed bed. Thus, for protein recovery in liquid fluidised beds, it is highly desirable to minimise the degree of mixing in order to mimic the adsorption characteristics found in a packed bed contactor with respect to capacity and resolution.

Several strategies have been reported in order to limit the mixing of adsorbent particles within liquid fluidised beds. One approach is to divide the bed into sections by the introduction of baffles into the contactor (Bujis and Wesselingh, 1980). Other approaches seek to keep the adsorbent beads in a fixed position or at least localise their movement in

order to achieve a stable fluidised bed which subsequently behaves like a packed bed, but with a greater voidage. For example, by using magnetically susceptible adsorbent particles a fluidised bed can be stabilised by subjecting it to a magnetic field. Such beds are claimed to exhibit little or no backmixing and can be operated continuously (Burns and Graves, 1985). The practical benefit of this approach, i.e. restricted movement of adsorbent particles and associated uncoupling of the bed expansion from fluidisation velocity, has subsequently been demonstrated by Zhang (1998). In this work, magnetically stabilised fluidised beds (MSFB) were exploited for (i) the direct recovery of the intracellular enzyme glyceraldehyde 3-phosphate dehydrogenase (G3PDH) from unclarified yeast disruptates and (ii) for the recovery of antibody fragments from *E. coli* fermentation broths. However, this technique requires complicated and relatively expensive equipment, particularly at large scale.

A simpler approach has been to design the physical properties of the solid phases in such a way that they generate an inherently stable fluidised bed. If the adsorbent beads have an appropriate distribution of sizes and/or densities, grading or classification of the adsorbent occurs within the bed with the larger/denser particles being located near the bottom of the bed and the smaller/lighter particles nearer the top. The segregation behaviour restricts the local mobility of the fluidised particles. Such a bed exhibits dispersion characteristics similar to a packed bed (Chase, 1994; Thömmes, 1997; Barnfield-Frej *et al.*, 1997; Thömmes *et al.*, 1995a). Thus, the hydrodynamic properties of a fluidised bed are combined with the chromatographic properties of a packed bed. The degree of classification is dependent on the ratio of the size of the largest and smallest particle within the bed. This ratio has been claimed to be at least 2.2 (Al-Dibouni and Garside, 1979; Karau *et al.*, 1997).

In order to account for the difference in the dispersion characteristics of the classified, stable fluidised bed and the conventional, well-mixed fluidised bed, the term 'expanded bed'

has been coined by several authors together with the leading manufacture of chromatography media and equipment (Amersham Pharmacia Biotech AB, 1997; Chase, 1994; Hjorth, 1997). In the work presented here, the term 'fluidised bed' will be used synonymously with 'expanded bed' to refer to adsorbents fluidised under conditions which seek to minimise particle mixing.

1.4.2 Design and operation of liquid fluidised beds

1.4.2.1 Matrices for fluidised bed adsorption

Particle fluidisation is achieved by pumping liquid upwards through a settled bed of adsorbent particles. At low fluidisation velocities, liquid merely percolates through the voids between the adsorbent beads as in a packed bed. Increasing the flow rate leads to point at which the settled beads start to move apart. If the velocity is further increased, the particles become suspended in the liquid. This point is defined as the minimum fluidisation velocity U_{mf} (see Figure 1.3). If the fluidisation velocity is increased above U_{mf}, the bed expands as the adsorbent particles move further apart. This results in a smooth, progressive bed expansion referred to as steady state fluidisation (Kunii and Levenspiel, 1969). A critical velocity is reached with further increase of fluidisation at which the bed destabilises as adsorbent particles begin to entrain from the bed. The flow velocity at this point is called the maximum fluidisation velocity or terminal velocity U_t. This velocity can be approximated using Stokes law (Equation 1.1) which describes the settling velocity of a single particle at infinite dilution.

$$U_t = \frac{\left(\rho_p - \rho_l\right) \cdot d_p^2 \cdot g}{18 \cdot \eta} \qquad \textit{Equation 1.1}$$

Since particles in a fluidised bed interact due to adhesion forces, particularly when fluidised at higher viscosities, they cannot be regarded as individual particles and hence

Figure 1.3. Operational window of fluidisation velocities.

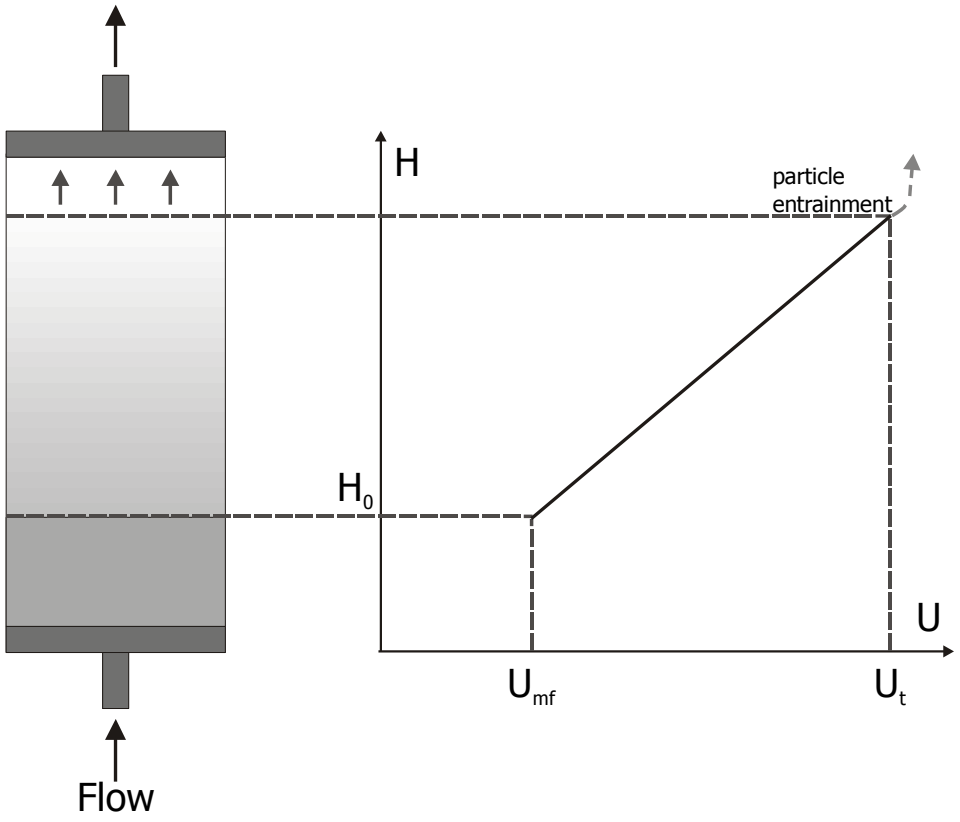

The operational window of a fluidised bed process is defined by the minimum fluidisation velocity U_{mf} at which a settled bed of adsorbent beads starts to fluidise and the terminal velocity (U_t)at which the bed stabilises and adsorbent beads are entrained from the bed.

Equation 1.1 only yields an estimation of the terminal velocity. However, Equation 1.1 clearly reflects the parameters which influence the terminal velocity of a particle and thus determine the operational window with regard to fluidisation velocity. The terminal velocity is proportional to the density difference between the particle (ρ_p) and the fluidising liquid (ρ_l), proportional to the square of the particle diameter (d_p), and inversely proportional to the fluid viscosity (η).

Early work exploiting extensively cross-linked agarose adsorbents originally designed for conventional, packed bed processes demonstrated the principal of operation and the potential of fluidised bed adsorption for processing particulate feedstocks (Chase and Draeger, 1992a; Draeger and Chase, 1991; Chase and Draeger, 1992b). However, it was found that these materials were not optimally suited since the combination of particle diameter and density allowed only low flow rates (e.g. 10-30 cm h^{-1}) which resulted in low overall productivities. Denser particles such as silica were more appropriate in this respect (Finette *et al.*, 1996; Dasari *et al.*, 1993). However, a drawback of silica-containing material is the limited stability at high pH values which makes it less suitable for biopharmaceutical production where alkaline conditions are commonly used for cleaning-in-place and sanitisation-in-place procedures.

The development of denser adsorbents enabled the use of higher flow rates and improved the stability of operation of expanded beds. Tailor-made adsorbents were produced using hydrophilic natural polymers such as cellulose, agarose or synthetic trisacrylate-based materials. In order to enhance the particle density, heavy, inert filler materials have been incorporated during assembly. The resulting composite materials included cellulose-titanium dioxide (Gilchrist *et al.*, 1994; Gibson and Lyddiatt, 1993) and dextran-silica (Morton and Lyddiatt, 1992). Other materials reported for the fabrication of denser adsorbents were glass

and zirconia. For example, Thömmes *et al.* (1995b) exploited custom-derivatised controlled pore glass particles for the purification of monoclonal antibodies. Zirconia-based materials exhibit a significantly higher density than silica (Zhu *et al.*, 1997). It has been demonstrated that even small particles (e.g. less than 50 μm in diameter) may be fluidised at linear flow rates similar to those used for silica or density-enhanced agarose particles having a greater diameter (Griffith *et al.*, 1997; Morris *et al.*, 1994). In another approach, McCreath and colleagues developed perfluoropolymer particles which were derivatised with dye ligands for the affinity purification of dehydrogenases from disrupted bakers' yeast (McCreath *et al.*, 1995; McCreath *et al.*, 1994). The increased density of the support (2.20 g ml^{-1}) also allowed the use of comparatively small particles (50-80 μm) at an acceptable linear flow velocity of 120 cm h^{-1}.

Agarose based materials have been commercialised specifically for fluidised bed adsorption by increasing their specific weight with incorporated quartz or steel particles (STREAMLINE^{TM}, Amersham Pharmacia Biotech AB, 1997; Hjorth, 1997). The densities so achieved have been quoted as 1.15 g ml^{-1} for agarose-quartz and 1.3 g ml^{-1} for agarose-steel composites. There are many studies published concerning the fluidisation behaviour of the STREAMLINE range of materials (Chang and Chase, 1996a; Chang *et al.*, 1995; Hansson *et al.*, 1994; Hjorth *et al.*, 1995; Thömmes *et al.*, 1995c). These materials are available with a range of ligand functionalities such as anion exchange (DEAE, Q), cation exchange (SP), chelating ligand (iminodiacetic acid for immobilised metal affinity chromatography, IMAC), protein A (affinity purification of antibodies) and phenyl groups (hydrophobic interaction chromatography, HIC; Färenmark *et al.*, 1999; Hjorth, 1997; Amersham Pharmacia Biotech AB, 1997). More recently, so-called pellicular adsorbents were defined as suitable for fluidised bed adsorption (Gibson and Lyddiatt, 1993). These adsorbents are characterised by a

dense core such as glass (Lihme *et al.*, 1998) or stainless steel (Palsson *et al.*, 2000a; Palsson *et al.*, 2000b) coated with a layer of porous material, e.g. agarose. Such matrices promise high rates of adsorption/desorption due to the absence of deep convective pores and the short diffusion distances within the thin porous layer which comprises the pellicle.

1.4.2.2 Column design for fluidised bed adsorption

In order to achieve a stable fluidised bed, the column has to fulfil some simple but important demands. A suitable liquid distribution is crucial to accomplish plug flow conditions within the bed and thus minimise particle dispersion. A prerequisite for the generation of an even velocity profile across the cross section of a column is an evenly distributed pressure drop across the distributor at the column inlet. Pressure drop fluctuations lead to the development of channels which are the most important influence upon inhomogeneity in an adsorption process (Bascoul *et al.*, 1993). Flow distribution can be achieved by using sieve plates, meshes, or a bed of glass ballotini (De Luca *et al.*, 1994; Lan *et al.*, 1999; Thömmes *et al.*, 1995c). Bascoul *et al.* (1988) investigated bed stability as a function of the distributor design showing that channelling in the lower part of a fluidised bed due to uneven flow distribution is reduced with increasing column length. This has led to the conclusion that the fluidised bed itself serves as an effective flow distribution system. More recently, a novel distributor design was introduced which uses a stirrer in the bottom of the contactor to distribute the incoming feedstock. This configuration divides the fluidised bed in a limited, well mixed zone at the bottom and a stable fluidised bed above it (Zafirakos and Lihme, 1999). Such contactors were included in the study presented here (see Chapter 3 and Chapter 4). Besides the demand for an even flow distribution, the distributor has to enable the unhindered passage of particulates without becoming blocked or damaging shear sensitive cells. Partial blockage of a distributor will cause channelling in the fluidised bed. Cell

breakage in the flow distributor can lead to the unwanted release of intracellular compounds which may impair the purification process of an extracellular product for whole broths.

Another important factor which bears upon bed stability is the column verticality. Van der Meer *et al.* (1984) have demonstrated that even small deviations from vertical alignment lead to significant inhomogeneity of liquid flow. These findings were confirmed by Bruce *et al.* (1998) who found that this effect is more pronounced in small-diameter contactors. In their work, the dynamic capacity of a 1 cm column, used for the capture of glucose-6-phosphate dehydrogenase (G6PDH) from unclarified yeast homogenate, was reduced by approximately 30% when misaligned by 0.185°. However, a 5 cm contactor operated under similar conditions appeared to be unaffected.

1.4.2.3 Experimental procedure

In principle, the experimental protocol of fluidised bed adsorption does not deviate from packed bed operations, but the main difference is the direction of the liquid flow. The sequence of steps of equilibration, sample application, wash, elution and cleaning (CIP) is performed in an upward direction although the last two might be undertaken in fixed bed mode. During equilibration, the matrix is fluidised and a stabilised fluidised bed is developed. Here, the classification within the bed with regard to particle size of the adsorbent particles may be detected by visual observation. At the same time, the matrix is primed for adsorption by the selection of a suitable buffer with respect to product-adsorbent interactions. Subsequently, the feedstock is applied to the fluidised bed. Target proteins are adsorbed while cells, debris and other particulates and contaminants pass through the bed. After sample application, residual biomass and unbound proteins are removed from the bed in a washing procedure. Elution may be performed either in packed bed or in fluidised bed mode. A common procedure has been to allow the adsorbent to settle and then to reverse the flow for

elution. Here, the upper adapter is lowered to the top of the settled bed. On the other hand, maintaining a fluidised bed during elution prevents particle aggregation and thus facilitates subsequent cleaning of the adsorbent (Lihme *et al.*, 1998; Hjorth, 1999). However, due to the greater interstitial volume of the fluidised bed, the elution volume is increased in comparison to fixed bed elution (Hjorth *et al.*, 1995). Following elution, the adsorbent is subjected to cleaning-in-place (CIP) procedures. These are important since the application of whole broth increases the contact of the adsorbent with nucleic acids, lipids, and cellular compounds which are commonly removed or reduced in conventional primary recovery steps prior to fixed bed column chromatography. Commonly used agents in CIP protocols are NaCl, NaOH, ethanol, acetic acid, urea and guanidine hydrochloride (Amersham Pharmacia Biotech AB, 1997; Chang *et al.*, 1995; Hjorth, 1997).

1.5 Aim of the study – primary purification of L-asparaginase from *Erwinia chrysanthemi* by fluidised bed adsorption

The aim of the study presented here was to develop a novel process for the primary purification of the intracellular enzyme L-asparaginase produced in *Erwinia chrysanthemi*. It was envisaged that the novel process would integrate discrete operations of cell disruption by bead milling with product capture by fluidised bed adsorption in order to minimise the processing time. L-asparaginase is known to be proteolytically sensitive (Lee *et al.*, 1989), and thus the rapid processing achieved by such an approach should benefit the overall yield and molecular fidelity of the end-product.

1.5.1 The clinical relevance of L-asparaginase

L-asparaginase catalyses the deamidation of L-asparaginase to produce L-aspartic acid and ammonia. The enzyme has been noted in a range of bacteria, fungi, plants, and mammals

and its presence in Gram-negative bacteria has been widely recorded (Wriston, 1985). The interest in L-asparaginases arises because some of these enzymes, particularly those from *Escherichia coli* and *Erwinia*, have proven to provide an effective treatment for acute lymphoblastic leukaemia (Wade and Rutter, 1970). The enzymes from *E. coli* and *Erwinia* are immunologically distinct, allowing an alternative therapy for a patient hypersensitive to one of these enzymes (Cammack *et al.*, 1972). The *Erwinia* L-asparaginase is a tetrameric molecule of relative high molecular mass 140,000, consisting of four identical subunits with an isoelectric point (pI) of 8.6.

1.5.2 Conventional purification of L-asparaginase from *Erwinia chrysanthemi*

Figure 1.4 depicts a comparison between the current commercial process and a proposed revision for L-asparaginase release from *Erwinia* cell paste and its primary purification. The long established *current* process exploits alkaline lysis of the cells and an adsorption step performed in batch mode following centrifugal clarification (Goward *et al.*, 1989). Cell lysis is achieved by adjustment of the pH of a cell suspension to 11.4. The pH is then incrementally lowered to 6.5 and then 4.8. At both pH values the broth is clarified by centrifugation. The pH of chemically lysed biomass is not directly adjusted to 4.8 in a single step in order to minimise loss of enzyme due to adsorption to cell debris (Goward *et al.*, 1992). Batch adsorption of the product is then performed in a stirred tank using a cation exchange CM cellulose matrix. The matrix is separated from the broth by centrifugation and eluted in batch mode with added salts. Commonly, the total process time to yield the primary extract amounts to approximately 20 h (batch size: 60 kg biomass).

In the proposed *integrated* process of bead milling and fluidised bed adsorption (see Figures 1.4 and 1.5) the disruptate would be directly fed from the mill into the fluidised bed

Figure 1.4. Comparative approaches to the purification of L-asparaginase from *Erwinia chrysanthemi*.

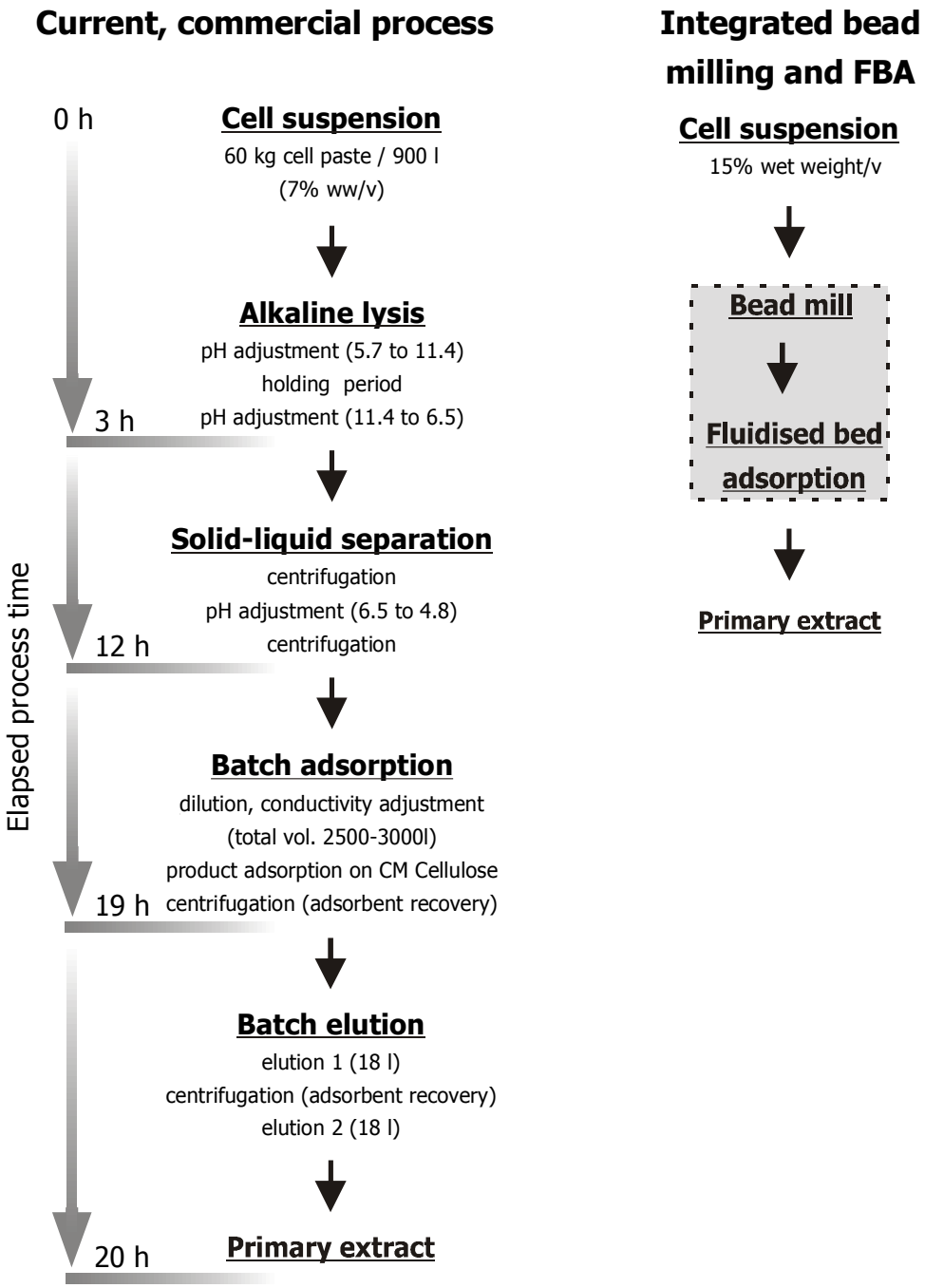

Comparison between the current production process and a proposed revision integrating bead milling and fluidised bed adsorption.

Figure 1.5. Experimental configuration for integrated bead milling and fluidised bed adsorption

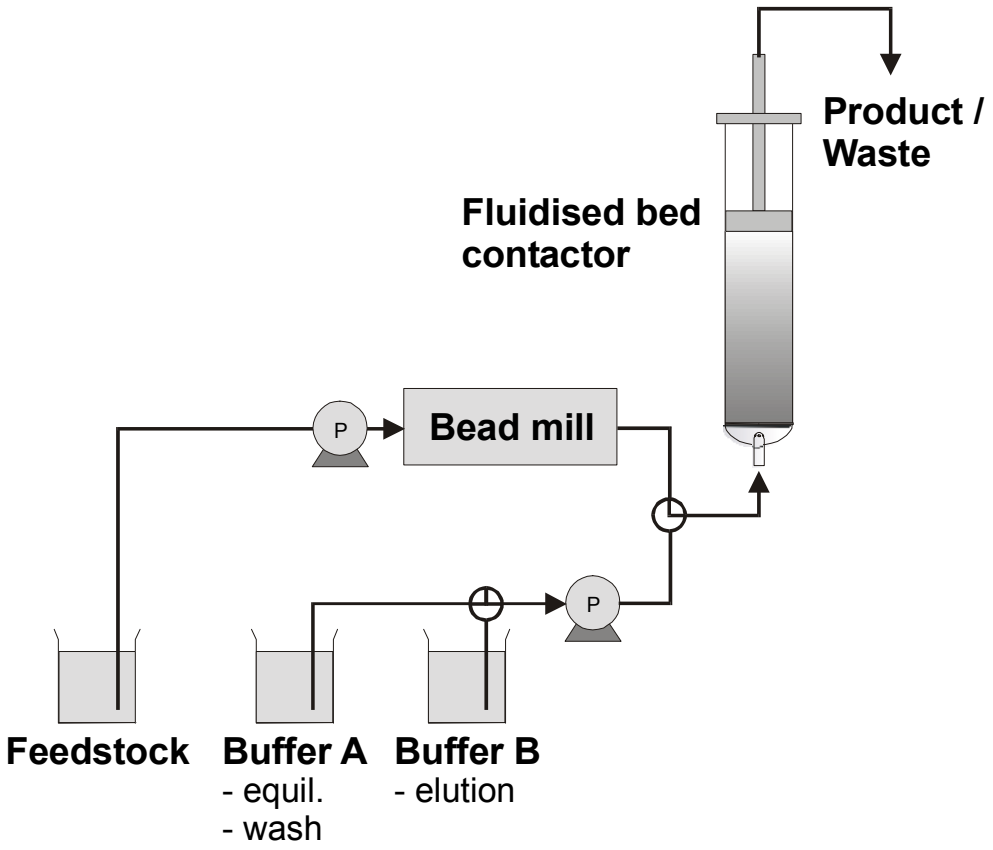

Cell suspension is fed to the bead mill and disruptate is directly introduced from the mill into the fluidised bed contactor. After loading of the disruptate, the fluidised bed is washed and subsequently eluted in fluidised bed mode.

contactor. Temporary storage of the disruptate is thus eliminated and exposure of the product to potential antagonists (debris adsorption, degrading enzymes, etc) is minimised. In addition, no clarification steps are required to process the broth which (i) reduces the number of unit operations, (ii) shortens the overall process time and (iii) reduces the capital costs.

1.5.3 Thesis outline

The study presented in Chapter 2 investigated the disruption of *Erwinia chrysanthemi* by bead milling. The aim was to establish an effective method for the release of the intracellular enzyme L-asparaginase and to identify potential process limitations. Raw material was supplied in the form of cell paste (CAMR, Porton Down, Salisbury) harvested by centrifugation after fermentation and frozen for storage and shipment. Feedstocks for bead milling were therefore prepared by thawing and re-suspending frozen cells. The feedstock conditions for cell disruption, in particular pH and ionic strength, were chosen with the aim to produce a disruptate suitable for immediate processing by exploiting cation exchange adsorbents. The back mixing characteristic of the bead mill was investigated by tracer analysis. Product release was tested both under feedstock re-circulation from a reservoir and single pass operation at various feed rates.

Chapter 3 summarises the establishment of a protocol for the primary purification of L-asparaginase from unclarified *Erwinia* disruptates by fluidised bed adsorption. Fluidisation characteristics and axial dispersion of candidate adsorbents were compared. Suitable adsorbents were chosen for further experimentation and their biochemical performance was assessed. Here, CM HyperD LS (Biosepra), a hyper-diffusive cation exchange adsorbent, and SP UpFront, a custom derivatised, pellicular stainless steel/agarose solid phase were employed. Product uptake rates were compared by batch adsorption studies and the influence

of fluidisation velocity and settled bed height on the adsorbent dynamic capacity was assessed by frontal analysis.

Chapter 4 summarises experiments which seek to demonstrate the feasibility of the integration of cell disruption by bead milling and product capture by fluidised bed adsorption (see Figure 1.4). At first a study concerning the primary purification of the enzyme G3PDH from brewers' yeast is presented. The aim was to review the practical feasibility of coupling the two unit operations whilst preserving precious stocks of *Erwinia* cell paste. Then, the integrated primary purification of L-asparaginase from *Erwinia* disruptates was investigated. Here, experimental conditions, established for the fluidised bed capture of L-asparaginase (see Chapter 3), were applied in larger scale contactors. The study included the comparison of the custom built BRG contactor (4.5 cm i.d.) with the commercially available UpFront contactor (5.0 cm i.d.) featuring a novel flow distribution system. Flow distributor designs were assessed by residence time distribution (RTD) analysis and the biochemical performance of the contactors was compared by frontal analysis online with cell disruption by bead milling. The purity of partially purified L-asparaginase recovered by fluidised bed adsorption was finally compared with samples derived from a conventional production process by SDS PAGE analysis in tandem with activity and total protein assays.

2 MECHANICAL CELL DISRUPTION OF *ERWINIA CHRYSANTHEMI*

2.1 Introduction

For the production of recombinant or native proteins and other bioproducts, a variety of common hosts are available such as *Escherichia coli* and *Saccharomyces cerevisiae*. For simple, unglycosylated proteins, the Gram-negative bacterium *E. coli* remains the recombinant host of first choice. There are several reasons for this, as discussed by Shuler and Kargi (1992). For example, it has been intensively studied and cloning techniques are well established for which strongly-inducible gene promotors are readily available. High growth rates can be achieved on simple media, and validated methods for endotoxin removal facilitate regulatory approval for new products. The yeast *S. cerevisiae* has the advantage of performing simple glycosylations. Its genetic system is also well understood and it is also capable of achieving relatively high growth rates.

Unfortunately, *E. coli* and *S. cerevisiae* both have a disadvantage as hosts for protein production in that they do not excrete high levels of proteins to the medium (Shuler and Kargi, 1992). Consequently, process methods for releasing macromolecular products from cells following fermentation are required. This involves breaking apart the cell envelope (i.e. cell wall and membrane) which isolates the intracellular content from the suspending medium and provides physical stability for the cell. A wide variety of disruption methods based on different mechanisms have been developed (see Table 2.1). Section 2.1.1 gives a brief review of the cell wall structure of bacteria and yeast. This information is important if the mechanism

Table 2.1 Classification of cell disruption techniques

MECHANICAL METHODS		
Bead mill		Agitators impart kinetic energy to beads in the cell suspension. Collisions of beads and shear forces cause cell disruption.
Homogeniser		A cell suspension is forced under high pressure through a discharge valve and impinges on an impact ring. The discharge pressure is regulated by a spring loaded valve rod.
Microfluidiser		Two streams of cell suspension are impacted on each other or a stream is impinged on a solid surface which causes disruption by liquid shear forces
NON-MECHANICAL METHODS		
Physical	**decompression**	Cell suspension is mixed with pressurised subcritical gas which enters the cell and expands on release of the applied pressure
	osmotic shock	Cell suspension equilibrated at high osmotic pressure is suddenly diluted. No disruption of strength-providing components. Release of proteins secreted to the periplasm.
	thermolysis	Heat treatment to release periplasmic or cytoplasmic proteins, results dependent on the type of the organism and its growth phase.
Chemical	**antibiotics**	Lysis caused by a particular mechanism, e.g. cell wall synthesis (β-lactam antibiotics). Effectiveness depends on the state of the culture, less effective for stationary cells.
	chelating agents	Disruption of the outer membrane of gram-negative bacteria caused by binding of divalent cations (Mg^{2+} and Ca^{2+}) releases periplasmic proteins, no release of cytoplasmic proteins.
	chaotropes	Chaotropes such as urea or guanidine disorganise the structure of water and thus weaken solute-solute interactions resulting in a solubilisation of hydrophobic membrane proteins.
	detergents	Due to their amphipathic nature, detergents (SDS, tetra alkyl ammonium salts, Triton X) interact both with water and lipid resulting in a solubilisation of membrane components.
	solvents	Non-polar solvents (e.g. toluene, chloroform) dissolve hydrophobic components of the cell wall (phospholipids)
	hydroxide	Alkaline lysis works by saponification of the lipids in the cell wall, extremely harsh, product must be stable at high pH.
Enzymatic	**lytic enzymes**	Foreign enzymes degrade the cell wall leading to lysis (e.g. glucanase and protease for yeasts, lysozyme for bacteria)
	autolysis	Host organism produces an enzyme which degrades the cell wall
	cloned-phage lysis	Lysis of bacteria after incubation with bacteriophages, e.g. T4, or cloned phage ϕX174 gene.

of disruption is to be understood. Section 2.1.2 gives a classification of different disruption techniques and 2.1.3 focuses on the bead mill as a mechanical method of cell disruption.

2.1.1 The cell envelope of bacteria and yeast

The cell wall structure of *E. coli* will be described as being representative of other Gram-negative organisms such as *Erwinia*. Basic structures of cell envelopes of *E. coli* and yeasts have been summarised by Middelberg (1995). The cell envelope of Gram-negative bacteria, such as *E. coli* and *Erwinia*, consists of a semi-permeable cytoplasmic membrane (innermost), an inter-membrane periplasmic space, a thin rigid wall layer comprised of peptidoglycan and a lipid-protein outer membrane bilayer (see Figure 2.1). The cytoplasmic membrane provides the major interactive barrier between the internal cell environment and the bulk medium which houses transport systems and actively maintains concentration gradients. It does not provide any significant structural strength and is readily disrupted by osmotic shock in the absence of the structural component layers. The mechanical strength is provided by the peptidoglycan layer which forms the basic framework of the cell envelope. It accounts for 10 to 20% of the cell envelope in terms of dry mass and consists of a series of glycan chains composed of N-acetylglucosamine (NAG) and N-actetylmuramic acid (NAM) linked by β(1-4)-glycosidic bonds. These chains are crosslinked together by peptide bonds formed between amino acid side chains (Höltje and Glauner, 1990). The strength of this structure is governed by the frequency of occurrence of peptide chains and their crosslinking (Engler, 1985). The outer membrane specific to Gram-negative bacteria consists of a lipid bilayer containing transmembrane proteins, phospholipids and lipopolysaccharids (LPS). Divalent cations play an essential role in stabilisation (Nikaido, 1973; Engler, 1985). The anisotropic nature of its bilayer configuration distinguishes it from the cytoplasmic membrane. Gram-positive bacteria, such as *Bacillus* lack the outer membrane component, but

Figure 2.1. Simplified structure of the wall of Gram-negative bacteria

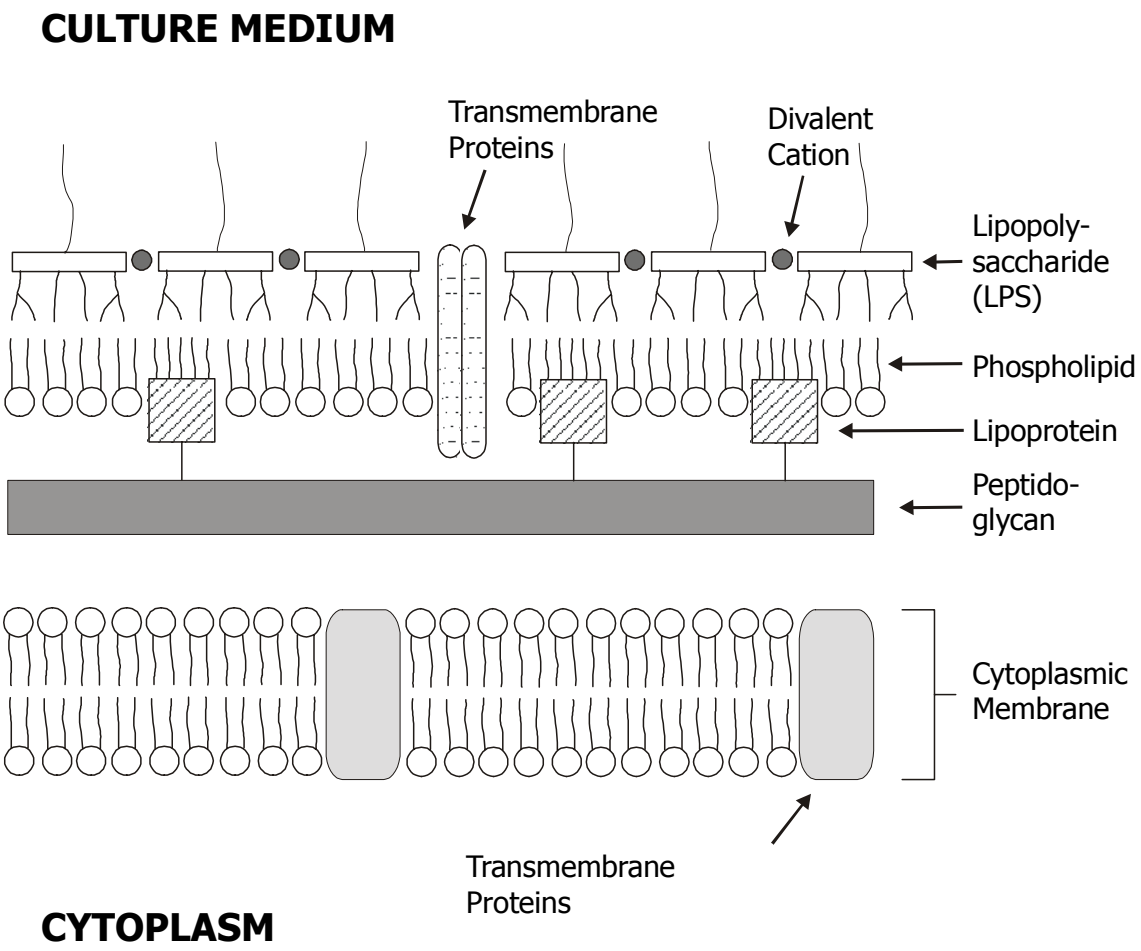

The cell wall structure of E. coli is depicted here schematically representative for other Gram-negative organisms such as Erwinia (redrawn from Middelberg, 1995). Common features of the cell envelope of Gram-negative organisms are the innermost, semi-permeable cytoplasmic membrane, an inter-membrane periplasmic space, a thin rigid wall layer comprised of peptidoglycan and a lipid-protein outer membrane bilayer.

in turn possess a more dominant peptidoglycan structure (Nikaido, 1973; Engler, 1985).

The cell cytoplasm of the yeast *S. cerevisiae* is encased in a lipid bilayer as in *E. coli*. This plasma membrane is separated from the cell wall by the periplasm. The wall is composed primarily of glucan, mannoprotein and chitin which form a crosslinked polysaccharide-protein structure which is considerably more complex than that of *E. coli* (Fleet, 1991). It accounts for approximately 15-25% of the dry cell weight.

2.1.2 Classification of disruption techniques

Different methods of cell disruption have been reviewed by several researchers (Harrison, 1991; Hughes *et al.*, 1971) partly focussing on larger scale operations (Middelberg, 1995; Kula and Schütte, 1987). Table 2.1 summarises methods used for cell disruption together with their principles of operation. Complete destruction of the cell wall in a non-specific manner is usually achieved by mechanical means exploiting solid shear (bead mill) and liquid shear forces (high-pressure homogeniser, microfluidiser). Non-mechanical methods are gentler and often only perforate or permeabilise cells rather than tearing them entirely apart. For example, chemical and enzymatic methods rely on selective interaction of a substance, or an enzyme respectively, with components of the cell wall or the membrane which allow product to seep out. However, chemical or enzymatic treatment at large scale may be costly and waste disposal of process additives may also cause problems. As a result, mechanical methods such as high-pressure homogenisers (HPH) or bead mills are preferred for large-scale applications (Agerkvist and Enfors, 1990; Kula and Schütte, 1987).

High-pressure homogenisers and bead mills were originally designed for different industrial applications but have recently been adapted for microbial cell disruption (Harrison, 1991; Middelberg, 1995). The former originated in food technology for the homogenisation of milk and milk products. Bead mills are also employed for the comminution of pigments in the

paint and lacquer industry and will be reviewed more closely in Section 2.1.3. Important operating parameters of the HPH with regard to the disruption of microorganisms, i.e. operating pressure, cell concentration, and design of the valve unit have been reviewed by several researchers (Chisti and Moo-Young, 1986; Kula and Schütte, 1987).

In order to maximise the disruption efficiency, combinations of disruption methods have been synergistically employed. Dean and Ward (1992) reported a combined treatment of *E. coli* with EDTA and lysozyme. Here, EDTA destabilised the outer membrane of the bacteria which enabled lysozyme to penetrate and hydrolyse the peptidoglycan layer leading to disruption of cells that are not osmotically stabilised. Vogels and Kula (1991) used a short treatment with a lytic enzyme or heat before mechanically disrupting *Bacillus cereus* in a bead mill or a HPH. The pre-treatment resulted in 98% disruption after a single homogeniser pass whereas untreated cells exhibited only 40% disruption.

Regardless of the mode of disintegration, cell disruption cannot be considered as an isolated process. It must interact and interface with both upstream and downstream operations. For example, considerable changes in peptidoglycan structure of bacteria occur during the transition from exponential to stationary phase, particularly with respect to the degree of crosslinkage (Pisabarro *et al.*, 1985) which increases resistance to cell disruption. Such findings agree with those by Engler and Robinson (1981) who reported that yeast cells growing at a higher growth rate were easier to disrupt. In addition, Gray *et al.* (1972) found that *E. coli* cells grown on complex media are more robust than cells grown on a simple synthetic medium. On the downstream side, the size of cell debris, generated by cell disruption, significantly influences solid-liquid separations (Clarkson *et al.*, 1993; Agerkvist and Enfors, 1990). Also, chemical/biological lytic agents (see Table 2.1) may complicate purification procedures. Moreover, the protein of interest will be the target of proteolytic

enzymes liberated from the same cell which limits process conditions and time and makes rapid processing of the disruptate essential (Kaufmann, 1997; Grodberg and Dunn, 1988; Kaufmann and Stierhoff, 1993). Consequently, a product capture step integrated with cell disruption would be expected to benefit the yield and molecular fidelity of most protein products. The optimal process in this respect would be a continuously operated cell disruption, e.g. achieved by bead milling, and a product capture step capable of handling particulate feedstocks such as fluidised bed adsorption (see Figure 1.5). Thus, holding periods due to the accumulation of disruptate as well as time consuming clarification steps are omitted. Such an integrated process was proposed earlier (Bierau *et al.*, 1999) for the purification of the intracellular enzyme glyceraldehyde 3-phosphate dehydrogenase (G3PDH) from unclarified yeast disruptates.

2.1.3 The bead mill

Mechanical cell disruption in a bead-mill has many attractive process characteristics including high disruption efficiency, high throughput and biomass loading, good temperature control and mills are commercially available from laboratory to industrial scale (Chisti and Moo-Young, 1986; Limon-Lason *et al.*, 1979; Schütte *et al.*, 1983; Zhang, 1998). In addition, the operational characteristic of single-pass and continuous operation recommends the bead mill as the ideal feedstock generator for direct sequestration of released products in a fluidised bed (Bierau *et al.*, 1999).

Bead mills consist of a mostly horizontally positioned, closed grinding chamber. On the motor-driven agitator shaft different impellers can be employed in the form of discs, rings or pins (Figure 2.2). These can be mounted centrically or eccentrically and impart kinetic energy from the rotating parts to the grinding elements which are suspended in the cell suspension. Cells are disrupted by shear forces generated by the radial acceleration of the beads as well as

Figure 2.2. The Dyno Mill KDL

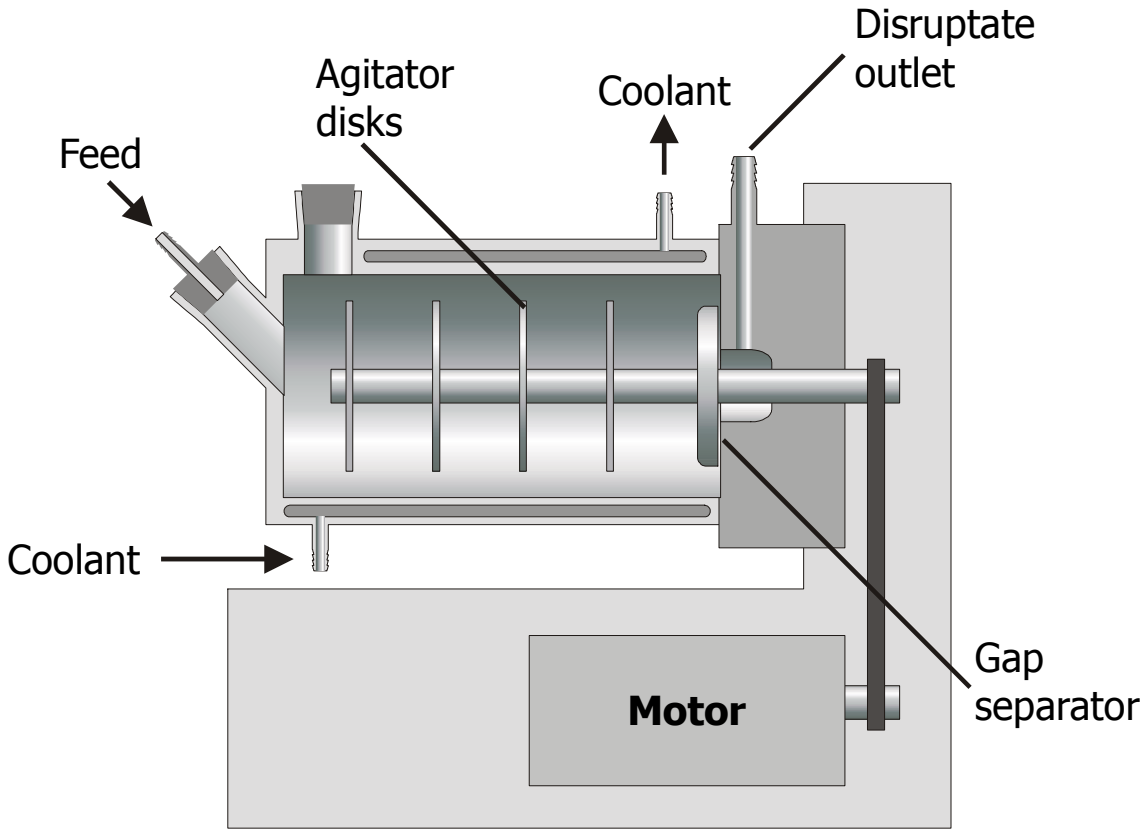

The volume of the disruption chamber is 600 ml. Four centrically mounted rotating discs impart kinetic energy to the grinding elements which are suspended in the cell suspension. The feed inlet and outlets are above tank level. Grinding beads are retained by the gap separator. Cooling of the processed liquid is provided via a jacket.

by bead collisions. Virtually all of the energy input is dissipated as heat, necessitating cooling of the chamber which is achieved by a cooling jacket. The continuous separation of the grinding elements from the suspension is accomplished using either dynamic sieves or coaxial ring slots integrated into the bearing housing. Commercially available mills differ in the ratio of diameter to length of the grinding chamber which is considered to be optimal between 1:2.5 to 1:3.5 (Kula and Schütte, 1987). Mills with grinding chambers between 50 ml and 275 litres are available for laboratory, pilot and production scale. The largest available bead mills can handle throughputs of up to 2000 l h^{-1} (White and Marcus, 1988; Asenjo and Patrick, 1990). Typical biomass loads were reported between 30 – 50% ww/v (Middelberg, 1995; Schütte *et al.*, 1983; Zhang, 1998).

Disruption of microorganisms by bead milling has been reviewed by a number of researchers (Middelberg, 1995; Harrison, 1991; Chisti and Moo-Young, 1986). The most important operational parameters with regard to cell disintegration were identified as the agitator speed (a normalised peripheral tip speed of the agitating elements is used for the comparison of different mills), the feed rate of the suspension, size and density of the beads, and cell size in the feed. Generally, by increasing tip speed the shear forces generated will increase, as does the collision frequency, both contributing to a higher disruption efficiency. However, at the same time this increases the temperature of the disruptate, the energy required to drive the agitator, and the erosion of the grinding beads. Kula and Schütte (1987) found an optimal peripheral tip speed in a Netzsch LME 4 mill of 8 m s^{-1} for yeast and 10 m s^{-1} for bacteria. Similar results had been reported by Limon-Lason *et al.*, (1979) who established an optimal tip speed of 10 m s^{-1} for the disruption of yeast in a Dyno Mill KD5. An optimal bead load of 80-85% chamber volume has been reported by several researchers (Schütte *et al.*, 1983; Rehácek and Schaefer, 1977). The optimum bead size was found to be

dependent on the size of the microorganism to be disrupted. Smaller bead diameters (< 0.5 mm) were found to be more suitable for the disruption of bacteria whereas larger beads (0.5 – 1 mm) seemed to be optimal for yeast (Kula and Schütte, 1987). The same study revealed also that cell size has a considerable impact on disruption efficiency. It was demonstrated that lower feed rates or even multiple passes were required for the disruption of bacteria (*B. cereus, Brevibacterium ammoniagenes, E. coli, Lactobacillus confusus*) in order to achieve an equivalent release of protein obtained for yeasts in single-pass operation (*S. carlsbergensis, S. cerevisiae*). As a result, biomass throughput for yeast was 4 to 10 times greater in comparison with bacteria.

It has been demonstrated that the protein release in bead mills in batch operation follows first-order kinetics. However, in continuous operation back mixing has to be taken into account which is a function of the feed rate and the stirrer geometry. Thus, the degree of disintegration, or the protein release respectively, is not inversely proportional to the feed rate (Kula and Schütte, 1987; Limon-Lason *et al.*, 1979).

Side-by-side comparison of disruption by bead milling with high pressure homogenisation, conducted by different researchers, revealed some process advantages for the bead mill such as a relatively high disruption efficiency in single pass operation as well as larger debris size distributions. The latter is favourable if a subsequent centrifugation or filtration of the disruptate is envisaged. Agerkvist and Enfors (1990) disrupted *E. coli* cells in a bead mill (Dyno Mill KDL, 0.6 l disruption chamber) and in a HPH (Manton Gaulin 15M-8TA). A single pass through the bead mill at a flow rate of 4.5 l h^{-1} (equivalent to 4 min mean residence time in the disruption chamber) yielded a release of 79 % of the cytoplasmic enzyme β-galactosidase. In order to achieve an equivalent degree of disruption in the HPH, three passes were required. The mean debris size generated was 217 nm for the HPH and 529

nm for the bead mill. It should be noted that in this study the operational flow rate in the HPH (approximately 200 l h^{-1} at a pressure of 60 MPa) was much greater than in the bead mill owing to the relatively small scale of the mill (0.6 l chamber volume). However, experiments by Schütte *et al.* (1983) (*Bacillus sphaericus*) employing a bead mill at a larger scale (Netzsch LME 20, 20 l chamber volume, 93 l h^{-1}) bettered the disruption efficiency achieved in a HPH (Manton Gaulin, 59 MPa, 54 l h^{-1}).

The bead mill used for the work presented here is a Dyno Mill KDL (see Section 2.2.1) which has been extensively characterised by Zhang (1998) for the disruption of waste brewers' yeast. Here, the feed rates employed (5-25 l h^{-1}) exhibited little influence upon the disruption efficiency (i.e. release of total protein and the enzyme G3PDH) which was routinely high. The amount of total protein and enzyme released increased at higher feedstock concentrations (e.g. 40 – 50% ww/v). A similar effect has been reported in other studies (Limon-Lason *et al.*, 1979). A comparison of two different bead materials (glass, 0.2-0.5 mm, 2.5 g ml^{-1} and zirconia, 0.3 mm, 6.0 g ml^{-1}) yielded only a slight increase in disruption efficiency (6 % higher release of G3PDH and 2 % higher release of total protein, (Zhang, 1998).

2.2 Materials and Methods

2.2.1 Bead milling of *Erwinia chrysanthemi*

Cell disruption was performed by bead milling in a Dyno Mill KDL-I (Willi A. Bachofen AG, Switzerland) consisting of a silicon-carbide lined stainless steel chamber (0.6 ml) cooled by re-circulating iced water (0°C), for configuration see Figure 2.2. The chamber was loaded with zirconia beads (0.3 mm, density 6 g ml^{-1}) to 83% settled volume occupancy (500 ml beads, packed volume). This corresponded to a free volume within the chamber of

approximately 250 ml. The agitator speed was 3200 rpm corresponding to a peripheral tip speed of the agitating discs of 10.5 m s^{-1}. Frozen cell paste was thawed and resuspended in buffer A (20 mM citric acid / tri-sodium citrate, pH 5.0) at 30 % wet weight per volume (ww/v). Due to medium contamination of the paste voidage, cell leakage and undefined buffer effects the pH commonly shifted to approx. 5.8 - 6.0 The cell suspension was adjusted to the desired pH (pH 5.5 if not stated otherwise) by the addition of 20 mM citric acid and diluted to the desired biomass concentration.

For single pass experiments, chilled cell suspension was fed from a well-mixed reservoir into the mill and the disruptate was collected in a holding vessel. For re-circulation experiments, both the inlet and outlet of the mill was connected to the same vessel containing 500 ml of a *Erwinia* suspension (30% ww/v). Before milling was commenced, the free volume of the chamber was filled with cell suspension which reduced the volume of cell suspension in the re-circulation reservoir to 250 ml during an experiment.

2.2.2 Residence time distribution in the disruption chamber as a function of the feed rate

An acetone solution (1% v/v) in distilled water was used as a tracer and a step-input was introduced into the bead mill while the UV absorbance at the outlet was recorded (single path monitor UV-1 and chart recorder, Pharmacia, Sweden) and interpreted in terms of concentration of the tracer. After reaching a steady reading (100% value) the input feed was switched back to water. From the curve obtained for decreasing UV absorbance the data characterising the residence time distribution were calculated. The time interval from switching the feed to water until the signal reached 50% of the full deflection was taken as the mean residence time, the time interval of the signal between 84.15% and 15.85% yielded the spread of the distribution, 2σ, (refer to Figure 3.2).

2.2.3 Alkaline lysis of *Erwinia chrysanthemi*

Cell paste was thawed and resuspended in buffer A (15% ww/v). The pH of the suspension was adjusted to 11.4 by the addition of 0.5 M NaOH. After 30 min of stirring the pH was re-adjusted to pH 5.5.

2.2.4 Total protein determination

A commercially available reagent (Pierce Chemical) was used for the routinely performed determination of total protein in various samples. The assay is based on a method reported by Bradford (1976). An acidic solution of the dye Coomassie Brilliant Blue G-250 exhibits an absorbance shift between 465 and 595 nm when binding with proteins. The dye primarily binds to arginine residues in proteins and interacts with other basic and aromatic residues. The reagent is compatible with a wide range of commonly used buffer substances and the sensitivity of the method allows the detection of protein concentrations as low as 1 μg ml^{-1}. Due to the different composition of analytes, the response of the assay varies with the protein measured. Thus, the assay yields results which represent equivalents to the standard protein used.

A standard curve was generated using bovine serum albumin (BSA) in concentrations of 0 – 30 μg ml^{-1} in buffer A (*Erwinia* experiments: citric acid / tri-sodium citrate, 20 mM, pH 5.5; yeast experiments: 10 mM Tris/HCl, pH 7.5 containing 1 mM EDTA). The standards were incubated with an equal volume of Coomassie reagent for 3 minutes at room temperature (e.g. 600 μl sample + 600 μl reagent). Then the absorbance at 595 nm was recorded against a blank (buffer + reagent). The standard curve (valid for a particular batch of reagent) was stored electronically using commercial software (Viglen Ltd., Middlesex, UK). Appropriately clarified and diluted experimental samples were treated in the same manner as

the standards (measured in duplicates) and the average total protein concentration was automatically estimated from the standard curve using the software.

2.2.5 L-asparaginase activity assay

The assay is based on the measurement of ammonium released by the action of L-asparaginase on asparagine.

$$\text{Asparagine} \longrightarrow \text{Aspartate} + NH_4^+$$

The assay procedure comprises two stages. In the first stage the enzyme present in the sample is incubated with its substrate and liberates ammonium from asparagine. In the second stage the amount of ammonium so formed is quantified by converting it into ammonia (NH_3) by the alkaline hypochlorite solution which then reacts with the phenol-nitroprusside to give a blue coloured complex.

Reagents required for the L-asparaginase activity assay are listed in Table 2.2 The solutions for the determination of ammonia are stable for extended periods (storage at 4 °C). The assay buffer was prepared on the day of use by adding an appropriate quantity of L-asparagine and BSA to stocks of 50 mM borate buffer (pH 8.5). Enzyme samples may be in the form of washed, whole cells or of cell free extracts, both in 50 mM borate buffer (pH 8.5). Disruptate samples or fractions collected from chromatography experiments were routinely clarified by centrifugation (7600 g, 10 min). Sample (e.g. clarified supernatant, 150 µl) was placed into reaction tubes (1.5 ml volume) which were placed in a water bath (37 °C). Pre-warmed assay buffer was added (750 µl) and the mixture was incubated for exactly 5 minutes at 37 °C. After incubation the enzyme reaction was terminated by the addition of 375 µl of TCA solution. The tubes were removed from the water bath and mixed on a vortex mixer. 30 µl from each tube was removed and placed into another 1.5 ml reaction tube. Then 735 µl of alkaline hypochlorite and 735 µl of phenol nitroprusside solution were added. The solution

was mixed on a vortex mixer and incubated for 30 min. After incubation the absorbance of the sample was measured in a spectrophotometer (Pharmacia Ultraspec III) at 625 nm against the blank (borate buffer, 50 mM, pH 8.5, containing no asparaginase). The background level of ammonium present in the sample can be accounted for by including a sample in the assay in which the TCA solution is added before the assay buffer. The enzyme activity was estimated using a standard curve. The standards (0.2 / 0.5 / 1.0 / 5.0 / 10.0 U ml^{-1}) were included with each set of samples to be measured. They were treated in the same manner as the samples and produced a linear curve. Both, standards and samples were measured in duplicates.

Table 2.2. Reagents for the L-asparaginase assay

Reagent	Ingredients	
Assay buffer	50 mM	Borate (tri-sodium tetraborate), pH adjusted to 8.5 (HCl, 1 M)
	10 mM	L-asparagine (Sigma Chemicals, Poole, UK)
	0.05 mg ml^{-1}	Bovine serum albumin (BSA)
Alkaline -	5 g l^{-1}	NaOH
hypochlorite	0.42 g l^{-1}	available chlorine hypochlorite (35 ml l^{-1} BDH-SPECTROSOL sodium hypochlorite, 12% available chlorine)
Phenol -	10 g l^{-1}	Phenol
nitroprusside	0.05 g l^{-1}	Sodium nitroprusside
TCA	70 g l^{-1}	Tri-chloro acetic acid (7%)

2.2.6 Exposure of purified L-asparaginase to milling conditions

The chamber of the mill was packed to 67% with glass beads (400 ml) while the remaining volume was filled with a solution of purified L-asparaginase (supplied by CAMR, Porton Down, Salisbury), dissolved in buffer A (~ 300 U ml^{-1}, 850 U mg^{-1}). Milling intervals of one minute were alternated with cooling intervals of one minute. Samples were taken after each milling interval and assayed for protein concentration and asparaginase activity.

2.2.7 Protein adsorption studies to grinding beads.

Grinding beads (glass, 0.2-0.5 mm and zirconia, 0.3 mm) at a settled volume of 2 ml were incubated with 4 ml of protein solution (L-asparaginase, BSA, lysozyme, 1 mg ml^{-1} in each case in buffer A, pH 5.0). During the experiment the test tubes were placed on a roller incubator to provide mixing. L-asparaginase activity or the protein concentration, respectively, were monitored over a time course of 20 min. Binding capacities of the beads were calculated from a material balance conducted after 20 min incubation time.

2.2.8 Protein adsorption studies to cell debris.

a) An *Erwinia* disruptate was prepared by bead milling as described in Section 2.2.1 (bead mill feed rate 5 l h^{-1}, 30% biomass ww/v, pH 5.0). A fraction of the disruptate was adjusted to pH 6.0 by addition of a small volume of NaOH. The following samples were prepared using disruptate both at pH 5.0 and pH 6.0 (buffer A at the respective pH): (i) blank, disruptate + buffer A (600 µl + 600 µl), (ii) disruptate + buffer A containing 2 M NaCl (600 µl + 600 µl), (iii) disruptate + buffer A containing 500 U ml^{-1} of purified L-asparaginase (850 U mg^{-1}), 600 µl + 600 µl, total addition of enzyme activity: 250 U/ml.

After incubation for 30 minutes on a roller mixer, the samples were clarified by centrifugation (7600g, 10 min) and the supernatant was assayed for L-asparaginase activity.

b) Samples from *Erwinia* disruptates (30 % ww/v, pH 5.5), generated at different bead mill feed rates, were mixed at equal volumes with buffer A containing 2 M NaCl and borate buffer (100 mM di-sodium tetraborate, pH 8.5), respectively. The latter shifted the pH of the sample towards basic conditions which facilitated the desorption of L-asparaginase from cell debris. After 30 min of incubation time the samples were clarified by centrifugation (7600g, 10 min) and the supernatant was assayed for L-asparaginase activity. The amount of desorbed

enzyme was quantified by the increase in enzyme activity in comparison with the blank (1:2 dilution in buffer A).

2.3 Results and discussion

2.3.1 Residence time distribution as a function of the feed rate

Due to the varied back mixing of feedstock within the grinding chamber there is no linear relationship between the feed rate and the mean residence time (MRT) of a fluid element introduced with the feedstock (Kula and Schütte, 1987). Residence time distribution measurements were performed in order to characterise different feed rates with regard to residence time in the milling chamber. The technique applied is generally used for the measurement of plate numbers in chromatography columns (see Section 2.2.1 and Figure 3.2, also described by Barnfield-Frej *et al.* (1997). Results of these measurements are depicted in Figure 2.3. It can be seen in the graph that both curves follow a similar trend and two distinct regions can be identified. At feed rates above 8 l h^{-1}, the change in MRT and the spread of the distribution (2σ) with feed rate was much reduced in comparison to lower feed rates. As a result, the MRT at low feed rates increased as a composite function of flow rate and increased back mixing as indicated by the steep increase in the spread. Relatively low values for the spread at higher feed rates (> 10 l h^{-1}) indicated reduced back mixing and an approach to plug flow behaviour. This confirmed the results of Kula and Schütte, (1987) who found that back mixing was reduced with increasing feed rates and therefore a tighter MRT distribution was generated. Results presented in Figure 2.3 were also in good agreement with Agerkvist and Enfors (1990) who reported similar MRTs obtained in a Dyno Mill KDL for feed rates between 4.5 and 9.0 l h^{-1}.

Figure 2.3. Mean residence time of a unit volume in the disruption chamber as a function of the feed rate.

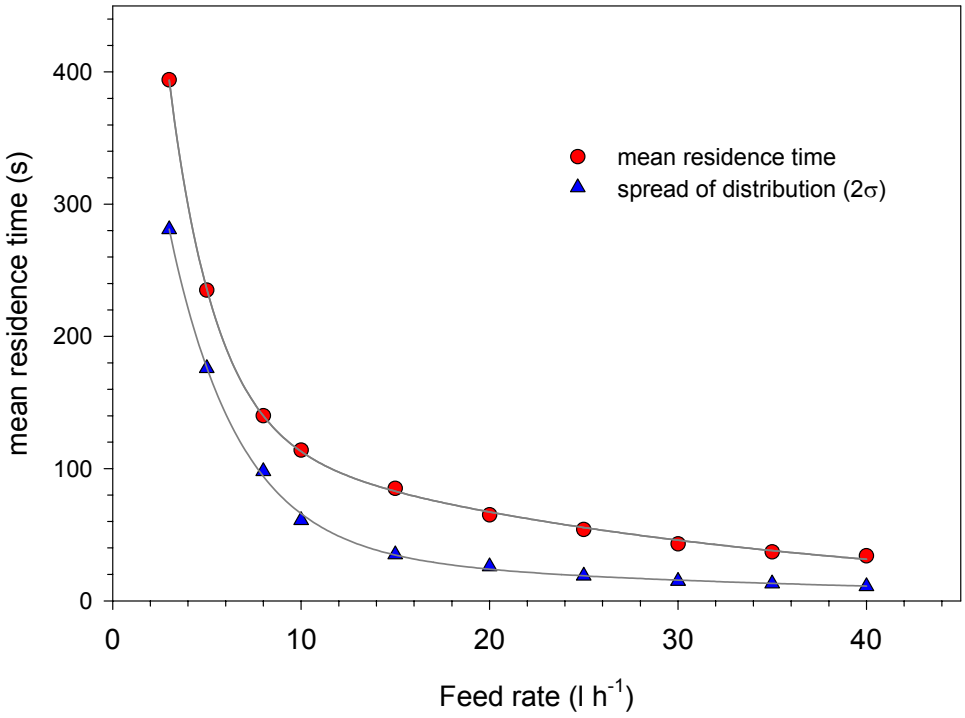

Dyno mill KDL, agitator speed 3200 rpm (tip speed 10.5 m s^{-1}), zirconia beads (0.3 mm), bead load 83%). An acetone solution in water (1% v/v) was used as a tracer. UV absorbance was measured at the outlet of the mill and interpreted in terms of concentration of the tracer. The mean residence was calculated as the time interval in which the tracer concentration decreases from 100% to 50%. The spread of the distribution is equivalent to the time interval in which the signal decreased from 84.15% to 15.85% (see Section 2.2.2 and Figure 3.2).

2.3.2 Re-circulation and single pass experiments

Scouting experimentation for the establishment of optimal milling conditions in single pass operation requires large quantities of experimental material (i.e. biomass suspension). It was therefore decided to employ re-circulation procedures for such experiments with *Erwinia chrysanthemi* to conserve precious stocks of cell paste. It was assumed that a combination of MRT data and that from the disruption of re-circulated feedstocks would indicate the range of flow rates best suited for single pass disruption of *Erwinia*. A cell suspension was prepared as described in Section 2.2.1 and re-circulated from a well mixed reservoir (500 ml) at a feed rate of 25 l h^{-1}. Samples were taken at intervals to monitor total protein concentration and L-asparaginase activity. The degree of cell disruption was assumed to be directly correlated to protein release and L-asparaginase activity in the processed suspension and the results of this experiments are depicted in Figure 2.4. The curve for total protein reached a plateau after about 4 min of re-circulation which indicted that the total achievable disruption of the cells was established. However, the data was less clear for the release of L-asparaginase which indicated a maximum value after 3 minutes which thereafter decreased continuously. Using the data depicted in Figures 2.3 and 2.4 a feed rate was estimated which was expected to yield a maximum enzyme release in single pass operation. With the given flow rate of 25 l h^{-1} (416 ml min^{-1}) a time of 1.2 minutes was required for one discrete pass of the feedstock volume (500 ml) through the disruption chamber (here, mixing in the reservoir was neglected and plug flow assumed). The maximum enzyme release was achieved after 3 min of re-circulation (see Figure 2.3). Such a period of re-circulation was judged equivalent to 2.5 discrete passes of the reservoir content through the disruption chamber at 25 l h^{-1}. For this feed rate, Figure 2.3 indicated a mean residence time within the disruption chamber of 54 s. After 2.5 passes the total residence time of the feedstock within the mill was thus 135 s which was expected to

Figure 2.4. Re-circulation of *Erwinia* cell suspension through the bead mill.

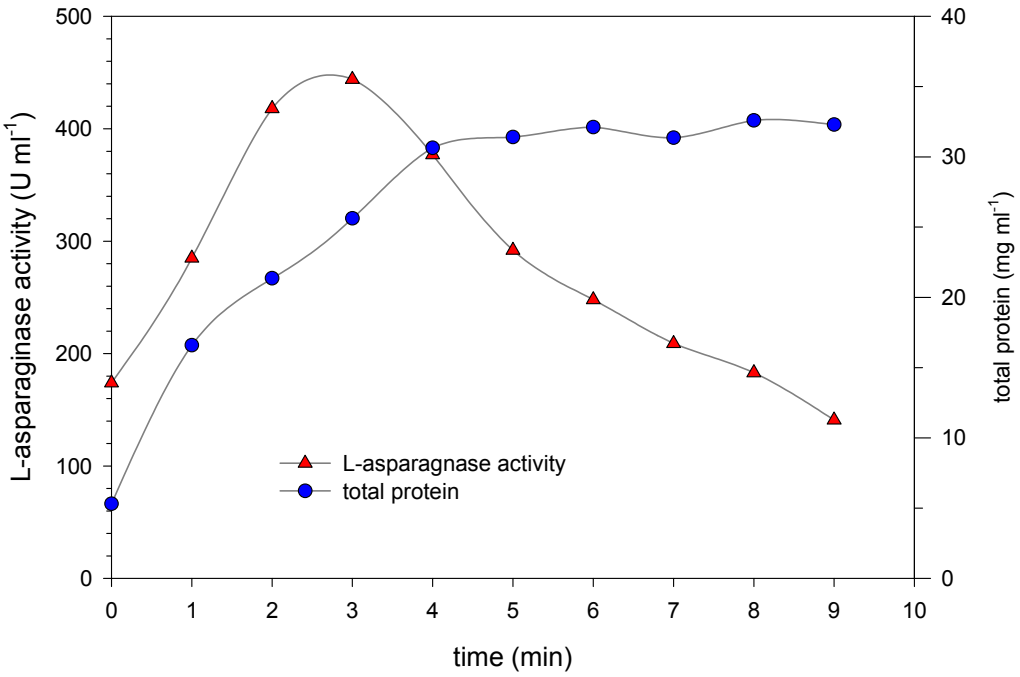

An Erwinia cell suspension (30% ww/v) was re-circulated from a reservoir (500 ml) through the bead mill operated at an agitator speed of 3200 rpm (tip speed 10.5 m s^{-1}) and a feed rate of 25 l h^{-1}. At given time intervals, samples were taken from the reservoir and subsequently assayed for total protein and L-asparaginase activity.

be equivalent to the mean residence time measured at a feed rate of 8 l h^{-1} (see Figure 2.3).

In order to verify this estimated optimum feed rate, single pass experiments were performed. Here, a cell suspension was prepared as described in Section 2.2.1 and passed through the mill at various feed rates covering the established optimum range (approximately 8 l h^{-1}). Figure 2.5 depicts the results obtained for two different batches of cell paste (obtained from different fermentations) and Table 2.3 summarises the maximum release of L-asparaginase in a side-by-side comparison with disruption of the respective *Erwinia* batches by alkaline lysis (see Section 2.2.3). Maximum enzyme release by bead milling was achieved at feed rates of 8 l h^{-1} (batch 1) and 10 l h^{-1} (batch 2), respectively. These results were in good agreement with the optimum feed rate estimated from re-circulation and MRT data (see Figure 2.3 and Figure 2.4).

Table 2.3. Comparison of L-asparaginase release from *Erwinia chrysanthemi* by bead milling and alkaline lysis.

Batch of cell paste	Bead mill			Alkaline lysis		
	Release[(1)] MU kg^{-1}	Protein mg ml^{-1}	Specific activity U mg^{-1}	Release[(1)] MU kg^{-1}	Protein mg ml^{-1}	Specific activity U mg^{-1}
1	3.4	5.5	96	4.5	4.3	158
2	3.8	5.4	105	4.6	4.0	174

[(1)] Release at optimum feed rate, batch 1: 8 l h^{-1}, batch 2: 10 l h^{-1} (see Figure 2.5)

The enzyme release by bead milling for Batch 1 and Batch 2 corresponded to 75% and 83% of the release achieved by alkaline lysis whereas the concentration of total protein released by bead milling was higher (Table 2.3). This might be explained by the precipitation of proteins during alkaline lysis which resulted in a lower total protein content of the lysate. A lower release of enzyme by bead milling in comparison with the alkaline lysis might be attributed to a combination of factors such as (i) incomplete disruption in the mill due to back

Figure 2.5. Single pass disruption of *Erwinia chrysanthemi*

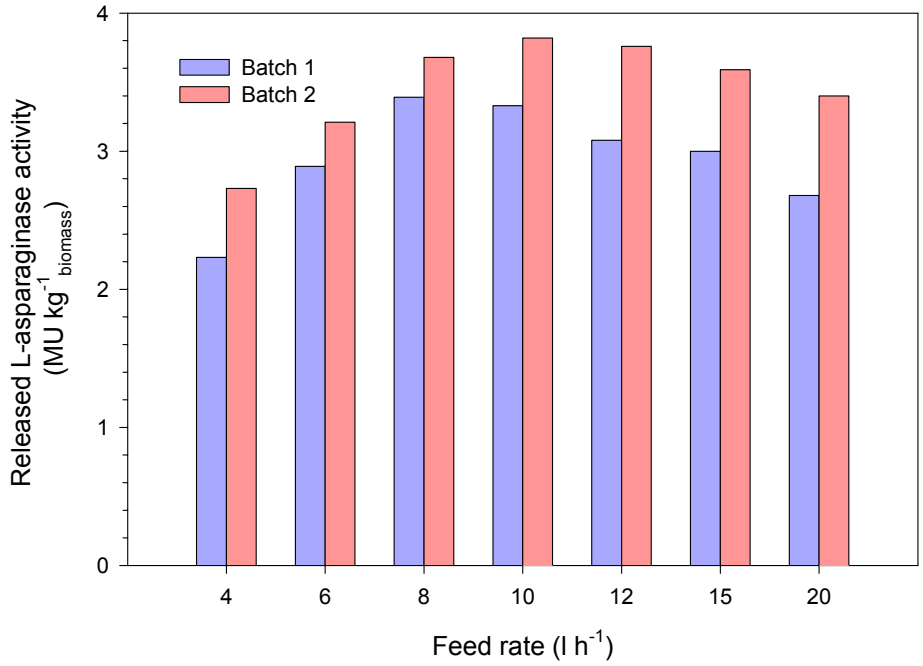

Release of L-asparaginase as a function of the bead mill feed rate for two batches of Erwinia chrysanthemi. Frozen cell paste was thawed and resuspended in buffer A (15% biomass ww/v) and exposed to bead milling at various feed rates. The initial enzyme activity of the cell suspension was 1.9 MU kg^{-1} for Batch 1 and 2.1 MU kg^{-1} for Batch 2 (batches of cell paste came from different fermentations).

mixing in the chamber, (ii) shear damage of the enzyme, or (ii) adsorption of the enzyme to grinding beads and/or oppositely charged cell debris or (see Section 2.3.3).

However, the disruption efficiency achieved here is in good agreement with results reported by Agerkvist and Enfors (1990) for the disruption of *E. coli* which is similar to *Erwinia* with regard to size and wall structure. In that study, a release of 72% of total protein and 74% of the cytoplasmic enzyme β-galactosidase was achieved in a single pass operation exploiting an equivalent Dyno Mill model (0.6 l chamber, 6 l h^{-1}, 80 % glass beads, 4500 rpm, results expressed relative to the release attained by 10 passes through a microfluidiser). In general, *Erwinia* cell suspensions were characterised by a relatively high initial L-asparaginase activity (before cell disruption, batch 1: 1.9 MU kg^{-1}, batch 2: 2.1 MU kg^{-1}). This observation appeared to be common in the processing of frozen cell paste and has been reported previously (Agerkvist and Enfors, 1990; Johnson and Hecht, 1994). For example Milburn and Dunnill, (1994) reported the leaching of the intracellular enzyme alcohol dehydrogenase (ADH) from freeze/thaw damaged *Saccharomyces cerevisiae* cells which appeared intact by light microscopy inspection. However, virus-like particles, expressed in the recombinant cells were retained which was attributed to their comparatively large size (> 20 nm).

As can be seen from Figure 2.5, higher feed rates than 10 l h^{-1} resulted in a decrease in released enzyme activity which suggested incomplete disruption. However, feed rates less than 8 l h^{-1} were also characterised by a decrease in measurable enzyme activity. Here, MRTs were longer than required for optimum enzyme release and therefore, this effect is comparable to the decline of enzyme activity depicted in Figure 2.4 at re-circulation times greater than 3 min. This phenomenon could be variously explained by (i) adsorption of L-asparaginase to cell debris and/or the grinding beads or (ii) enzyme inactivation due to

susceptibility to shear forces. Such effects are discussed in the following Section 2.3.3. The temperature of the disruptate routinely did not exceed 25 °C during the milling processes. Previous experiments did not indicate a loss of enzyme activity in samples stored at room temperature (20 – 22°C) over this period of time and thus, it was judged likely that damage due to temperature-induced stresses could be excluded.

2.3.3 Loss of L-asparaginase activity during bead milling

2.3.3.1 Susceptibility of L-asparaginase to shear forces

In order to investigate the possibility that the loss of L-asparaginase activity during the milling experiments mentioned above might be caused by susceptibility of the enzyme to shear forces, a solution of purified enzyme in buffer was exposed to similar experimental conditions to those used during previous experiments (see Section 2.2.6). Due to the absence of cell material in the system, adsorptive losses to cell debris could be excluded. Here, glass beads (diameter 0.2-0.5 mm) were used instead of zirconia beads because this experiment was performed in a Dyno Mill type fitted with a glass chamber which was not designed for the use with the zirconia material. Due to limited material availability, a packing of only 400 ml of glass beads was employed. The settled volume occupied 67% of the chamber compared with 83% in the re-circulation and single pass experiments. The use of a lower bead loading reduced the number of bead collisions and would therefore result in a lower efficiency of disintegration (Kula and Schütte, 1987). However, this difference was not judged critical with respect to the general purpose of this experiment (shear sensitivity of enzyme products). Results of this experiment are depicted in Figure 2.6. Enzyme activity exhibited a considerable loss of about 90% within one minute of initiating the treatment. Thereafter, the activity was judged to remain at a constant level. The protein concentration declined

Figure 2.6. Purified L-asparaginase exposed to milling conditions.

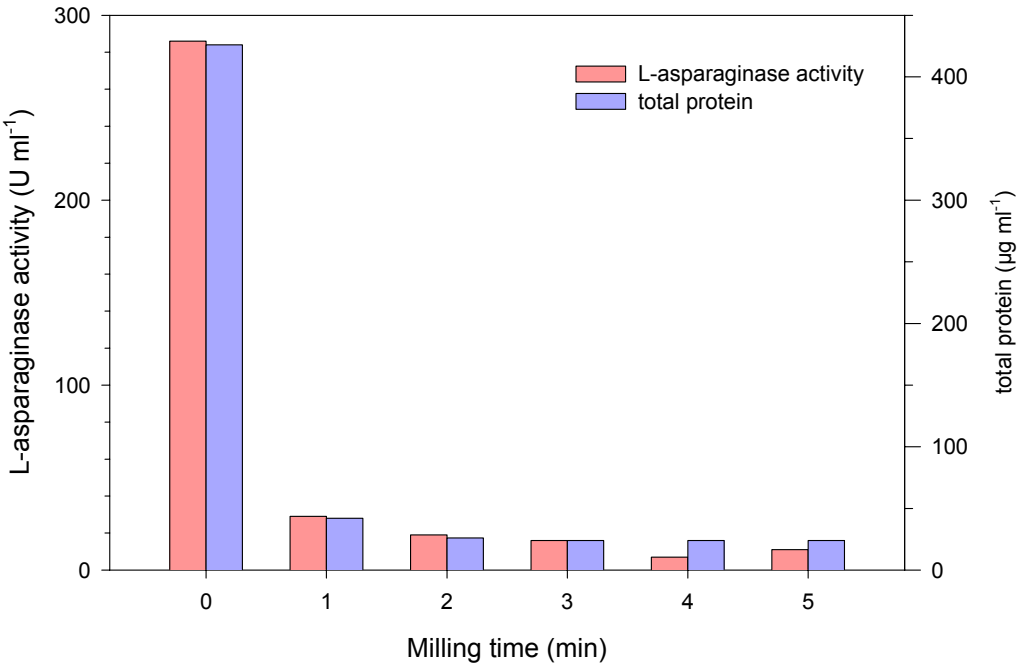

Purified L-asparaginase (300 U ml^{-1}, in buffer A, pH 5.0) was exposed batch-wise to conditions similar to those during the milling experiments (glass beads, bead occupancy 67%, settled volume 400 ml, agitator speed: 3200 rpm, see Section 2.2.1). Samples were taken after each milling interval of 1 minute and assayed for protein concentration and L-asparaginase activity. Between each milling interval the chamber was allowed to cool. The temperature of the solution did not exceed 25°C.

proportionally to the enzyme activity which suggested that protein was sequestered out of solution, presumably due to adsorption to the glass grinding beads. From the data depicted in Figure 2.6 an effective binding capacity of 0.29 mg of L-asparaginase per ml of settled volume of glass beads could be calculated. However, it could not be excluded from such experimental data that enzyme was partially inactivated by shear forces.

2.3.3.2 Adsorption of L-asparaginase to grinding beads

To analyse the adsorption characteristics of the glass and zirconia grinding beads, a batch binding experiment was performed (see Section 2.2.7). The time course of the experiment for glass beads is depicted as an example in Figure 2.7 and binding capacities of the grinding beads are summarised in Table 2.4.

Table 2.4. Binding capacities of grinding beads for various proteins

Capacity (mg ml^{-1})	L-asparaginase	BSA	Lysozyme
Glass beads	0.27	0.16	0.24
Zirconia beads	0.46	0.35	0.04

Glass and zirconia grinding beads were incubated with various protein solutions to study their adsorption characteristics. Protein adsorption was estimated by a mass balance for a 20 min incubation time.

The respective proteins used in the experiment were purified L-asparaginase (pI = 8.6), BSA (pI = 4.8) and lysozyme (pI = 10.5) chosen on the basis of different isoelectric points. However, with regard to their pI, a simple cation exchange mechanism for the observed adsorption is not evident from the results. The two basic proteins, L-asparaginase and lysozyme, exhibit quite disparate capacities on zirconia whereas on glass they are very similar. The binding capacity of glass for L-asparaginase in this experiment (0.27 mg ml^{-1}) approximates the value of 0.29 mg ml^{-1} estimated in Section 2.3.3.1. From the time course of

Figure 2.7. Protein adsorption to glass beads.

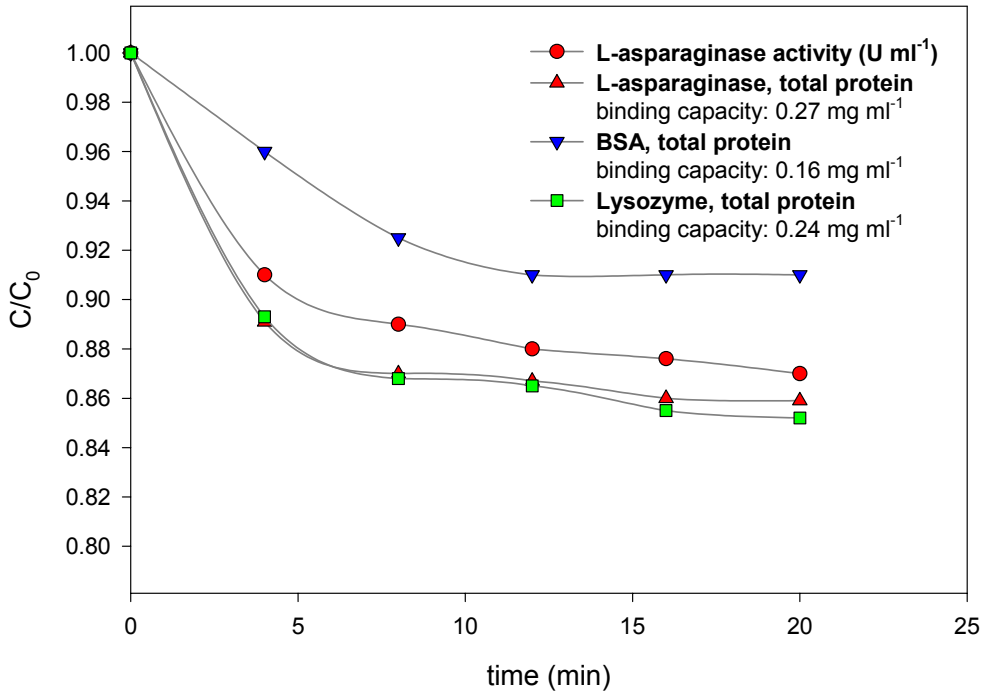

2 ml of glass beads (A) and zirconia beads (B) were incubated for 20 minutes with solutions of purified L-asparaginase, BSA and lysozyme (1 mg ml^{-1}). Binding was investigated by difference analysis and expressed as mg protein per ml of beads (20 min incubation time).

the experiment for glass beads (depicted in Figure 2.6) it is apparent that the decline in L-asparaginase activity is proportional to the measured total protein values. Both observations imply that the enzyme loss discussed in Section 2.3.3.1 should largely be attributed to product adsorption to the grinding beads. However, it would be expected that the grinding beads would be rapidly saturated in an extended cell disruption process and that such interactions are thus negligible

2.3.3.3 Adsorption of L-asparaginase to cell debris

To examine adsorptive interactions between L-asparaginase and the cell debris generated by bead milling, batch binding experiments were performed in which cell debris (in a disruptate) was evaluated in a fashion analogous to the performance of an ion exchange matrix (see Section 2.2.8, a). The aim was to establish whether debris-bound L-asparaginase could be desorbed/eluted by an elevated salt concentration. A second objective was to investigate whether the addition of a defined amount of pure L-asparaginase to cell debris was reflected in a decrease in activity of the sample which would be indicative of adsorption. As can be seen from Figure 2.8, a similar disruptate sample showed a significantly higher enzyme activity in the blank at pH 6.0 as compared to pH 5.0. This indicated that a fraction of the available L-asparaginase (pI = 8.6) in the disruptate was adsorbed to the cell debris and further, that such adsorptive interactions decreased with increasing pH. In addition, the sample containing 1 M NaCl at pH 5.0 exhibited a higher activity than its corresponding blank (disruptate in buffer A), which demonstrated that debris bound enzyme could be desorbed by the elevated salt concentration. The same observation could not be found at pH 6.0. Here, both the blank and the sample containing 1 M NaCl exhibited corresponding enzyme activities which, however, matched the elevated activity of the sample at pH 5.0

Figure 2.8. Adsorptive interactions of L-asparaginase with cell debris in *Erwinia* disruptates.

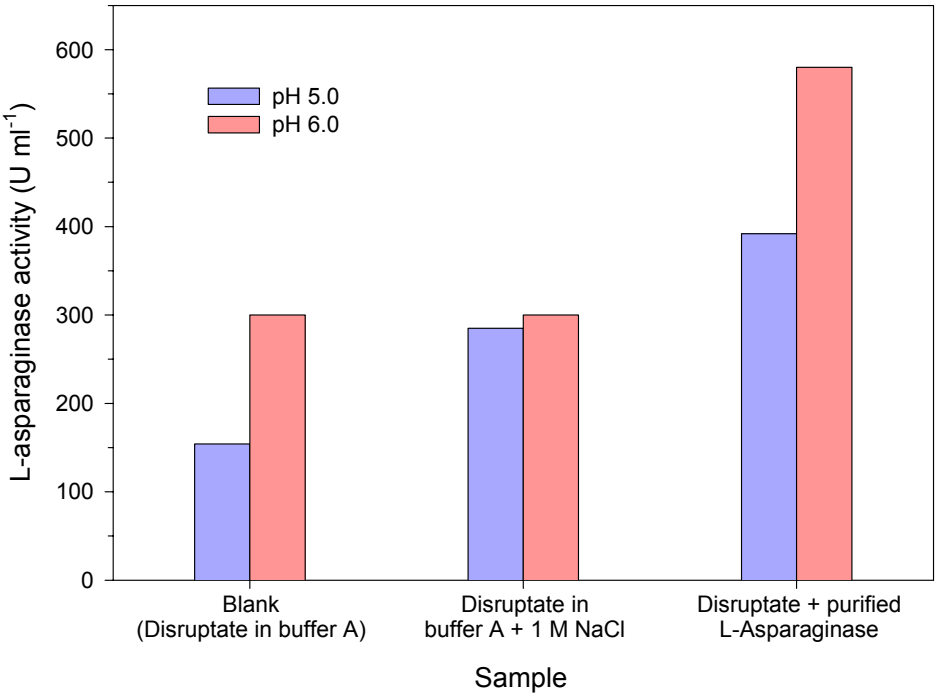

Erwinia disruptate from a milling experiment (containing debris) was mixed at equal volumes with (i) buffer A (blank), (ii) buffer A containing 2 M NaCl, and (iii) buffer A containing a charge of purified L-asparaginase (total addition 250 U ml^{-1} L-asparaginase), see Section 2.2.8. After incubation for 30 min the samples were clarified by centrifugation and assayed for asparaginase activity.

containing 1 M NaCl. This suggested that enzyme/debris interactions at pH 6.0 were minimal and that desorption of debris bound enzyme could also be achieved by shifting the pH towards the pI of L-asparaginase. At both pH values, the experimental addition of L-asparaginase at 250 U ml^{-1} could be fully accounted for in system supernatants indicating that no additional enzyme was adsorbed by the debris. This would imply that debris was already saturated with enzyme under the circumstance of the experiment.

Figure 2.9 depicts the influence of the bead mill feed rate, i.e. the mean residence time within the grinding chamber, upon the adsorption of L-asparaginase on cell debris. Here, disruptates generated at different feed rates were exposed to an elevated salt concentration (1 M NaCl) and a pH shift (from 5.5 to 8.2) in order to stimulate the desorption of debris bound enzyme (see Section 2.2.8, b). The chart (Figure 2.9) illustrates the increase in enzyme activity following this treatment compared with the blank (disruptate diluted with buffer A). Under the given milling conditions (see Section 2.2.1), the amount of L-asparaginase which could be desorbed from cell debris increased considerably with decreasing feed rates. This suggested that the comminution of cell fragments, a process enhanced at lower feed rates (i.e. prolonged MRT in the grinding chamber), resulted in increased adsorption of L-asparaginase presumably due to the increase in specific surface area available for interaction. In addition, the pH shift which approached values close to the pI of L-asparaginase desorbed considerably more enzyme than the elevated salt concentration. It should be noted that the fraction of debris bound L-asparaginase, when compared to the total available enzyme activity (enzyme activity in the clarified supernatant plus debris bound enzyme), could be as high as 25%. For example compare Figure 2.9: L-asparaginase released by pH shift at 4 l h^{-1}: 1.3 MU kg^{-1} with Figure 2.5, batch 2: maximum release of L-asparaginase by bead milling 3.8 MU kg^{-1}.

Figure 2.9. Desorption of L-asparaginase from cell debris in disruptates generated at different feed rates.

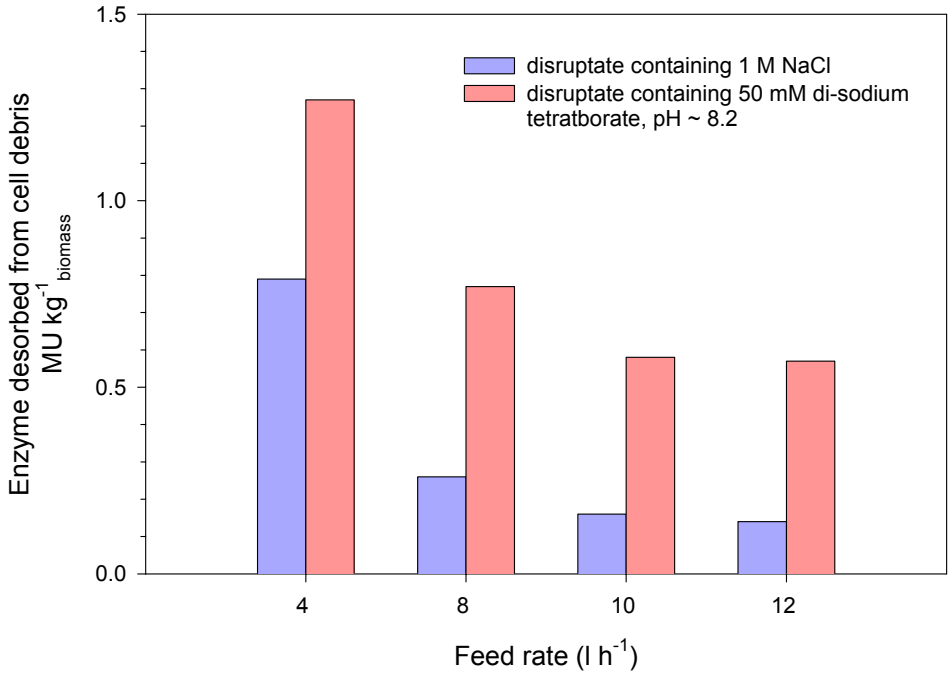

Disruptates generated at different feed rates (see Section 2.2.1) were mixed at equal volumes with 2 M NaCl in buffer A and 100 mM borate buffer (di-sodium tetraborate, pH 8.5). Desorption of L-asparaginase was calculated by the increase of enzyme activity against the blank (1:2 dilution with buffer A).

2.4 Interim conclusions

It was demonstrated that *Erwinia chrysanthemi* can be efficiently disrupted by bead milling in a single-pass operation for the effective release of the enzyme L-asparaginase. Here, the feedstock conditions for cell disruption, i.e. pH and ionic strength, were chosen with the aim of producing a disruptate suitable for immediate processing by cation exchange chromatography in fluidised bed contactors operated immediately downstream and in the same time frame. However, under these conditions optimisation of the bead mill feed rate, i.e. the mean residence time within the milling chamber, was crucial in order to achieve a high disruption efficiency whilst minimising adsorptive losses of the enzyme to cell debris. The losses of enzyme activity recorded in re-circulation and single pass experiments appeared to result from a combination of different causes. Batch adsorption studies using glass and zirconia grinding beads yielded a measurable adsorptive capacity of the beads for purified L-asparaginase. Such interactions, however, were expected to become secondary when a complex mixture of biological molecules, such as a bacterial disruptate, was processed. Clearly the interactions of L-asparaginase with cell debris were predominant and of an electrostatic nature since they are a function of the pH and the salt concentration of the disruptate.

Despite the higher specific activity in the alkaline disruptate (see Table 2.3), some general process advantages recommend bead milling as the method for disrupting *Erwinia* rather than alkaline lysis. During the latter, the viscosity of the broth increases considerably when the pH is adjusted to alkaline conditions. Therefore, the biomass load at lysis is limited in order to ensure homogenous mixing and to avoid the risks of extreme local pH values. The neutralised disruptate is also characterised by a comparatively high ionic strength which will commonly require further dilution if ion exchange chromatography is planned as a subsequent

step (Goward *et al.*, 1989; Goward *et al.*, 1992). In addition, chemical lysis is performed batch-wise which ultimately results in extended hold-up periods, in particular at larger scales of operation, while processing the disruptate. Such hold-up risks time-dependent product modification, inactivation or degradation by system antagonists (Goward *et al.*, 1992; Lee *et al.*, 1989). A single-pass disruption, however, as achieved by bead milling, would offer the advantage to integrate the cell disruption with an immediate product capture step (refer to Figure 1.5). Thus, the product is initially retained in the intact cell where it is less susceptible to an antagonistic attack and then removed immediately upon cell disruption from the potentially hostile environment of the disruptate. Such an approach is described and evaluated in Chapter 4.

It was demonstrated by Agerkvist and Enfors (1990) for the disruption of *E. coli* cells that multiple passes (2-3) were necessary in high-pressure homogenisation (Manton Gaulin 15M-8TA at 60 MPa) in order to achieve equivalent disruption efficiencies to those obtained by bead milling in single-pass operation. In addition, the mean particle size of debris generated by high-pressure homogenisation was considerably smaller in comparison with the bead mill disruption. Thus, it might be predicted that, under the given feedstock conditions (see Section 2.2.1), disruption of *Erwinia* in a HPH would result in increased enzyme-debris interactions due to the increased debris surface area (see Section 2.3.3.3). Single-pass disruption of brewers' yeast in a high-pressure system has been reported by Rito-Palomares and Lyddiatt (1996). In their studies, a CSL Z-series homogeniser (Constant Systems Ltd, Warwick), operated at 207 MPa and 54 l h^{-1}, achieved disruption efficiencies which were equivalent to those accomplished by a single pass from a Dyno Mill KDL (0.6 l chamber volume, 15 l h^{-1}, 3200 rpm, glass beads 0.2 – 0.5 mm) or four discrete passes from a APV-Gaulin type homogeniser (15M-8BA, operated at 55 MPa). However, the operating pressure

had to be considerably higher than those commonly employed in HPH (30 – 70 MPa) in order maximise the degree of disruption. As a consequence, it might be expected that the size range of debris, generated under such operating conditions, would be further reduced which again would promote product-debris interactions.

3 FLUIDISED BED ADSORPTION OF L-ASPARAGINASE FROM ERWINIA DISRUPTATES – METHOD DEVELOPMENT

3.1 Introduction – Analysis of operating parameters

Adsorption in stable fluidised beds was originally carried out exploiting adsorbent solid phases which had been developed as conventional packed bed materials. The influence of mass transport (Chase and Draeger, 1992a), axial mixing (Draeger and Chase, 1990), and the influence of biomass on equilibrium and breakthrough (Draeger and Chase, 1991) for model proteins on Sepharose were investigated in studies where stable fluidisation was achieved. However, because of the physical properties of the exploited material, bed expansion was limited to inconveniently low linear flow velocities (10 – 30 cm h^{-1}) resulting in low overall productivities. Based on these studies, Chase and Draeger (1992a) formulated idealised criteria which should be met by fluidised bed adsorbents. Thus:

- size and density of the matrix should result in a significant difference in the terminal settling velocity of adsorbent particles and biomass in the feedstock.
- a distribution of particle size and density should allow for the development of a classified fluidised bed exhibiting reduced axial mixing in the solid and liquid phases.
- mass transport capability of the adsorbent should be sufficient for use in a fluidised bed.
- the adsorbent should be resistant to fouling by biomass, nucleic acids, and lipids contained in the feedstock.

Various articles published in recent years have been concerned with the investigation of operating parameters which influence particle fluidisation as well as adsorption performance.

Common analytical studies included physical characterisation of adsorbents, batch binding experiments and frontal analysis. Physical characterisation includes the investigation of the bed expansion behaviour as a function of fluidisation velocity and residence time distribution (RTD) analysis in order to assess the degree of axial dispersion in a fluidised bed. Batch binding experiments are commonly employed to assess equilibrium adsorption capacities and rates of adsorption/desorption. Frontal analysis investigates protein breakthrough at varying linear flow velocities and is a standard experiment to elucidate the limitation of protein adsorption by residence time (discussed in Thömmes, 1997).

Some key publications have been selected and will be discussed here, since the presented work therein covers a wide variety of issues in connection with the method development of fluidised bed processes. The main parameters which have been identified as governing a fluidised bed process were the settled bed height of the adsorbent (SBH), the superficial flow velocity (u), axial dispersion, fluid viscosity, and particle/biomass content of the feedstock.

Hjorth *et al.* (1995) investigated the influence of matrix volume, i.e. SBH, and the superficial flow velocity upon the breakthrough capacity of fluidised ion exchangers (STREAMLINE). Increasing the flow velocity was shown to reduce the dynamic capacity of a given bed of adsorbent. This effect was more pronounced during the adsorption of bovine serum albumin (BSA) on STREAMLINE DEAE when compared with lysozyme adsorption on STREAMLINE SP which was attributed to the difference in molecular weight and hence diffusivity between the two proteins. In addition, it was demonstrated that a minimum settled bed height was required in order to achieve a high adsorption efficiency. This behaviour was attributed to the existence of flow irregularities at the column inlet which can be overcome above a certain bed height. These findings were in accordance with Bascoul *et al.* (1988) who

investigated bed stability as a function of the distributor design. It was shown that channelling in the lower part of a fluidised bed due to uneven flow distribution was reduced with increasing expanded bed height.

Chase and Draeger (1992b) reported a negative influence of cells on the binding of BSA to a fluidised anion exchanger. It was shown that the presence of yeast cells reduced the equilibrium binding capacity, and this was attributed to the binding of cells to the outer adsorbent surface and subsequent blocking of the matrix pores. Cation exchanger adsorbents, however, were less affected by the presence of yeast cells. Cell/adsorbent interactions were also observed by Erickson *et al.* (1994) who described association of mammalian cells to a protein A coated controlled pore glass adsorbent during the capture of antibodies from CHO cell culture broth. These interactions led to the formation of aggregates between cells and the adsorbent and reduced the efficiency of the overall process. A systematic study of cell/adsorbent interactions was presented by Feuser *et al.* (1999) who used a pulse response technique to quantify the adsorption of various cell types (yeast, Gram positive and negative bacteria, mammalian cells and yeast homogenate) to a range of commercially available matrices (STREAMLINE). Cells and cell debris were found to interact with the ligands of agarose based resins mainly by electrostatic forces. In agreement with the finding of Chase and Draeger (1992b) anion exchangers showed the most severe interactions, whilst cation exchange and affinity adsorbents appeared to be less affected.

Barnfield-Frej *et al.* (1994) investigated the influence of *E. coli* homogenate concentration in the feed during the adsorption of recombinant annexin V to STREAMLINE DEAE. It was found that under the given conditions, i.e. adsorbent density and flow rate, increased feedstock viscosity promoted by biomass concentrations greater than 7 – 8% dry weight caused particle elutriation ($H/H_0 > 5$). In addition, the formation of flow channels in

the bed was observed at biomass concentrations greater than 8% dry weight. This clearly suggested that the particle density of the commercially available STREAMLINE adsorbents needs further improvement to facilitate higher throughput of biomass.

Thömmes *et al.* (1995a) examined axial dispersion by RTD analysis in fluidised beds as a function of flow velocity and fluidised bed height to diameter ratio (H/d). Axial dispersion was quantified by the dimensionless Bodenstein number (Bo) which is a measure of the overall axial dispersion in a given experimental setup. These results were correlated for two representative adsorption systems (SP derivatised adsorbent for the capture of monoclonal antibodies from hybridoma supernatant and BSA from a buffer solution) operated under conditions similar to those of the RTD experiments. It was found that axial mixing was decreased, reflected by an increase in Bo, both by an increase in H/d and by an increase in linear velocity (u). Subsequent adsorption experiments confirmed the trend observed during RTD measurements, i.e. an increased dynamic capacity at increased H/d ratios. Varying the linear velocity at a constant H/d ratio resulted in a broad range of u where capacity was only slightly affected. This was attributed to the diffusion characteristic of the protein in the pores of the adsorbent. A packed bed experiment was performed in order to isolate the effect of pore diffusion from the effect of dispersion. This resulted in a clear reduction of the dynamic capacity at an intermediate linear velocity. Consequently, a shift from dispersion-controlled to diffusion-controlled adsorption was proposed.

Chang and Chase (1996b) measured the influence of feedstock viscosity and flow velocity, or bed expansion respectively, on the adsorption efficiency of a model system (lysozyme binding to STREAMLINE SP). Here, viscous feedstocks were simulated by the inclusion of glycerol in the adsorption buffers. Increased viscosity resulted in an increased mass transfer resistance. Due to reduced diffusivities, the protein uptake in batch binding

experiments was slower and dynamic capacities, assessed by frontal analysis, were reduced. RTD analysis exhibited increased axial dispersion, reflected by a reduced number of theoretical plates (N), both at increased feedstock viscosities and increased flow velocities. A comparison of different operating regimes, i.e. adsorption at a constant linear velocity or at a constant bed expansion, revealed a clear difference in the achieved dynamic capacities. However, when the processing time for the entire purification cycle, i.e. equilibration, loading, washing, and CIP, was taken into account the relative productivities (defined as the amount of adsorbed protein divided by the adsorbent volume and the total processing time) were found to be almost the same when employing different operating modes with identical process feedstocks. Here, in the calculation of the productivity, the reduction in dynamic capacities, found at higher flow velocities, was compensated by shorter processing times and thus yielded similar values. However, such findings are expected to be system specific and vary with the properties of the target molecule, such as (e.g. diffusivity) and the adsorbent solid phase (e.g. rate of adsorption).

Karau *et al.* (1997) investigated the influence of the adsorbent particle size and operating conditions on the adsorption performance. Here, the commercially available matrix STREAMLINE (120 – 300 μm) was fractionated by wet sieving and two fractions with a narrower size range (120 – 160 μm and 250 – 300 μm) were generated. RTD analysis revealed that dispersion in the liquid phase was minimal when the unfractionated material, i.e. with a wide size distribution was fluidised. Both, the smaller and the larger fraction exhibited a higher degree of dispersion, reflected by lower Bodenstein numbers. Frontal analysis using BSA as a model protein resulted in a enhanced dynamic capacity for the smaller fraction which was attributed to shorter diffusion paths within the matrix.

The results reported in the literature reviewed above may thus be summarised as follows.

- Axial dispersion in a fluidised bed is reduced at increasing ratios of H/d and by a wide size distribution of the adsorbent particles. However, no common trend is identified in the influence of the flow velocity on axial dispersion. Various experiments exploiting different adsorbents and contactors yielded inconsistent results.
- Dynamic capacity is enhanced at higher H/d ratios due to the dampening of flow irregularities in longer beds. Higher dynamic capacities are also achieved when the mean particle diameter of a specific adsorbent was reduced owing to shorter diffusion paths within the particles and an increased specific surface area.
- Increased viscosity reduced dynamic capacities at given flow velocities due to the reduced diffusivities of the target proteins whilst equilibrium capacities are unaffected. In addition, it is observed that high feedstock viscosities may cause channelling and destabilisation of fluidised beds.
- Cell/adsorbent interactions may reduce static capacity of adsorbents and can impair bed stability by promoting aggregate formation. As a consequence, harsh regeneration conditions may be required in order to release tightly bound cellular material.

In essence, the publications summarised here, confirmed the requirements of adsorbents formulated by Chase and Draeger (1992a), i.e. the need for increased specific weight and enhanced mass transport capabilities of the adsorbent. In addition, it is evident that a systematic development of a fluidised bed process for the purification of a specific target protein must meet a number of specific criteria. An adsorbent has to be selected which achieves stable fluidisation at a reasonable flow velocity for a given feedstock viscosity. Suitable ligand chemistry should facilitate efficient capture of the target molecule and

minimise cell/debris-adsorbent interactions which may reduce the adsorbent capacity or diminish bed stability. The adsorption process needs to be characterised by batch binding and frontal analysis since equilibrium and dynamic capacity for the target molecule will be influenced by both the product properties (molecular weight, surface charge, hydrophobicity) and feedstock properties such as viscosity, pH, ionic strength and the presence of contaminants.

This chapter summarises the establishment of operating conditions for the initial fractionation of L-asparaginase from unclarified *Erwinia* disruptates by fluidised bed adsorption. Fluidisation characteristics, i.e. bed expansion and axial dispersion of candidate adsorbents were investigated (see Section 3.3.1). Two adsorbents, CM HyperD LS and SP UpFront, were selected for fluidised bed experimentation. A suitable pH for the efficient adsorption of L-asparaginase from *Erwinia* disruptates was established (see Section 3.3.2). Batch adsorption studies were employed in order to investigate and address comparative aspects of adsorption kinetics of the pellicular prototype SP UpFront and the macroporous CM HyperD LS (see Section 3.3.3). Scouting experiments were performed in small-scale, packed and fluidised beds (see Section 3.3.4). Section 3.3.5 summarises experiments which investigated the effect of superficial flow velocity and settled bed height on the dynamic capacity of the adsorbents.

3.2 Materials and Methods

3.2.1 Fluidised bed contactors

Three different contactors were used in the experiments described here. A commercially available contactor (UpFront Chromatography) and two custom-built contactors (referred to as BRG contactors, Biochemical Recovery Group, School of Chemical Engineering,

University of Birmingham) were employed. A schematic depiction of the contactors is given in Figure 3.1. The UpFront contactor (1 cm i.d.) distributed the feed by a magnetic stirrer located directly above the feedstock inlet in the bottom of the column. Spent charge left the column via a glass tube which was adjustable in height and was sealed airtight in the top lid. The BRG contactors (1.0 and 2.5 cm i.d.) comprised a glass column with a hemispherical inlet. In the 1 cm contactor, the latter was separated from the column by a stainless steel mesh (98 μm) acting to retain the matrix particles and distribute the incoming flow of feedstock. In the 2.5 cm BRG contactor, a 2 cm bed of glass beads (710-1180 μm) served as a flow distributor. Both BRG contactors were fitted with an adjustable top adapter (plunger) in order to minimise headspace.

3.2.2 Adsorbent materials used

Table 3.1 Summary of the adsorbents used in scouting experimentation

Adsorbent	Particle size (μm)	Density (g ml^{-1})	Supplier	Adsorbent type
SP Spherodex LS	100 – 300	1.32	Biosepra	Cation-exchange derivative
Ceramic CM HyperD LS	100 – 300	1.41	Biosepra	Cation-exchange
Macrosorb K6AX	100 – 400	1.27	PhaseSep	Underivatised composite matrix
UpFront glass/agarose	100 – 300	1.52	UpFront	Underivatised pellicular matrix, glass core
UpFront steel/agarose	76 – 151		UpFront	Underivatised pellicular matrix, steel core
	151 – 323			Underivatised pellicular matrix, steel core
SP UpFront	76 – 151	2.72		SP derivative of UpFront steel/agarose
	151 – 323	2.35		SP derivative of UpFront steel/agarose
CM Zirconia	68	3.22	Biosepra	Cation-exchange

3.2.3 Measurement of bed expansion characteristics

A given amount of adsorbent particles was loaded into a fluidised bed contactor corresponding to a settled bed height (SBH or H_0) of 15 cm. This settled bed was fluidised by increasing the flow velocity stepwise until the a maximum degree of expansion was achieved

Figure 3.1. Fluidised bed contactors for small-scale experiments

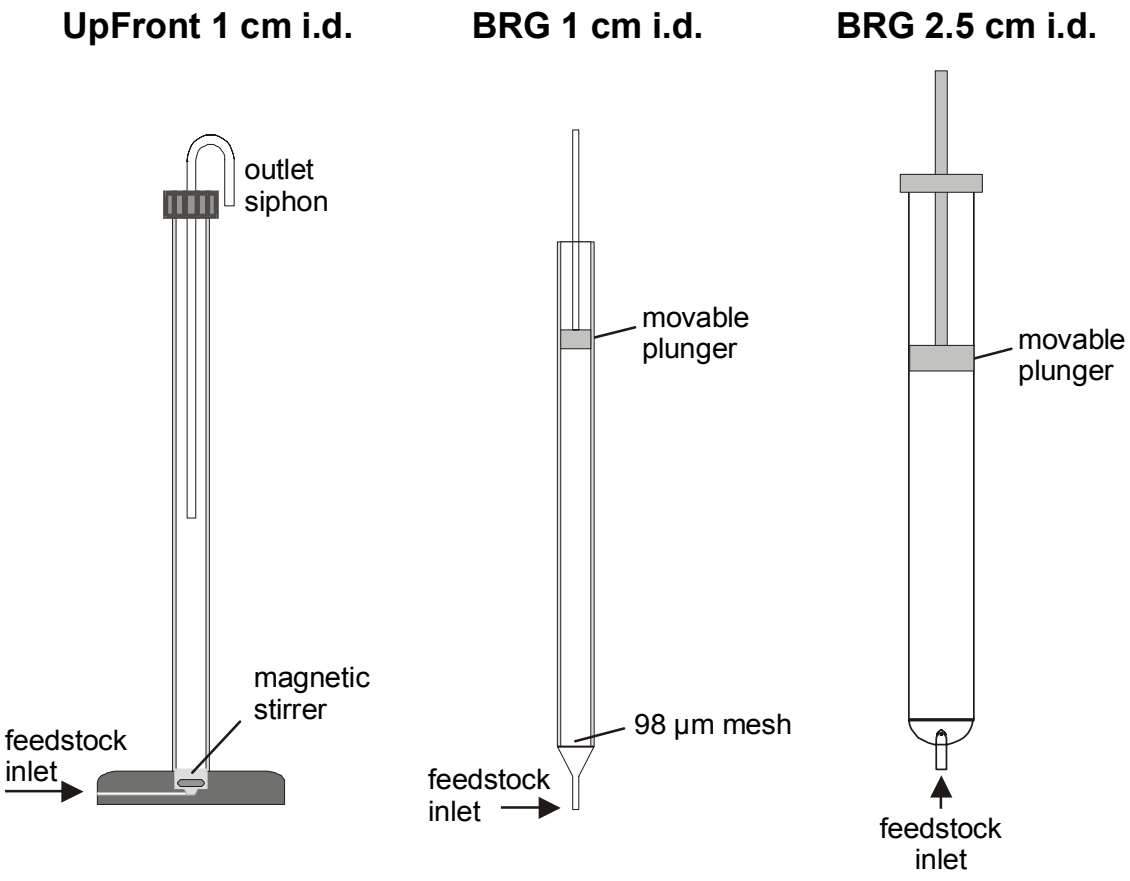

Three different fluidised bed contactors were used in method scouting, i.e. the commercially available UpFront contactor (1.0 cm i.d.) and two custom built contactors (BRG contactors,1.0 and 2.5 cm i.d., Biochemical Recovery Group, School of Chemical Engineering, University of Birmingham). Flow distribution in the UpFront contactor was achieved by a magnetic stirrer located directly above the feedstock inlet in the bottom of the column. The BRG 1 cm contactor was fitted with a 98 µm stainless steel mesh and in the BRG 2.5 cm contactor a 2 cm bed of glass beads (710-1180 µm) served as a flow distributor.

(diffuse surface of the fluidised bed). The flow velocity was then decreased stepwise and after each step the bed was allowed to stabilise (approximately 10 min). The height of the fluidised bed (H) was recorded after a stable value was achieved and the degree of bed expansion was calculated according to Equation 3.1.

Equation 3.1

$$\text{Degree of expansion} = \frac{H - H_0}{H_0} \cdot 100\%$$

3.2.4 Measurement of axial dispersion

A bed of adsorbent particles was fully expanded using buffer A at the test flow rate. When a stable fluidised bed height was attained, the top adapter was lowered to a position approximately 5 mm above the expanded bed surface. The fluid, loaded into the contactor by a peristaltic pump, was switched to the tracer solution (a dilute acetone solution, 1% v/v). The UV absorbance of the acetone was measured in the exit stream from the column using a UV monitor and a positive step input was recorded on a chart (see Figure 3.2). When the UV signal was stable at maximum absorbance (100%), the feed was changed back to buffer and this event was marked on the recorder paper. The decrease of UV absorbance (negative step input) was recorded until the signal stabilised at baseline level (0%). The time interval from switching the feed to water until the signal reached 50% of the full deflection was taken as the mean residence time (t), the time interval of the signal between 84.15% and 15.85% yielded the spread of the distribution (2σ). The number of theoretical plates (N) was calculated according to Equation 3.2 (average value from at least three runs at each test flow rate).

Equation 3.2

$$N = \frac{t^2}{\sigma^2}$$

Figure 3.2. UV signal recording during the test procedure for the determination of the number of theoretical plates

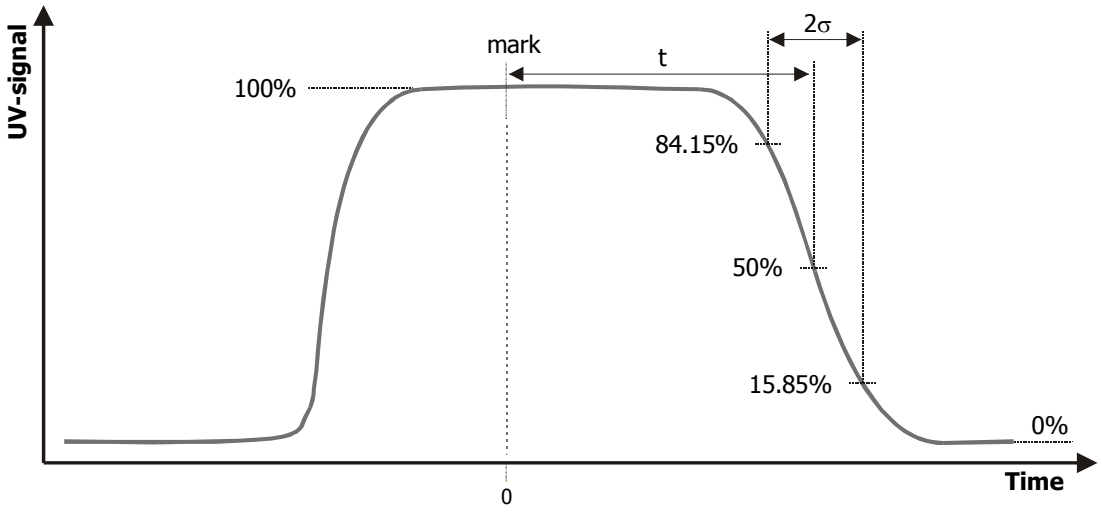

3.2.5 Derivatisation of UpFront steel/agarose by sulphonation

UpFront steel/agarose was derivatised by sulphonation in order to obtain a strong cation-exchange derivative of the base material. A method described by Burton and Harding (1997) was used where activation of the matrix was achieved by allyl glycidyl ether (AGE). The matrix was washed with de-ionised water and suction dried, then the matrix was suspended in 0.3 M NaOH containing 3 ml AGE per 10 g of suction dried matrix. This slurry was mixed on a roller incubator for 48 h. After reaction, the slurry was drained in a sintered funnel and washed with deionised water to remove base and byproducts. The matrix was then added into a solution containing sodium metabisulphite (0.5 g ml^{-1}) and sodium sulphite (0.4 g ml^{-1}), 10 g of activated matrix in a volume of 4 ml. The slurry was placed on a roller incubator and allowed to react for 48 h.

3.2.6 Effect of disruptate pH on the adsorption performance of various cation exchangers

A batch binding experiment was performed in which adsorbents (SP Spherodex LS, CM HyperD LS, and SP UpFront) were contacted with *Erwinia* disruptate at various pH values (see Table 3.2 for mixture compositions). The experimental disruptate was spiked with a charge of L-asparaginase sufficient to saturate the adsorbent at the given pH (the required activity level was estimated from an adsorption isotherm generated in a preliminary experiment, data not shown). As a control, disruptate was incubated with purified L-asparaginase in the absence of an adsorbent. Thus, it was possible to compensate for adsorption of L-asparaginase to cell debris and estimate the binding capacity of the cell debris.

Table 3.2. Composition of the batch binding experiments (at varied pH conditions)

Component	Volume	Note
Adsorbent in buffer A	1 ml	1:1 slurry in buffer A at respective pH
Purified L-asparaginase	2 ml	in 40 mM citric acid / tri-sodium citrate at respective pH, approximately 25,000 U ml^{-1}
Disruptate	2 ml	generated at 34 % biomass (ww/v), cells suspended in water (method see section 2.2.1)
Total	5 ml	adsorbent in disruptate (15 % biomass in 20 mM citric acid / tri-sodium citrate at respective pH)

The pH values investigated were investigated in the range of 4.0 – 7.0 in increments of 0.5 pH units for SP Spherodex and pH 5.0 to 6.0 in increments of 0.1 pH units for CM HyperD and SP UpFront. The reaction tubes were placed on a roller incubator. After an incubation time of 4 h at room temperature, the adsorbent was allowed to settle and a sample of the unclarified disruptate was removed for enzyme analysis. Cell debris in the sample was eliminated by centrifugation (7600g, 10 min) and the clear supernatant was assayed for

asparaginase activity. Binding capacities were calculated by a mass balance established from the original and intermediate concentration of the enzyme.

3.2.7 Batch uptake of purified L-asparaginase by CM HyperD LS and SP UpFront

Defined settled volumes of adsorbent (0.25 / 0.5 / 1.0 / 1.5 / 2.0 / 3.0 ml), were equilibrated in buffer A. At t = 0 min a solution of purified L-asparaginase (specific activity approximately 825 U mg^{-1}, supplied by CAMR, Porton Down) in buffer A was added (final concentration 2 mg ml^{-1}, total liquid volume 25 ml). The reaction tubes were placed on a roller incubator at room temperature, and at given time intervals the tubes were removed from the roller and, after the matrix was allowed to settle (approx. 5 - 10 sec), a small sample of the supernatant was removed and assayed for protein concentration (see Section 2.2.4).

3.2.8 Fluidised bed experiments

Adsorbent particles were loaded into a fluidised bed contactor corresponding to a given settled bed height (SBH) or settled bed volume (SBV) respectively. This settled bed was fluidised using equilibration buffer (buffer A) by increasing the flow velocity stepwise until the desired flow velocity for feedstock loading was achieved. The adsorbent bed was equilibrated in buffer A at the same pH as the feedstock used where at least 10 SBV of equilibration buffer were passed through the bed. After equilibration, the inlet was switched to the feedstock (e.g. unclarified disruptate). Feedstock application was performed until a desired adsorbent saturation was achieved. Washing of the adsorbent bed was achieved by passing 10 to 15 settled bed volumes of equilibration buffer through the bed. If not stated otherwise, elution was routinely achieved by a step input of buffer B (citric acid / tri-sodium citrate, 20 mM containing 1 M NaCl, pH 5.5 if not stated otherwise) in fluidised bed mode at

a linear flow velocity of 100 cm h^{-1}. Spent charge was collected in fractions and routinely assayed for L-asparaginase activity (see Section 2.2.5) and total protein concentration (see Section 2.2.4). Dynamic capacities were estimated from the L-asparaginase challenge required to achieve 10 % breakthrough, i.e. C/C_0=0.1.

3.3 Results and Discussion

3.3.1 Physical characterisation of adsorbent matrices – degree of bed expansion and assessment of axial dispersion

Before running a fluidised bed process, it was necessary to determine the bed expansion characteristic of the chosen adsorbent, i.e. variation of expanded bed height with the fluidisation velocity and variation of expansion with physical properties of the feedstock. Besides being an important design feature, the degree of bed expansion may be used as a quick and simple measure of bed stability (Amersham Pharmacia Biotech AB, 1997; Chang *et al.*, 1995). The bed expansion of adsorbent particles at a given fluidisation velocity is governed by the size and density of the particles and the viscosity of the mobile phase, as expected from the Stokes law (see Equation 1.1). Figure 3.3 depicts the bed expansion of various matrices as a function of the superficial flow velocity when fluidised in buffer. The strong influence of particle size becomes apparent from the curve for CM Zirconia. Although it has the highest specific weight of the adsorbents tested, it exhibits the highest degree of bed expansion at a given flow velocity and this can be attributed to a small particle size (68 μm). On the other hand, Macrosorb K6AX, despite its comparatively low specific weight, was characterised by a shallow expansion curve attributable to a large mean particle diameter (size range 100 – 400 μm).

Figure 3.3. Bed expansion of various adsorbents as a function of the superficial flow velocity

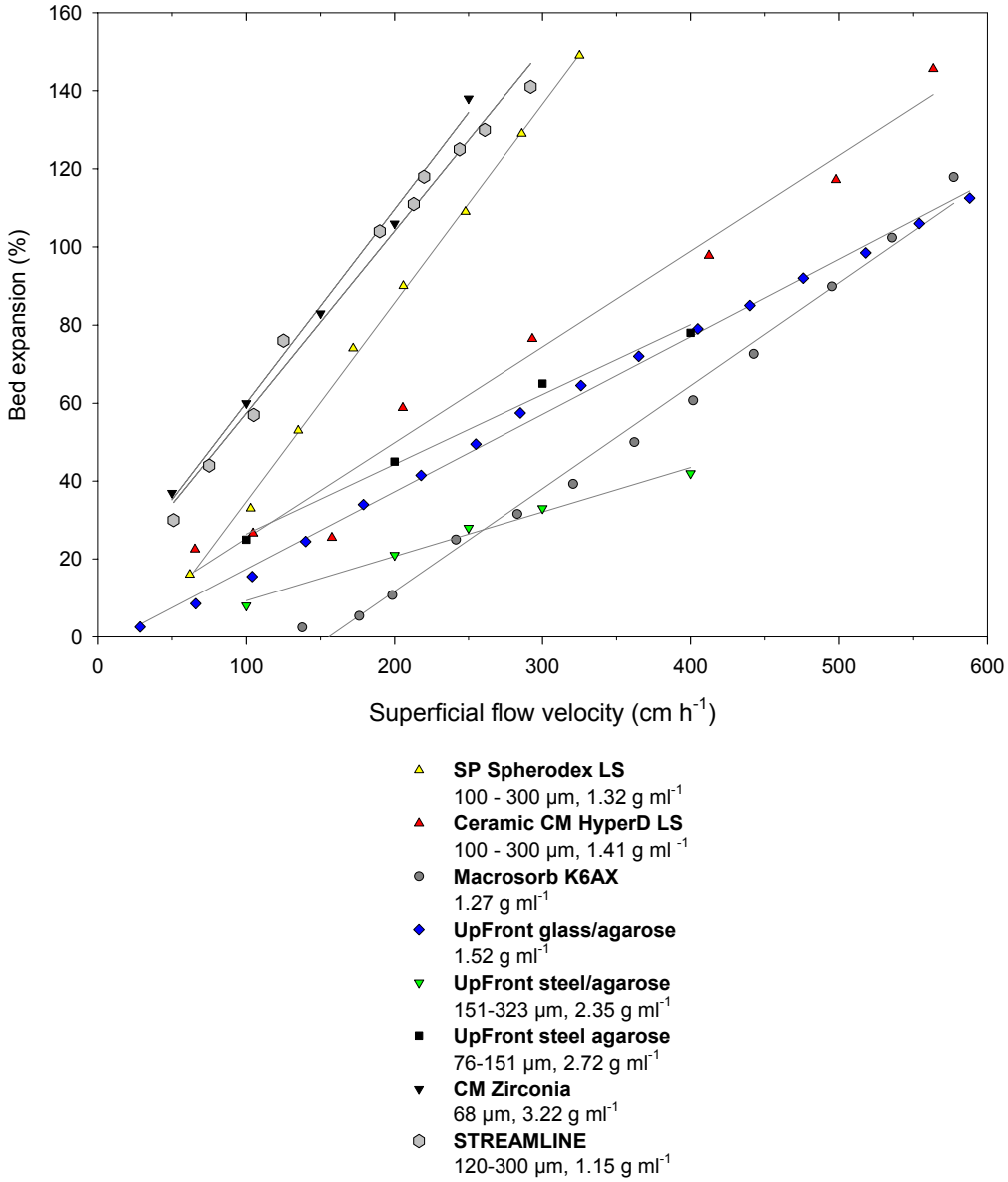

Bed expansion of various adsorbents in buffer. A constant volume of adsorbent, corresponding to a settled bed height of 15 cm was fluidised using buffer A either in a 4.5 cm internal diameter BRG contactor (SP Spherodex LS, Ceramic CM HyperD LS, Macrosorb K6AX, UpFront glass agarose, STREAMLINE) or in a 1 cm UpFront contactor (UpFront steel agarose, CM Zirconia. Densities and size ranges of the adsorbents are given with the symbols above.

A minimum degree of bed expansion is required in order to provide sufficient voidage for the particulates in the feedstock to pass unhindered through the contactor. At the same time, a shallow trend of increasing expansion height is desirable since increased voidage at a constant flow rate constrains fluid side mass transport (Thömmes, 1997). In addition, the low degree of expansion associated with particles of appropriate specific weight and diameter allows the adoption of higher flow rates to facilitate throughput maximisation and a more efficient exploitation of the length of a contactor. Loading a viscous feedstock, e.g. a cell disruptate, increases expansion of a fluidised bed operated with a given particle type. This effect is depicted in Figure 3.4 and also in Figure 4.3. It can be seen that the expansion of a bed at a given flow velocity increases by a factor of 2 – 3 when fluidised in cell disruptates containing 15 % biomass (ww/v, viscosity approximately 2.1 mPa·s). This fact underpins various implications: for a given settled bed height the required contactor length increases with the velocity and viscosity driven expansion of the adsorbent material. Under such circumstances, the diffusion distances for the adsorption process are increased with the voidage which could impair the adsorption efficiency. Therefore, it is desirable to maintain a minimal bed expansion which can be achieved by enhancing particle density at fixed particle diameter.

Measurement of the axial dispersion, i.e. the deviation from plug flow movement of fluid elements in an adsorbent bed (both fixed and fluidised), is commonly performed by residence time distribution (RTD) analysis of step or pulse signals (Levenspiel, 1972). It has been demonstrated that RTD data can be successfully correlated to the adsorption performance of FBA experiments (Barnfield-Frej *et al.*, 1997; Chang and Chase, 1996b; Thömmes *et al.*, 1995a; Lan *et al.*, 1999). In addition, RTD measurements may be used as a measure of bed stability and functional testing of complete systems (Amersham Pharmacia Biotech AB,

Figure 3.4 Increased bed expansion in biomass containing feedstocks

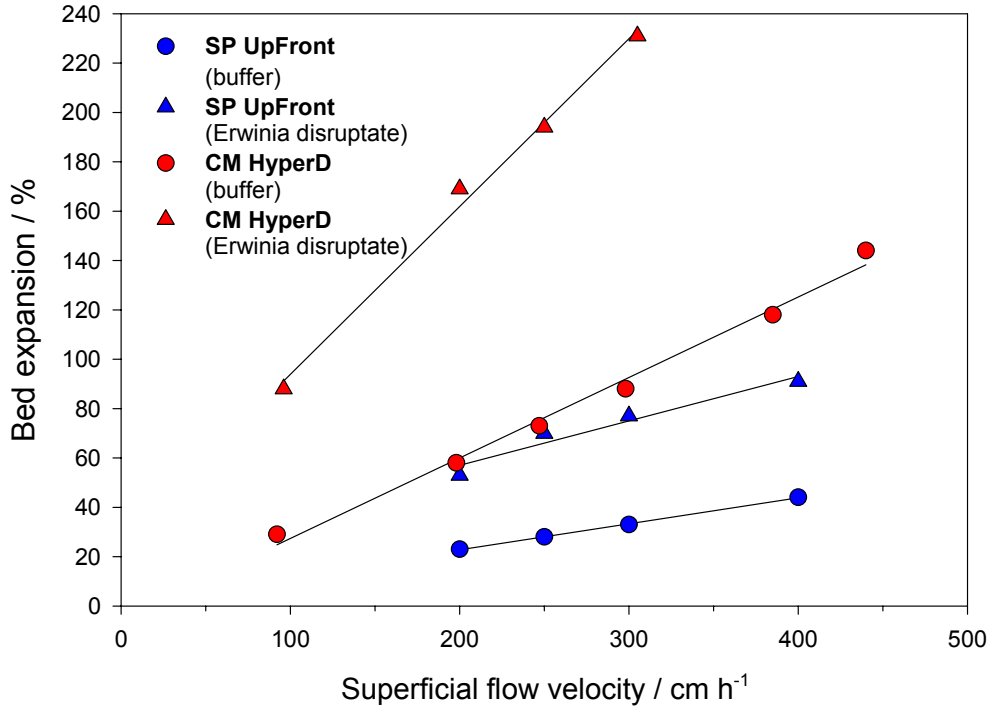

Bed expansion of SP UpFront (151 – 323 µm, 2.35 g ml^{-1}) and CM HyperD LS (100-300 µm, 1.41 g ml^{-1}) in buffer A and Erwinia disruptate 15 % biomass ww/v, SBH 15 cm. Bed expansion of SP UpFront was determined in a 1 cm contactor (UpFront Chromatography), CM HyperD LS was used in a 2.5 cm BRG contactor.

1997). For example by using a step input of a tracer solution the number of theoretical plates (N) can be calculated from the mean residence time of the tracer and the variance of the output signal, representing the broadening of an introduced sample zone. This method (see 3.2.4 for details) was employed in work presented here in order to characterise and compare various candidate adsorbents or base matrices respectively, applicable for the fluidised bed capture of L-asparaginase. Measurements were made with regard to degrees of axial dispersion and bed stability when materials were fluidised under similar conditions. Figure 3.5 depicts the height equivalent to one theoretical plate (HETP), calculated by dividing the number of theoretical plates (N, see Equation 3.2) by the height of the fluidised bed (H), as a function of the superficial flow velocity. Within the range of flow velocities employed, a common trend could be observed with all the adsorbents. At a low range of flow rates, i.e. 100 cm h^{-1}, a decrease in HETP with increasing flow velocity was found. For some adsorbents (UpFront steel/agarose, CM HyperD LS and UpFront glass/agarose) there appeared to be a minimum HETP value at an intermediate flow velocity with a slight increase in HETP at higher flow velocities. This might suggest that in a given contactor configuration each adsorbent is characterised by a range of flow velocities at which the degree of axial dispersion is at a minimum. Macrosorb K6AX exhibited the highest HETP values at flow velocities commonly employed for fluidised bed adsorption (200 – 400 cm h^{-1}). This might be attributed to the irregular shape of the particles causing a high degree of particle movement within the fluidised bed (due to a variation in settling velocity with spatial position of the particle). This was clearly evident by visual inspection. Another trend depicted in Figure 3.5 for all adsorbents with the exception of CM HyperD LS, was that the higher the density of an adsorbent (i.e. the lower its bed expansion and voidage) the lower was the HETP value at a

Figure 3.5. Theoretical plate height as a function of the superficial flow velocity.

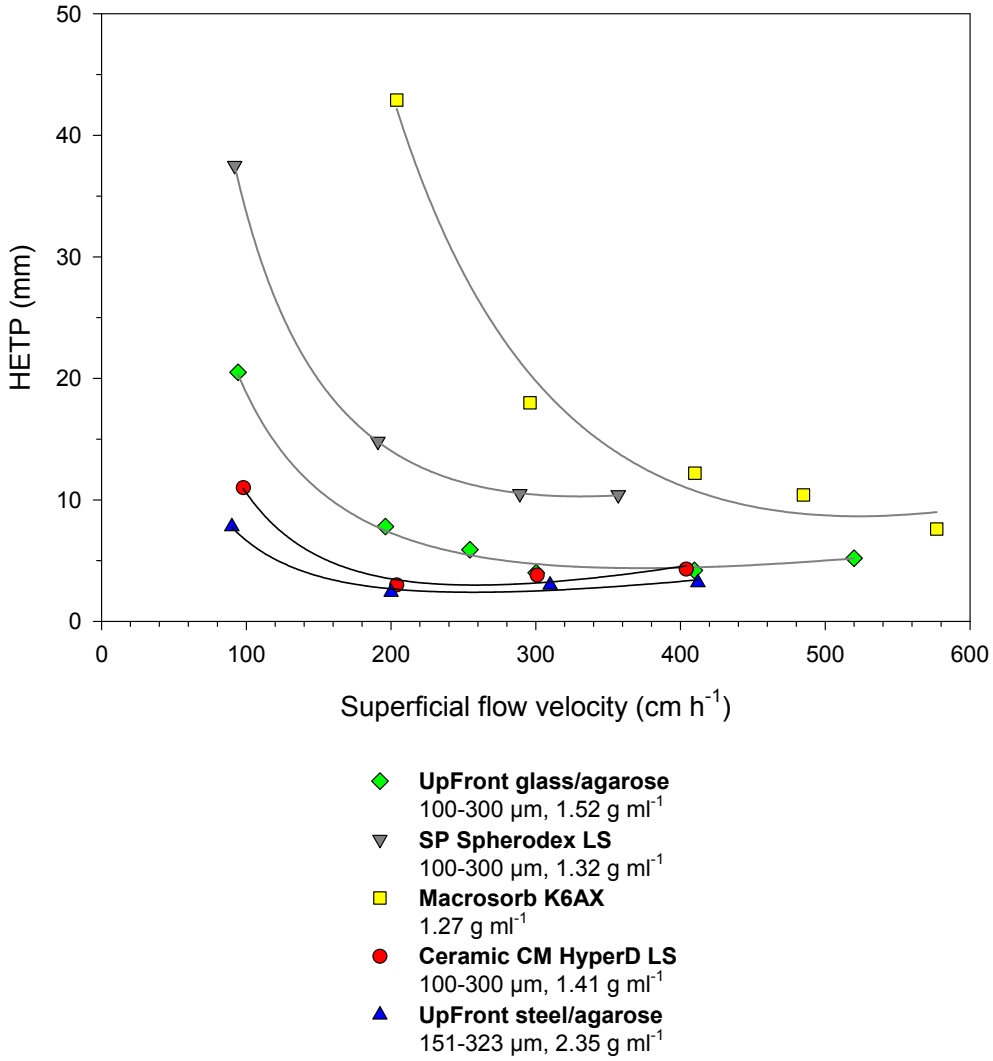

Adsorbents were fluidised in a 4.5 cm BRG contactor (SBH 15 cm) fitted with a 98 µm stainless steel mesh serving as a flow distributor. The number of theoretical plates was calculated from a negative step input signal using a dilute acetone solution as a tracer (see 3.2.4 for test procedure).

given flow velocity. This might suggest that the movement of equally sized particles in a fluidised bed is reduced for beads with increased density.

The results obtained here were in good agreement with Lan *et al.* (1999) who employed a similar contactor (BRG contactor, 2.5 cm i.d., SBH 15.8 cm, 98 μm mesh distributor) for negative step input RTD analyses (as described in Section 3.2.4). In that study HETP values of 12.2 mm for STREAMLINE DEAE (100 – 300 μm, 1.2 g ml^{-1}) and 8.5 mm for DEAE Spherodex LS (100 – 300 μm, 1.35 g ml^{-1}) were found for fluidisation in buffer at 200 cm h^{-1}. Chang and Chase (1996b) reported an HETP value for STREAMLINE SP of 10.5 mm (STREAMLINE contactor, 5 cm i.d. SBH 10 cm, 300 cm h^{-1}). Increasing the viscosity of the mobile phase by the inclusion of glycerol at 25 and 32% caused a higher bed expansion or higher voidage respectively and resulted in a fivefold and tenfold increase in HETP when the flow velocity was kept constant at 300 cm h^{-1}. However, maintaining a constant bed expansion of 100%, i.e. a constant voidage, at increased viscosities yielded an increase in HETP of only 10% for buffers containing 25% and 32% glycerol. Here, flow velocities to achieve 100% bed expansion in 0% glycerol were 300 cm h^{-1}, at 25% glycerol 121 cm h^{-1} and at 32% glycerol 88 cm h^{-1}. This might suggest that axial dispersion is reduced at low degrees of bed voidage, which can either be achieved by the reduced bed expansion of an adsorbent with a high specific weight or by reduced flow velocities at higher feedstock viscosities. Judged by the measured HETP values, UpFront steel/agarose and CM HyperD LS exhibited superior fluidisation characteristics which recommended them for further experimentation in the fluidised bed adsorption of L-asparaginase.

3.3.2 The effect of disruptate pH on the adsorption performance of CM HyperD LS and SP Spherodex

In order to identify a suitable pH for the capture of L-asparaginase by the two cation exchange matrices, a series of batch binding experiments was performed (see 3.2.5). Figure 3.6 depicts the equilibrium binding capacities of three adsorbents achieved at various pH values when challenged with an *Erwinia* disruptate (disruptates were spiked with a standard charge of purified L-asparaginase in order to provide a sufficient amount of enzyme to saturate the adsorbent). Initially, L-asparaginase binding was investigated for SP Spherodex LS. It can be seen that the capacity of this adsorbent significantly declined at pH values greater than 4.5 and approximated to zero at pH 6.0. From control samples, i.e. disruptate incubated with a charge of purified enzyme in the absence of an adsorbent, the adsorption of L-asparaginase to cell debris could be estimated. The curve for the debris bound enzyme followed the same trend, i.e. a clear decrease between pH 4.0 and 5.0 (see Figure 3.6). Allowing for the proportional ratio of L-asparaginase binding to matrix and debris, it appeared favourable to adopt an operational pH between 4.5 and 5.0 for further experimentation. However, experiments employing unclarified *Erwinia* disruptates at pH values below 5.5 were compromised by precipitates and flocs which fouled both the meshes fitted to columns as flow distributors as well as the narrow fittings of small-scale columns. Therefore it was concluded that pH conditions for the effective adsorption of L-asparaginase were best established between values of 5.0 and 6.0. CM HyperD and SP UpFront, tested at values between pH 5.0 and 6.0, exhibited a considerably higher capacity in comparison with SP Spherodex LS which confirmed applications for the former adsorbents in a suitable pH range (5.0 – 5.6). However, binding capacity diminished when pH 6.0 was approached.

Figure 3.6. Influence of the disruptate pH on the equilibrium binding capacity of various adsorbents.

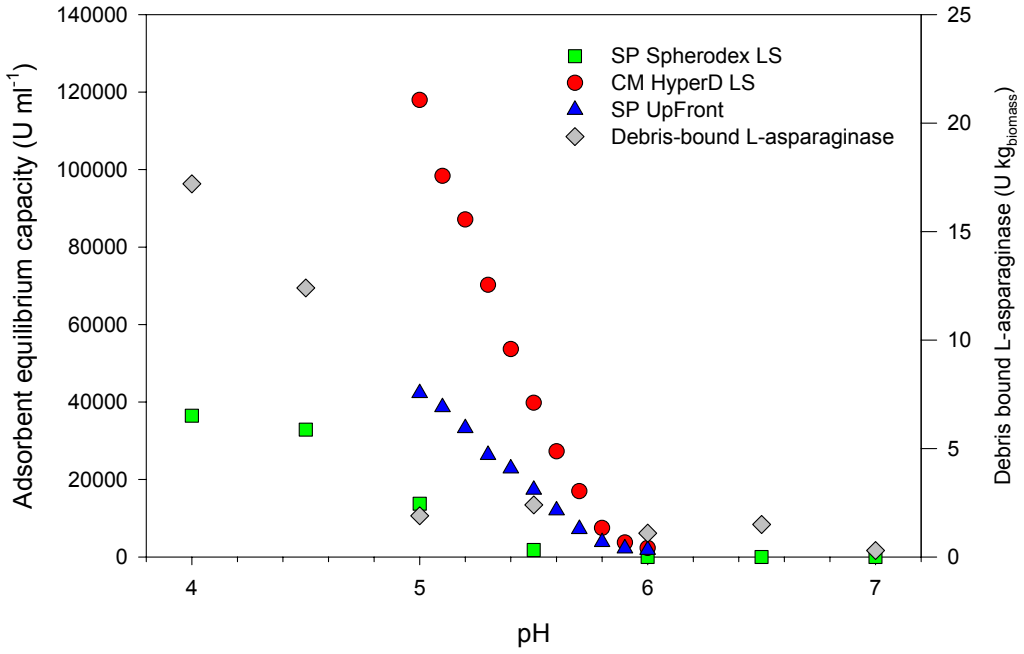

Matrix, equilibrated in buffer A at the relevant pH, was incubated for four hours with Erwinia disruptate, 15% ww/v original biomass, spiked with purified L-asparaginase. Debris binding was analysed by incubating the disruptate with purified L-asparaginase at the relevant pH values in the absence of an adsorbent. Binding capacities were estimated from a mass balance established from the original and intermediate concentrations of the enzyme.

3.3.3 Batch-uptake of purified L-asparaginase by Ceramic CM HyperD LS and SP UpFront

CM HyperD and SP UpFront (strong cation-exchange SP derivative of UpFront steel/agarose, see 3.2.5) represent two different types of adsorbent solid phases (see Figure 3.7). The commercially available CM HyperD is a composite stationary phase comprising a rigid, high-porosity skeleton (polystyrene-coated silica) which is filled with a polyacrylamide-based hydrogel. The skeleton provides mechanical strength while the soft gel provides adsorption or ion-exchange sites for the interaction with the solutes to be separated (Boschetti, 1994; Fernandez and Carta, 1996). The unique feature of this resin is that adsorbed proteins can move freely between charges in the functionalised gel (Wright *et al.*, 1999; Weaver and Carta, 1996). These so-called hyper-diffuse particles are therefore claimed to be characterised by rapid intraparticle mass transfer kinetics and high dynamic capacities.

In conventional, rigid macroporous adsorbents, adsorption takes place at an available binding site within a pore. The saturation of available adsorption sites progresses from the surface into the interior of the bead. Such adsorbents will commonly have high intraparticle mass transfer resistances and reduced dynamic capacities at increased flow velocities (discussed in Afeyan *et al.*, 1990; Skidmore *et al.*, 1990; Wright *et al.*, 1999). Various reports demonstrate a superior performance of hyper-diffusive resins in comparison with macroporous adsorbents. Weaver and Carta (1996) compared the hyper-diffusive S-HyperD-M (Biosepra) with POROS 50 (PerSeptive Biosystems) which is a macroporous adsorbent claimed to achieve convective flow within pores. Despite a larger particle size, S-HyperD exhibited considerably higher equilibrium and dynamic capacities during the adsorption of lysozyme from buffer solutions. Wright *et al.* (1998) and Wright *et al.* (1999) compared the macroporous STREAMLINE SP with the hyper-diffusive S-HyperD LS under batch binding

Figure 3.7. Structural characteristics of a macroporous, hyper-diffusive and a pellicular adsorbent

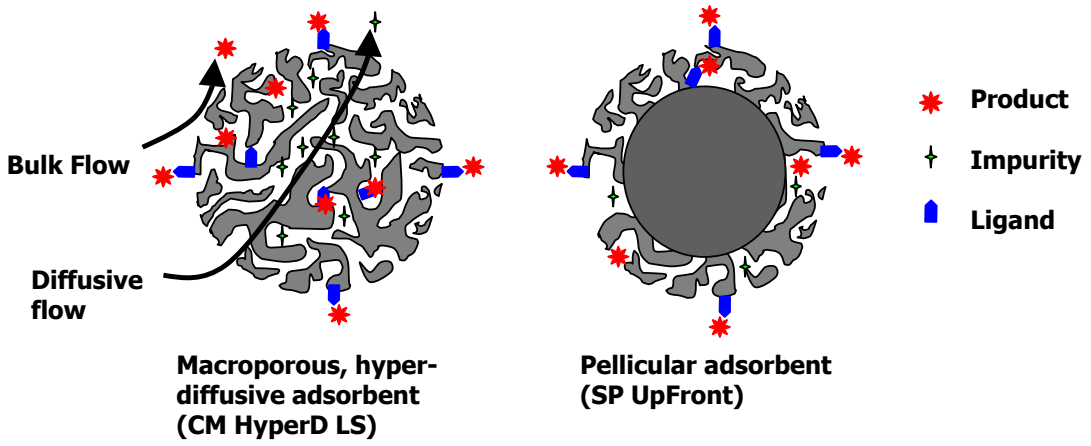

CM HyperD LS, a so-called hyper-diffusive adsorbent, comprises a megaporous, rigid and non-reactive skeleton filled with a homogeneous, macroporous continuum (polyacrylamide-based hydrogel). SP UpFront, a pellicular adsorbent, comprises a non-porous, solid core (stainless steel) coated with a comparatively thin layer of porous material (agarose). The depth of the porous agarose layer of the pellicular SP UpFront (bead size range 151-323 µm) was estimated as 40% of the bead radius, i.e. a 20 µm agarose layer on a 60 µm stainless steel bead (calculation based on the densities of the core and coating material and the composite bead). Redrawn from Zhang et al. (2000), not to scale.

and frontal analysis exploiting lysozyme as a model protein. It was found that increased flow velocity and feedstock viscosity affected the adsorption performance of STREAMLINE SP to a significantly higher degree than S-HyperD.

The prototype adsorbent SP UpFront has a more limited pellicular structure, i.e. a comparatively thin retentive agarose layer on the surface of a non-porous steel core (see Figure 3.7). The depth of the porous agarose layer of the pellicular SP UpFront (bead size range 151-323 μm) was estimated as 40% of the bead radius, i.e. a 20 μm agarose layer on a 60 μm stainless steel bead (estimations were based on difference analysis of the densities of the core and coating material and the composite bead). In such a particle, the volume fraction of the agarose shell would correspond to 78% and of the steel core to 22% of the total particle volume. Pellicular particles reduce bulk intraparticle mass transfer limitations by minimising diffusion distances for product (Weaver and Carta, 1996; Boschetti, 1994) but at the expense of volumetric capacity. Thus, it might be predicted that such particles attain adsorption equilibrium more rapidly than conventional macroporous particles. On the other hand, the equilibrium capacity of pellicular matrices is expected to be reduced in comparison with an equivalently sized macroporous or hyper-diffusive continuum by virtue of a reduced volume for adsorption.

In order to investigate and address comparative aspects of adsorption kinetics, a series of batch binding experiments were designed and performed (see 3.2.7). Uptake of purified L-asparaginase in buffer A as a function of incubation time for the two adsorbents is depicted in panel A of Figure 3.8 and adsorption isotherms are given in panel B. It can be seen from panel A that enzyme adsorption by SP UpFront was more rapid and reached a steady state value at about 20 min of incubation time, whereas in the case of CM HyperD LS significant adsorption was still detectable at times up to 60 min. A higher rate of adsorption for the pellicular

Figure 3.8. Batch adsorption of L-asparaginase to SP UpFront and CM HyperD LS

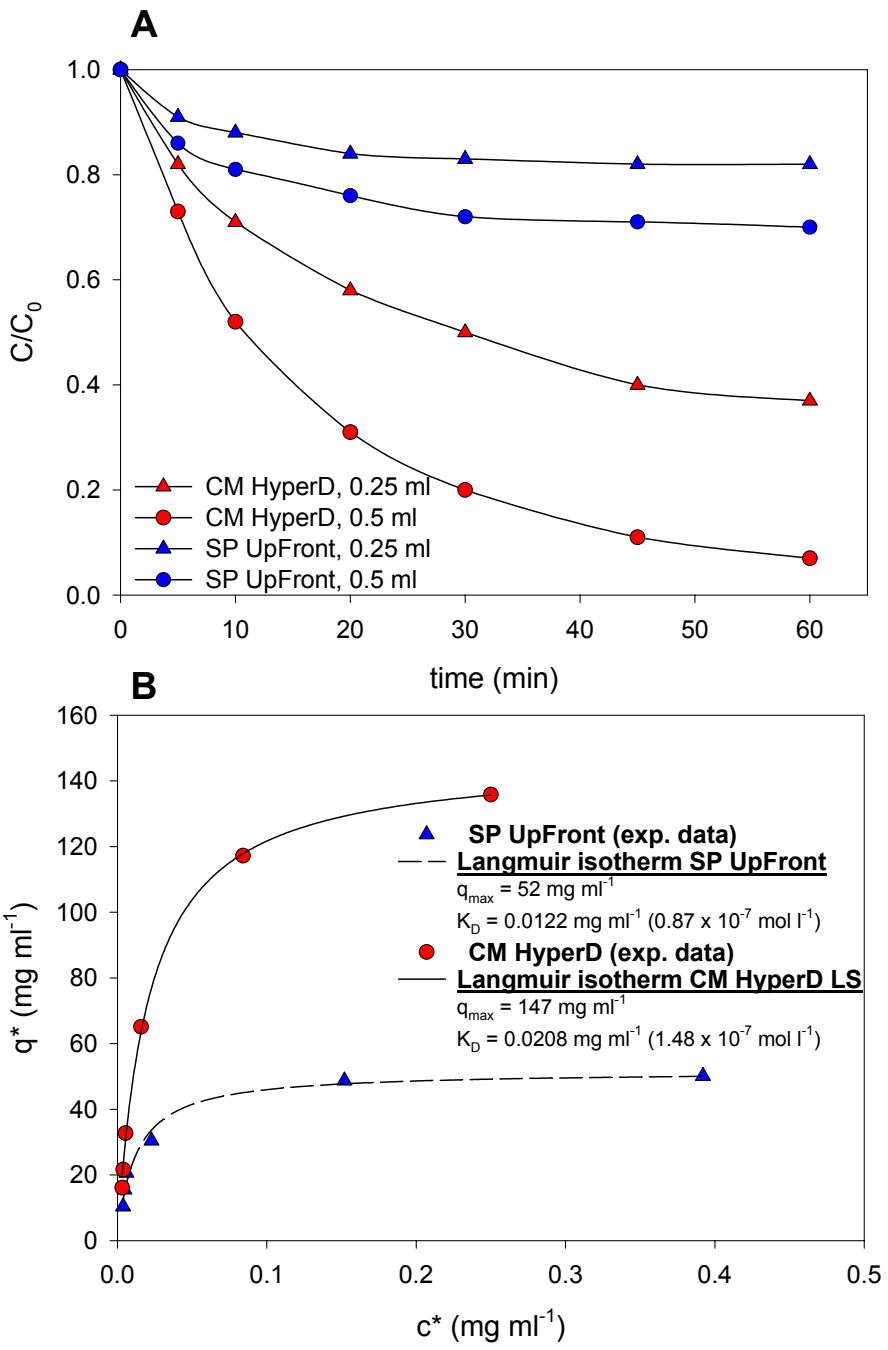

Selected settled adsorbent volumes (0.25 / 0.5 / 1.0 / 1.5 / 2.0 / 3.0 ml) were incubated with purified L-asparaginase in buffer A (25 ml total volume). Panel A: uptake of L-asparaginase by the cation adsorbents as a function of time. Panel B: adsorption isotherms of the adsorbents compiled from equilibrium data (adsorption time > 120 min).

adsorbent may also be indicated by a lower apparent K_D value for SP UpFront (see adsorption isotherms, panel B in Figure 3.8). However, the difference in K_D is comparatively small and it has to be noted that the determination of K_D from a plot of c*/q* vs. c* (c*, q*: liquid phase and solid phase concentration of the analyte at equilibrium) is usually affected by a considerable degree of experimental error. Adsorption isotherms exhibited a threefold higher equilibrium capacity for CM HyperD LS which confirmed the prediction made from the structural differences of the two adsorbents. A threefold difference in capacity, e.g. CM HyperD LS 21000 U ml^{-1} and SP UpFront 6800 U ml^{-1}, was also evident from small-scale fluidised bed and packed bed adsorption experiments (curves 2 and 5 in Figure 3.10, refer to page 86). However, it was estimated that the inert core reduces the volume of the pellicular bead only by 22% in comparison with an equally sized, macroporous continuum. The considerably lower capacity of SP UpFront in comparison with CM HyperD might therefore be attributed to a lower ligand concentration in the pellicular adsorbent (SP UpFront 76 µmol ml^{-1}, CM HyperD LS >250 µmol ml^{-1} according to the manufacturer) and/or to a limited accessibility of the ion-exchange groups in the porous layer.

Preliminary batch binding experiments comparing SP and CM derivatives (i.e. strong and weak cation exchangers) of the same base matrix (Sepharose, Amersham Pharmacia) revealed almost identical uptake rates and equilibrium capacities at the relevant pH (see Figure 3.9. This suggested that the different performance of SP UpFront and CM HyperD with regard to L-asparaginase uptake (Figure 3.8, panel A) can be attributed to their differences in resin structure rather than their different cation exchange chemistries. CM derivatives of UpFront stainless steel and SP derivatives of HyperD were not available for this study.

Figure 3.9. Batch adsorption of purified L-asparaginase on SP and CM Sepharose

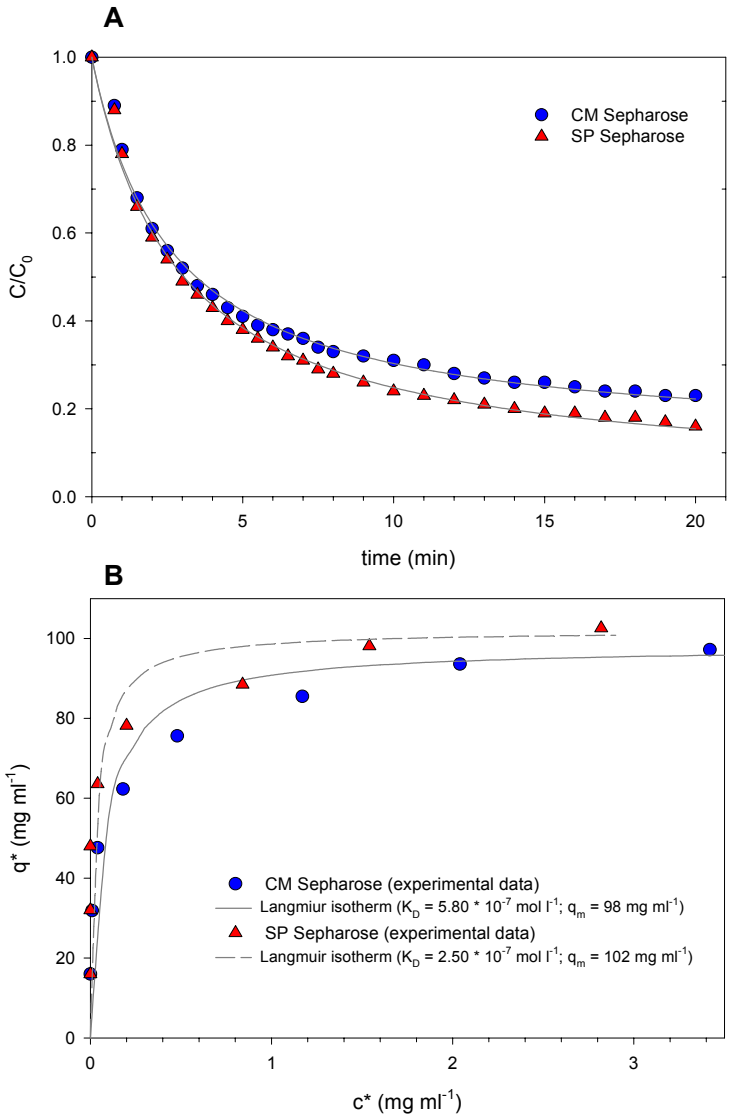

Panel A. Batch uptake of purified L-asparaginase by CM and SP Sepharose. One ml of adsorbent was stirred in a solution of purified L-asparaginase (5 mg ml^{-1} in buffer A, pH 5.5, total volume 20 ml). Supernatant was continuously drawn from the vessel through a fritted device and pumped through a UV detector for the monitoring the protein concentration. Panel B. Adsorption isotherms for CM and SP Sepharose compiled from batch binding experiments. A constant amount of adsorbent (settled volume 0.5 ml) was incubated over night with purified L-asparaginase in buffer A at various concentrations (2-16 mg ml^{-1}, total volume 5 ml).

3.3.4 Small-scale packed bed and fluidised bed experiments

Figure 3.10 depicts various packed and fluidised bed experiments exploiting CM HyperD and SP UpFront as adsorbents (washing and elution profiles of enzyme activity for the beds is depicted in Figure 3.11). Previously generated *Erwinia* disruptate (15% original biomass, ww/v, see Section 2.2.1) was used as a feedstock. For fluidised bed experiments, unclarified feedstock was employed. For packed bed experiments the disruptate was clarified by centrifugation (5800 g, 30 min). Fouling problems in the 1 cm BRG contactor using the steel mesh as distributor in conjunction with unclarified feedstocks also required the use of clarified disruptates.

It can be seen from Figure 3.10, that the dynamic capacities achieved by CM HyperD are considerably higher (approximately threefold) in comparison with pellicular SP UpFront (both operated in an UpFront 1 cm contactor), which was already evident from batch binding experiments (see Figure 3.8). The dynamic capacity at $C/C_0 = 0.1$ in the UpFront contactor was 21000 U ml^{-1} (experiment 5) which exceeded that in the BRG contactor (14500 U ml^{-1}, experiment 6) by approximately 45 % and rivalled values recorded in the packed bed (22500 U ml^{-1}, experiment 4). Besides the dynamic capacity, the shape of the breakthrough curve was additionally almost identical to the packed bed. This indicated a very low degree of axial mixing and therefore a high stability of the fluidised bed in the UpFront 1 cm contactor. The BRG contactor exhibited a lower dynamic capacity and a slightly shallower increase in product breakthrough which was attributed to minor bed instabilities promoting channelling phenomena.

SP UpFront was tested at two different size ranges, i.e. 76 – 151 µm (experiment 3) and 151 – 323 µm (experiment 2, see Figure 3.10). However, despite the size difference both adsorbents achieved comparable dynamic capacities of 6100 U ml^{-1} (76 – 151 µm) and 6800

Figure 3.10. Small-scale packed bed and fluidised bed experiments

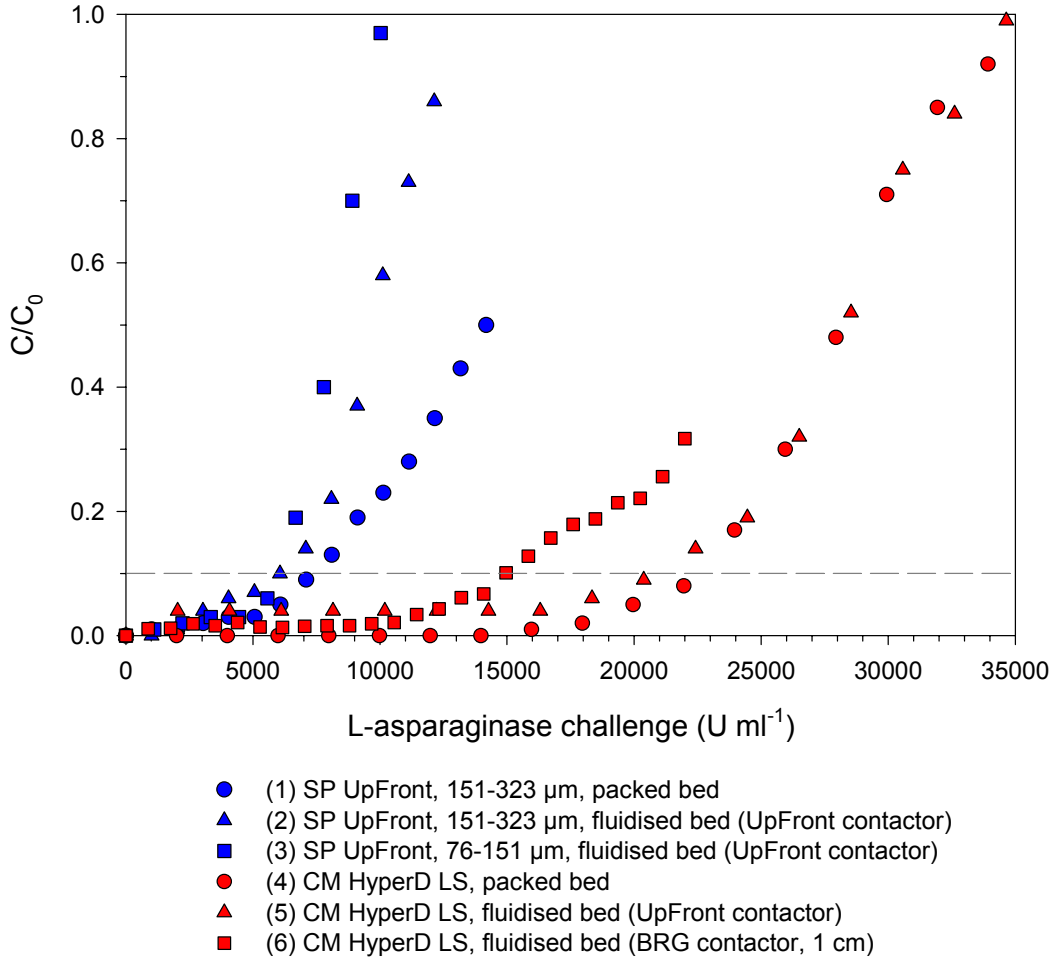

Experiment	Contactor (see 3.2.1)	Feedstock	u (cm h^{-1})	H/H_0	dyn. capacity at C/C_0=0.1 (U ml^{-1})
(1) SP UpFront, 151-323 µm	Packed bed, SBV 2 ml	clarified	100	-	7500
(2) SP UpFront, 151-323 µm	UpFront 1 cm, SBH 15 cm	unclarified	200	1.4	6800
(3) SP UpFront, 76-151 µm	UpFront 1 cm, SBH 15 cm	unclarified	200	1.6	6100
(4) CM HyperD LS	Packed bed, SBV 2 ml	clarified	100	-	22500
(5) CM HyperD LS	UpFront 1 cm, SBH 15 cm	unclarified	200	2.4	21000
(6) CM HyperD LS	BRG 1 cm, SBH 15 cm	clarified	200	2.3	14500

Disruptate was previously generated by bead milling (see Section 2.2.1). For fluidised bed experiments unclarified feedstock was used. For packed bed and fluidised bed experiments employing the BRG 1 cm contactor the disruptate was clarified by centrifugation (5800 g, 30 min). Estimated dynamic capacities are given as the amount of L-asparaginase applied per ml of adsorbent (L-asparaginase challenge) at C/C0 = 0.1.

Figure 3.11. Elution profiles of L-asparaginase in small-scale packed and fluidised beds

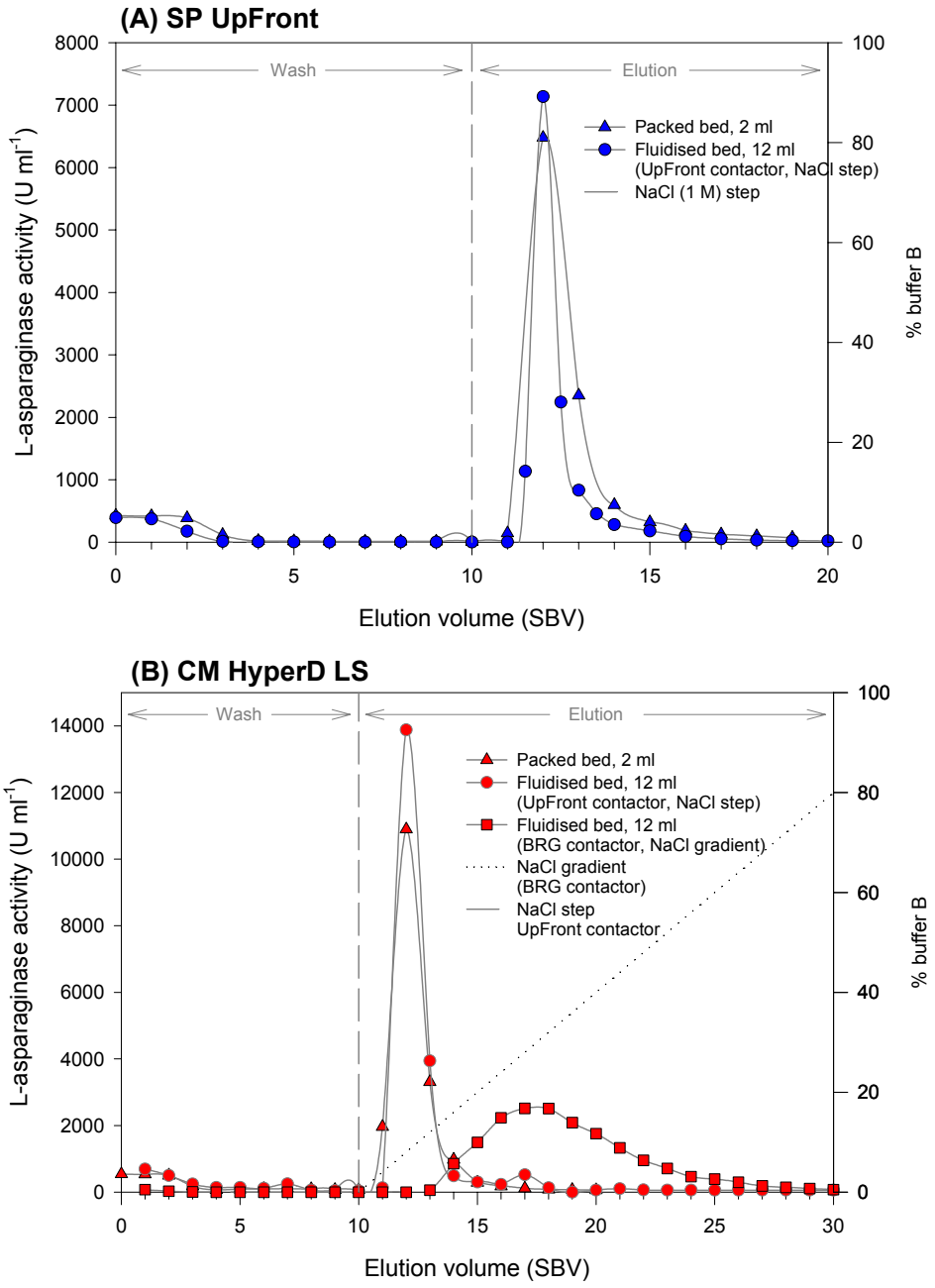

Beds were loaded as shown in Figure 3.10. Elution in packed and fluidised beds was achieved by a step input of buffer B (citric acid / tri-sodium citrate, 20 mM, pH 5.5 containing NaCl 1 M) at a superficial flow velocity of 100 cm h^{-1} (Panel A: SP UpFront, Panel B: CM HyperD LS). In the BRG contactor (CM HyperD LS) elution was achieved by a linear salt gradient (0-100 % buffer B).

U ml^{-1} (151 – 323 μm). Packed bed adsorption employing SP UpFront (151 – 323 μm, experiment 1) resulted in a slightly higher dynamic capacity in comparison with the fluidised bed experiments.

Figure 3.12 depicts the adsorption of purified L-asparaginase in packed beds by SP UpFront and CM HyperD LS. Once more, an approximatly threefold difference in dynamic capacity for the two structurally distinct adsorbents was established. However, it was evident from a comparison of Figure 3.10 with Figure 3.12 that the capacity for L-asparaginase was greatly reduced when the enzyme was adsorbed from a disruptate rather than from a buffer solution. Clearly this can be attributed to the nature of the disruptate as a complex mixture of biological molecules which may interact with the adsorbents and thus reduce the number of adsorption sites available for a specific target molecule. In addition dynamic capacities are reduced with increased feedstock viscosity (Chang and Chase, 1996b; Wright *et al.*, 1999). However, the presence of particulates, i.e. cells and cell debris did not appear to substantially affect the performance of the adsorbents, since the use of both clarified and unclarified feedstocks yielded almost identical dynamic capacities and breakthrough curves (Figure 3.10, compare experiments 4 and 5 for CM HyperD and experiments 1 and 2 for SP UpFront). Thus, cell/adsorbent or debris/adsorbent interactions appeared to be minimal under the given feedstock conditions. This was in accordance with findings of Feuser *et al.* (1999) who found insignificant interactions of various cell types with cation exchange matrices, a significant advantage over anion exchange processes.

Figure 3.11 depicts a comparison of elution profiles of various experiments using SP UpFront in panel A and CM HyperD in panel B (loading of these beds is depicted in Figure 3.10). It can be seen for both adsorbents that a step elution using buffer B (citric acid / tri-sodium citrate, 20 mM containing 1 M NaCl) resulted in a sharp peak of enzyme activity. The

Figure 3.12. Adsorption of purified L-asparaginase in packed beds

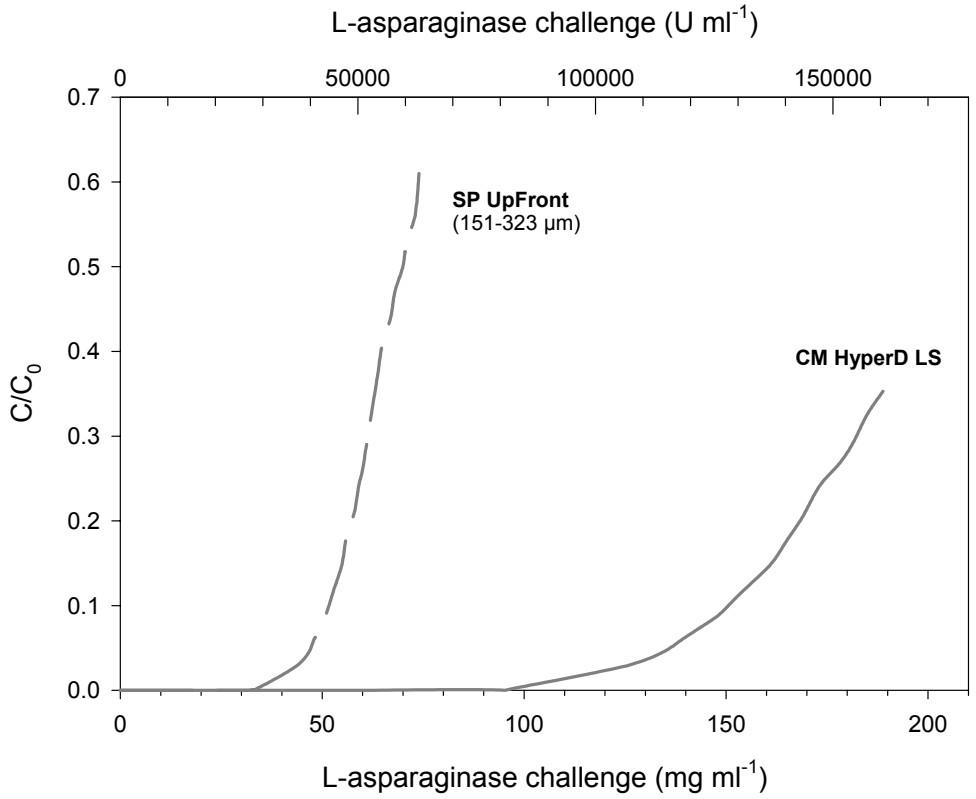

Packed bed adsorption of purified L-asparaginase in buffer A (964 U ml^{-1}, 1.1 mg ml^{-1}) on SP UpFront and CM HyperD LS. Bed dimensions: d=1 cm, H_0= 2.5 cm, 2 ml adsorbent. Loading flow velocity 100 cm h^{-1}. Detection of L-asparaginase by continuous UV-absorption of the effluent at 280 nm.

peak volume achieved in packed beds and fluidised beds was almost identical (approximately 2 settled bed volumes, SBVs) which again demonstrated a low degree of axial mixing in the small-scale fluidised beds (the different peak heights in panel A and B of Figure 3.11 were the result of different degrees of adsorbent bed saturation). A gradient elution (0-1.0 M NaCl) performed in the BRG contactor resulted in an unsatisfactory broad peak of L-asparaginase activity. Bed instabilities causing channelling in the BRG system might have contributed to the comparatively broad nature and asymmetric tailing of the enzyme peak. However, during a separate experiment a step elution using 0.4 M NaCl (conditions derived from the salt concentration at peak maximum during gradient elution, see Figure 3.11) yielded only 9 % of bound enzyme (data not shown). This suggested that the peak broadening during gradient elution could be attributed to the slow increase in ionic strength and that an ionic shock (> 0.6 M) necessary to front off the enzyme. All experiments depicted in Figure 3.11 exhibited a high percentage of recovered enzyme (> 80 % of bound product).

3.3.5 Effect of flow velocity and settled bed height on the dynamic capacity of CM HyperD LS and SP UpFront

This section summarises various primary purification experiments in which L-asparaginase was captured from unclarified *Erwinia* disruptates employing CM HyperD and SP UpFront as the fluidised adsorbents. For CM HyperD experiments a 2.5 cm BRG contactor was used. However, due to limited availability of the prototype adsorbent, the experiments employing SP UpFront were performed in a 1 cm UpFront contactor. In the first set of experiments, the fluidised beds were operated at a constant settled bed height of 15 cm and feedstocks were applied over a range of flow velocities (200 – 400 cm h^{-1}). Panel A in Figure 3.13 (CM HyperD LS) and Figure 3.14 (SP UpFront) depicts the breakthrough curves with respect to L-asparaginase activity achieved at various flow velocities. In addition,

Figure 3.13. Primary purification of L-asparaginase by fluidised bed adsorption from unclarified *Erwinia* disruptate on CM HyperD LS

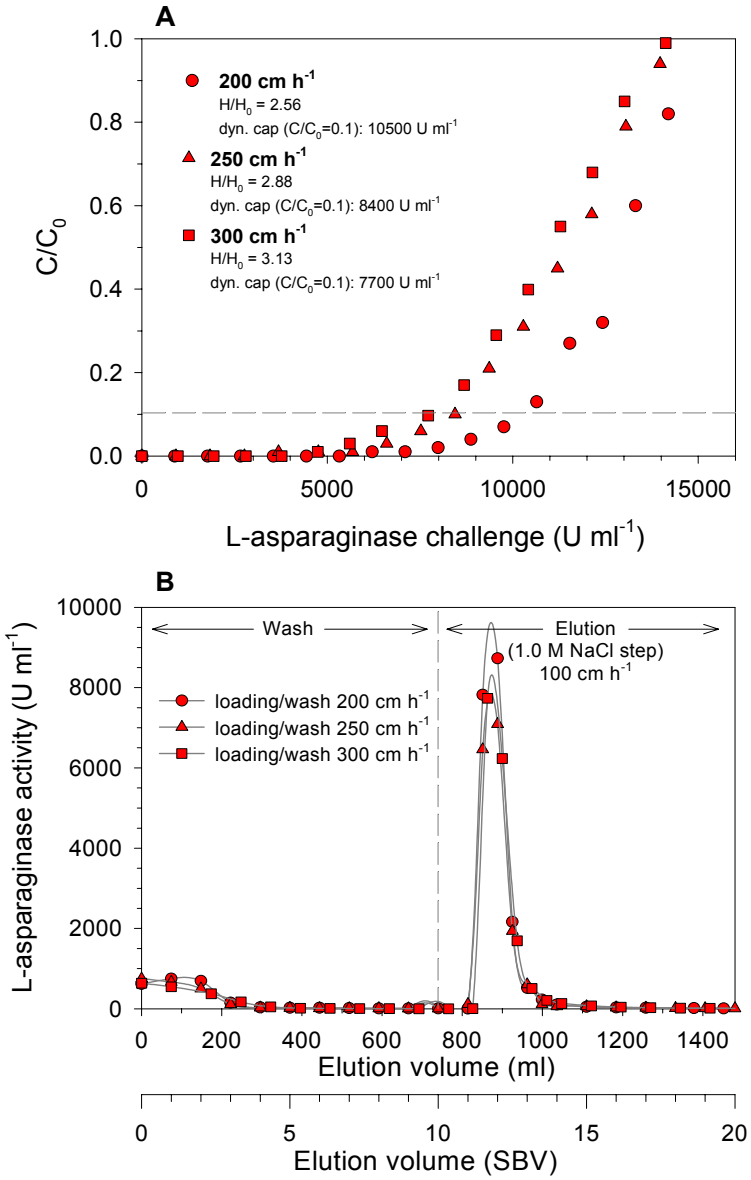

Panel A: Disruptate was previously generated by bead milling and applied to the contactor (BRG 2.5 cm, SBH 15 cm, SBV 74 ml). Estimated dynamic capacities are recorded as the amount of L-asparaginase applied per ml of adsorbent (L-asparaginase challenge) at C/C_0 = 0.1. Panel B: Following the loading to approximate saturation (depicted in panel A) beds were washed using buffer A at the loading flow velocity (initial enzyme activity during the wash corresponds to the feed concentration, C/C0 = 1) . Elution was performed in fluidised bed mode at 100 cm h^{-1} (1 M NaCl step).

Figure 3.14. Primary purification of L-asparaginase by fluidised bed adsorption from unclarified Erwinia disruptate on SP UpFront

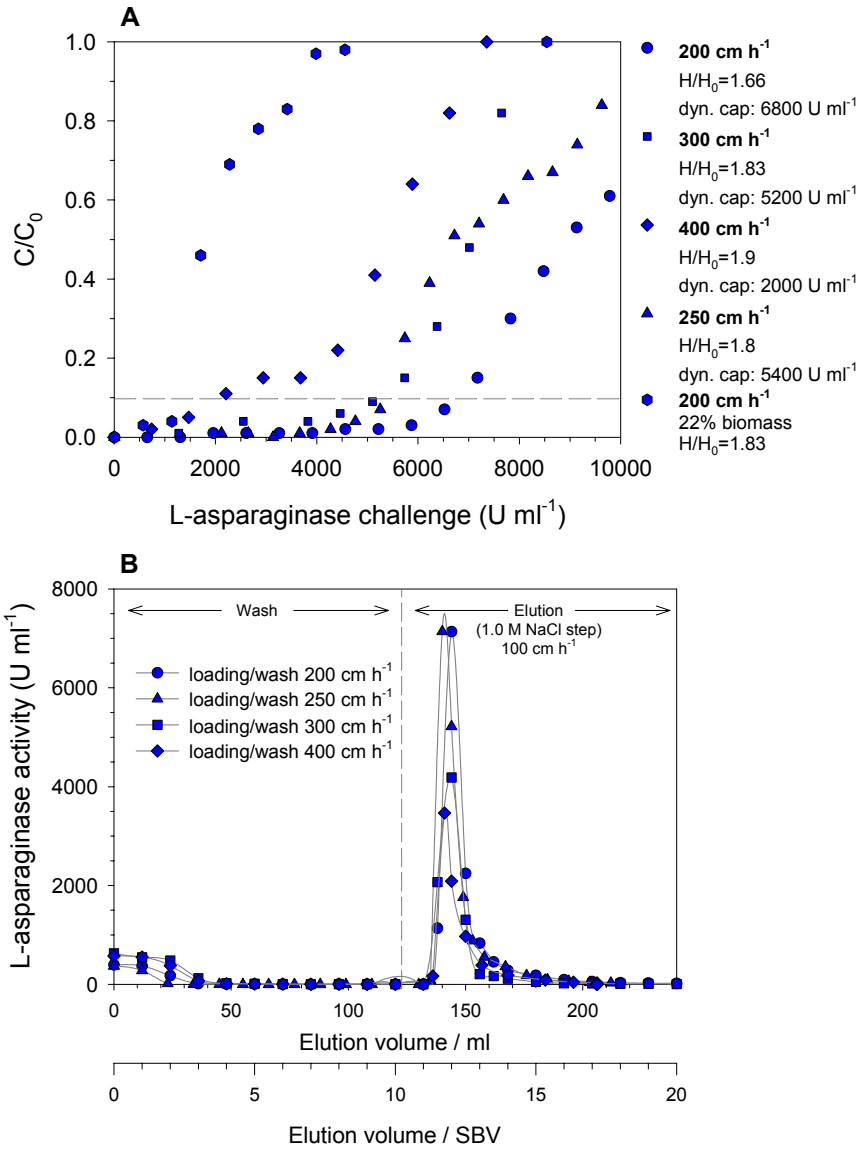

Panel A: Disruptate was previously generated by bead milling and applied to the contactor (UpFront 1.0 cm, SBH 15 cm, SBV 12 ml). Estimated dynamic capacities are recorded as the amount of L-asparaginase applied per ml of adsorbent (L-asparaginase challenge) at C/C_0 = 0.1. Panel B: Following the loading to approximate saturation (depicted in panel A) beds were washed using buffer A at the loading flow velocity (initial enzyme activity during the wash corresponds to the feed concentration, C/C0 = 1) . Elution was performed in fluidised bed mode at 100 cm h^{-1} (1 M NaCl step).

washing and elution profiles of enzyme activity for the beds are shown in panel B of the respective figures. Figure 3.15 summarises the dynamic capacities achieved by the two adsorbents at various flow velocities. Here, in order to facilitate a comparison, the results were normalised to the dynamic capacities (where $C/C_0 = 0.1$) achieved at 200 cm h^{-1} by the respective adsorbent. Productivities were estimated as the amount of enzyme adsorbed at 10% product breakthrough divided by the settled volume of the adsorbent (SBV) and the time required to load, wash and elute the fluidised bed, these result are given in Table 3.3. Additionally, the effect of settled bed height was studied by performing frontal analysis at different settled bed heights (7 – 22 cm) employing a constant loading flow velocity (250 cm h^{-1}). These results are summarised in Figure 3.16.

Table 3.3. Productivities of CM HyperD LS and SP UpFront achieved at various flow velocities

Flow velocity	Productivity CM HyperD LS (U ml^{-1} min^{-1})	Productivity SP UpFront (U ml^{-1} min^{-1})
200 cm h^{-1}	56	42
250 cm h^{-1}	59	43
300 cm h^{-1}	65	46
400 cm h^{-1}	-	26

Loading, washing and elution of the beds is depicted in Figure 3.13 and in Figure 3.14. The productivity at a given flow velocity was estimated as the amount of enzyme adsorbed at 10% product breakthrough (dynamic capacity at $C/C_0 = 0.1$) divided by the settled volume of the adsorbent and the total process time (loading to $C/C_0 = 0.1$ at the respective flow rate; wash of 10 SBV at the respective flow rate; elution of 5 SBV at 100 cm h^{-1}, 100% desorption assumed).

At a constant settled bed height both adsorbents exhibited a gradual decrease in dynamic capacity (estimated from the L-asparaginase challenge required to achieve 10 % breakthrough, i.e. C/C_0=0.1) with increasing flow velocity (see Figures 3.13 and 3.14).

Figure 3.15. Dynamic capacities and fluid residence time of CM HyperD LS and SP UpFront as a function of the superficial flow velocity

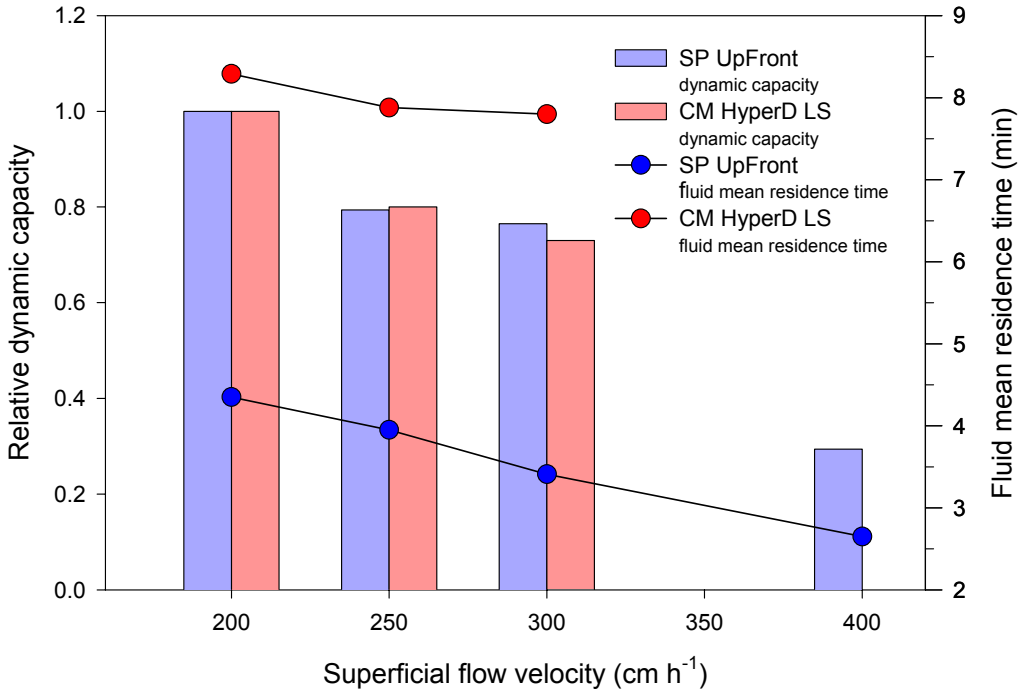

This bar diagram was compiled from data depicted in Figures 3.13 and 3.14. Adsorbent settled bed height was 15 cm (SP UpFront in 1 cm UpFront contactor, CM HyperD in 2.5 cm BRG contactor) whilst Erwinia disruptate (15% biomass ww/v) was used as feedstock. In order to facilitate a comparison, dynamic capacities are normalised relative to that achieved at a loading flow velocity of 200 cm h^{-1}. The mean residence time of a fluid element was calculated using the superficial flow velocity, the fluidised bed height and the bed voidage.

Figure 3.16. Effect if the settled bed height (SBH) on the dynamic capacity of CM HyperD and SP UpFront

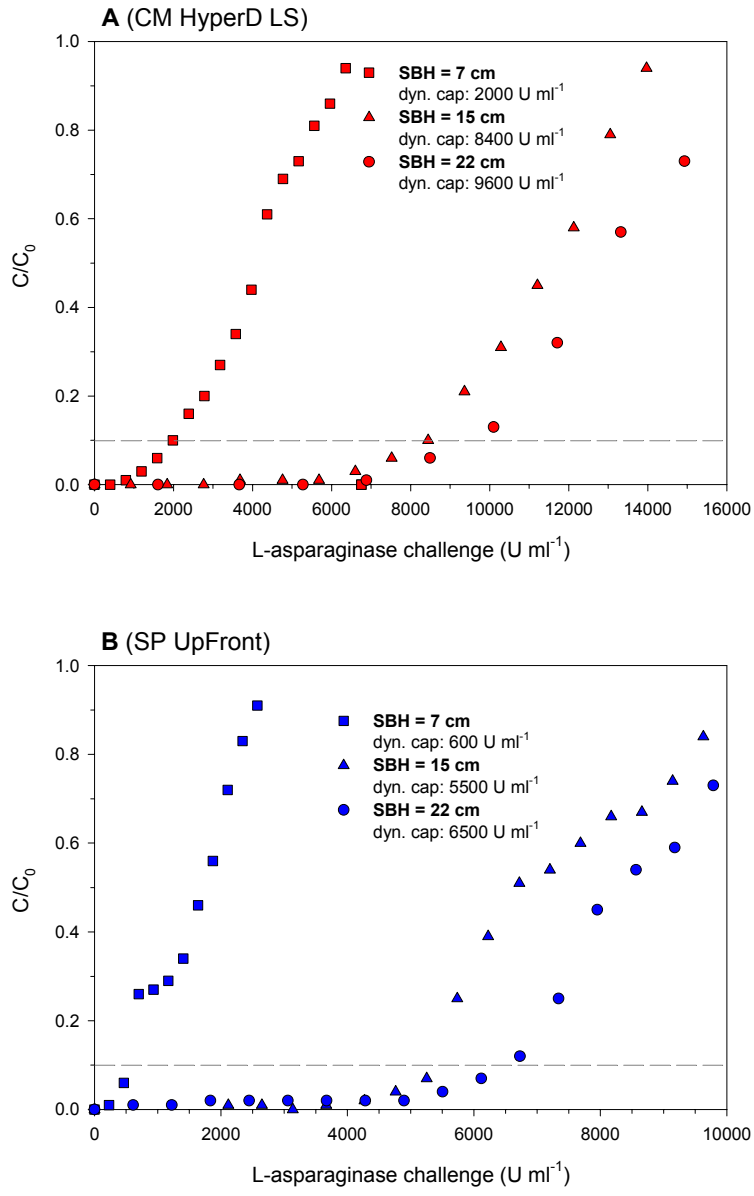

The settled bed heights of the adsorbents are given with the graph symbols. Adsorbents were equilibrated in buffer A and the feedstock (containing 15 % biomass (ww/v) was applied at a linear flow velocity of 250 cm h^{-1}. Estimated dynamic capacities are taken as the amount of L-asparaginase applied per ml of adsorbent (L-asparaginase challenge) at C/C_0 = 0.1. Panel A. CM HyperD LS, BRG contactor, 2.5 cm i.d. Panel B. SP UpFront, UpFront contactor, 1 cm i.d.

Estimated productivities varied only to a small degree with operating flow velocities (summarised in Table 3.3). Here, shorter processing times at higher flow velocities (during loading and washing) compensated for decreases in dynamic capacities. Both adsorbents appeared to be equally affected by the increase in superficial flow velocity. This became apparent as a proportional decrease in capacity after normalising the dynamic capacity results (Figure 3.15). Increasing the loading flow velocity from 200 to 300 cm h^{-1} resulted in a throughput increase of 50%, whereas the dynamic capacities of the adsorbents were only reduced by 24% (SP UpFront) and 27% (CM HyperD) respectively. This was judged acceptable in the face of a 50% increase in throughput and was also reflected by an increase in productivity (see Table 3.3). For SP UpFront the degree of bed expansion at a given flow velocity and likewise the bed voidage were considerably lower in comparison with CM HyperD owing to its higher specific weight (see Figure 3.4 and legends in Figure 3.13 and 3.14). Consequently, the interstitial velocities within the fluidised beds were higher which in combination with a reduced bed height resulted in greatly reduced mean residence times of a unit volume of feedstock (given in Figure 3.15) within the fluidised beds. However, the higher uptake rate of SP UpFront (Figure 3.8) appeared to compensate for the shorter contact times since both adsorbents exhibited similar influences of the flow velocity on their respective adsorption performances.

The dynamic capacities achieved with CM HyperD LS in the 2.5 cm BRG contactor were lower in comparison with the experiments performed in the 1 cm UpFront contactor (see Figure 3.10) which indicated a higher degree of axial mixing in the BRG contactor. At higher flow velocities, i.e. 300 cm h^{-1}, the top of the fluidised bed became increasingly diffuse which aggravated the determination of the true value of the expanded bed height (EBH). Also, small amounts of adsorbent particles were elutriated from the bed and could be found in the flow-

through. This suggested that a linear flow velocity of 300 cm h^{-1} approached the upper limit for operating CM HyperD under the given feedstock viscosity (that represented a disruptate generated from 15% biomass).

For SP UpFront, a loading flow velocity of 400 cm h^{-1} resulted in early product breakthrough and a clear reduction in dynamic capacity and productivity. Also included in Figure 3.14 is a data plot which depicts the loading of a disruptate containing 22% biomass ww/v at 200 cm h^{-1}. Here, immediate high breakthrough of product occurred even at a comparatively low loading velocity. Visual inspection of the bed revealed extensive channelling which suggested that the increased viscosity associated with elevated biomass loading adversely affects the bed stability and thus the adsorption process. Similar effects, i.e. the development of flow channels and particle elutriation, were reported by Barnfield-Frej *et al.* (1994) when STREAMLINE DEAE was challenged with *E. coli* homogenate containing more than 8% biomass (dry weight).

Figure 3.16. depicts the effect of the adsorbent settled bed height upon adsorption performance. Again, CM HyperD and SP Upfront exhibit a similar behaviour. At a settled bed height of 7 cm, L-asparaginase breakthrough began significantly earlier than at 15 or 22 cm. The experiments at 15 cm SBH showed a characteristic breakthrough curve, i.e. a prolonged phase of negligible product breakthrough followed by an approach to saturation with a significant increase in enzyme levels in the outlet stream. A further increase in SBH from 15 to 22 cm resulted in only a slight increase in dynamic capacity of 14 % for CM HyperD and 20 % for SP UpFront. Similar results were reported by Hjorth *et al.* (1995) employing STREAMLINE SP for the adsorption of lysozyme. It was found that the dynamic capacity increased considerably when the settled bed height was increased from 5 cm to 10 cm. Further increases in settled bed height up to 30 cm resulted in a less pronounced increase in

breakthrough capacity. RTD analysis performed at the settled bed heights employed for frontal analysis experiments (7, 15, and 22 cm) revealed increased HETP values, i.e. increased axial dispersion, with decreasing settled bed heights (Hjorth *et al.*, 1995). This suggested that the reduced dynamic capacity found at a SBH of 7 cm was caused by an increased degree of axial dispersion, possibly caused by uneven flow distribution. These flow irregularities were incrementally dampened with increasing SBH, reflected both by the decrease in HETP at a given flow velocity (refer to Figure 3.17) and a considerable increase in dynamic capacity at 15 SBH (panel A, Figure 3.16.). These results suggested that for both adsorbents a minimum settled bed height was required for an economic exploitation of the adsorbent capacity. Here, a SBH of 15 cm yielded satisfactory results and dynamic capacities could be improved only slightly by a further increase in SBH.

For both adsorbents, a wash volume of 5 settled bed volumes, applied at various flow velocities, was normally sufficient to reduce the concentration of contaminating debris (as judged from the total protein concentration, see Section 2.2.4) in the effluent of the fluidised bed by more than 95% (see panels B in Figure 3.13 and 3.14). Despite the reduction in dynamic capacity of CM HyperD LS during the scale-up from the 1 cm BRG to the 2.5 cm BRG contactor (see Figures 3.10 and 3.13) the elution volume remained constant at approximately 2 settled bed volumes (step elution employing 1 M NaCl in fluidised bed mode at 100 cm h^{-1}). Table 3.4 summarises data concerning the eluates obtained from the two adsorbents. It can be seen that the recovery values were consistently high ranging between 70 and 86% of the adsorbed enzyme recovered in the peak eluted fractions. Specific activities and purification factors exhibited some variation which might be attributed to the use of different batches of cell paste necessarily employed in the feedstock preparation.

Table 3.4. Eluates obtained from CM HyperD and SP Upfront

Experiment	loading/ wash (cm h^{-1})	Feed enzyme activity (U ml^{-1})	Feed total protein (mg ml^{-1})	Feed specific activity (U mg^{-1})	Eluate enzyme activity (U ml^{-1})	Eluate total protein (mg ml^{-1})	Eluate specific activity (U mg^{-1})	Purif. factor	Recovery (%)
CM HyperD	200	430	5.58	77	6169	16.02	385	5.0	76
	250	561	5.66	99	5368	11.51	466	4.7	76
	300	489	5.89	83	5233	12.54	417	5.0	82
SP UpFront	200	663	6.37	104	3562	5.96	598	5.7	75
	250	525	5.96	88	3892	7.37	528	6.0	86
	300	638	6.07	105	2489	5.65	441	4.2	80
	400	504	5.54	91	2346	5.46	430	4.7	70

This table was compiled from the loading and the elution of fluidised beds employing CM HyperD LS and SP UpFront at various flow velocities (as depicted in Figures 3.13 for CM HyperD and 3.14 for SP UpFront). Data given for the eluates represent the pooled fractions of the respective elution peak (depicted in panel B of Figures 3.13 and 3.14).

$$\text{Purif. factor} = \frac{\text{eluate specific activity}}{\text{feedstock specific activity}}$$

$$\text{Recovery} = \frac{\text{total enzyme activity in eluate}}{\text{total enzyme adsorbed}}$$

$$\text{total enzyme adsorbed} = \sum \text{flowthrough fraction volume} \cdot (C_0 - C_{\text{fraction}})$$

Figure 3.17. Axial dispersion of CM HyperD LS at different settled bed heights

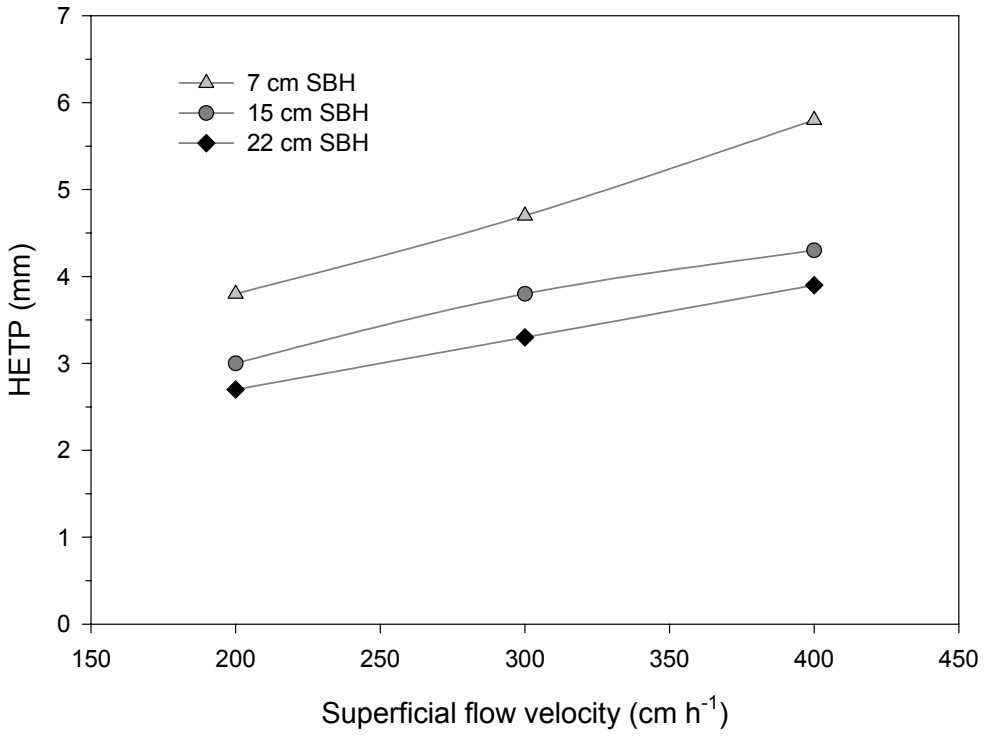

The adsorbent was fluidised in a 4.5 cm BRG contactor. The number of theoretical plates was calculated from a negative step input signal using a dilute acetone solution as a tracer (see 3.2.4 for test procedure).

3.4 Interim conclusions

Candidate adsorbents for the FBA of L-asparaginase from *Erwinia* disruptates were physically characterised, i.e. their bed expansion and axial dispersion characteristics were studied. Scouting experiments were performed which investigated the adsorption capacity of cation exchange adsorbents for L-asparaginase as a function of disruptate pH. Two cation exchange adsorbents, the hyper-diffusive CM HyperD LS and the pellicular SP UpFront, were employed in a side-by-side comparison which demonstrated the feasibility of the fluidised bed capture of L-asparaginase from unclarified *Erwinia* disruptates. The adsorption characteristics, i.e. uptake rate and equilibrium binding capacity, of the two adsorbents were investigated in batch binding experiments and the effect of loading flow velocity and adsorbent settled bed height on the dynamic capacity were studied using frontal analysis.

It was found that the elevated viscosity of biomass-containing feedstocks, such as yeast or bacterial disruptates, significantly increased the expansion of a fluidised bed in comparison with fluidisation in buffer solutions. An increased viscosity may limit the operational window of a fluidised bed process with regard to loading flow velocity for a given adsorbent, characterised by its particle density and size range. Such a limitation was identified for CM HyperD LS when unclarified *Erwinia* disruptate (15% biomass ww/v) was loaded into a fluidised bed at 300 cm^{-1}. Here, the surface of the fluidised bed became increasingly diffuse and small amounts of adsorbent particles were elutriated from the bed. In addition, high feedstock viscosity may compromise stable fluidisation and lead to poor adsorption performance (e.g. see Figure 3.14 for the application of a 22% ww/v *Erwinia* disruptate). Increased particle density, e.g. by the incorporation of heavy filler materials such as stainless steel in SP UpFront, considerably decreased the degree of bed expansion at a given linear flow velocity. Such adsorbent properties enable the use of higher flow velocities and/or the

use of higher feedstock viscosities and thus facilitate the maximisation of biomass throughput. RTD analysis indicated reduced HETP values with increasing particle density (Figure 3.5). Due to their superior fluidisation characteristics, CM HyperD and SP UpFront were targeted for further experimentation. Due to a comparatively low particle density, it was expected that materials such as STREAMLINE (1.2 g ml^{-1}) would be less suitable for the application with *Erwinia* disruptates since operating flow velocities and/or biomass loadings would be more restricted.

Batch binding experiments employing *Erwinia* disruptate at various pH values revealed a narrow window of operation with regard to pH for the effective adsorption of L-asparaginase by cation exchange adsorbents. Low pH values, i.e. below 5.0 were characterised by increased adsorption of L-asparaginase and the tendency of the disruptate to form precipitates which were capable of clogging mesh distributors or narrow column fittings. However, matrix capacities were diminished when pH 6.0 was approached. Thus, a pH of 5.5 was chosen as a trade-off between matrix capacity and reduced adsorption of L-asparaginase to cell debris.

In a side-by-side comparison of CM HyperD LS with SP UpFront adsorbents, batch binding experiments revealed a higher uptake rate for the pellicular SP UpFront. However, the equilibrium capacity of CM HyperD turned out to be considerably higher owing to the structural differences of the adsorbents (i.e. a greater volumetric capacity for the latter) combined with a higher ligand concentration. The use of disruptate reduced the adsorbent capacities for L-asparaginase considerably in comparison to the adsorption of purified enzyme from buffer solution. However, clarified and unclarified disruptates yielded corresponding dynamic capacities and thus, debris/adsorbent interactions appeared to be minimal. Despite their different adsorption characteristics, the dynamic capacities of both adsorbents were

equally affected by variations in flow rate and settled bed height during frontal analysis. Here, the higher uptake rate of SP UpFront found in batch binding experiments, did not turn out to be exploitable under the given experimental conditions. This might be attributed to the considerably shorter liquid residence times in fluidised beds comparison with CM HyperD due to a lower degree of bed expansion. For both adsorbents, step elution in expanded bed mode yielded consistently high elution efficiencies and peak volumes which were equivalent to packed bed elution.

The two adsorbents employed in this study exhibited different characteristics which can be separately exploited to benefit specific process requirements. On the one hand, CM HyperD LS, representing a macroporous, hyper-diffusive continuum, distinguished itself by its high capacity for L-asparaginase but was restricted with regard to operating flow velocity by a moderate density. However, due to its commercial availability and its advantages with regard to binding capacity, CM HyperD LS was expected to perform best in integrated recovery experiments (see Figure 1.5) and was thus used exclusively used for further experimentation.

The pellicular SP UpFront, on the other hand, is ideal by virtue of its elevated density for applications with high flow velocities and/or high viscous feedstocks. A reduced bed expansion, achieved by increased particle density can improve the economical use of a fluidised bed contactor, i.e. a given amount of matrix required comparatively less contactor volume during operation. The mass transfer characteristics of the pellicular structure also encourage novel routes to the design of an adsorptive step in downstream processing. For example, it would be conceivable to process a batch of feedstock by using a manifold of appropriately down-scaled fluidised beds which could be characterised by short cycle times of adsorption, desorption and cleaning/re-equilibration (Morton and Lyddiatt, 1994a). These

beds would be operated in such a way that one bed is used for product adsorption while others are being eluted or re-equilibrated for re-use in processing the same batch of feedstock (see Figure 3.18). Advantages of such a multi-bed system would be a reduced adsorbent inventory, short residence times for feedstocks and applicability with both fermentation and disruption operations. Hamilton *et al.* (1999) reported the successful implementation of multiple fluidised beds as an external loop to a productive bioreactor for the direct product sequestration of an extracellular protease integrated with the fermentation process. Dense, pellicular adsorbents, operated at high fluid velocities and viscosities with low bed expansions and rapid adsorption/desorption rates appear to be ideal for such applications and are the subject of further study (Jahanshahi and Lyddiatt, personal comm.).

Figure 3.18. Principle of a multi-fluidised bed system.

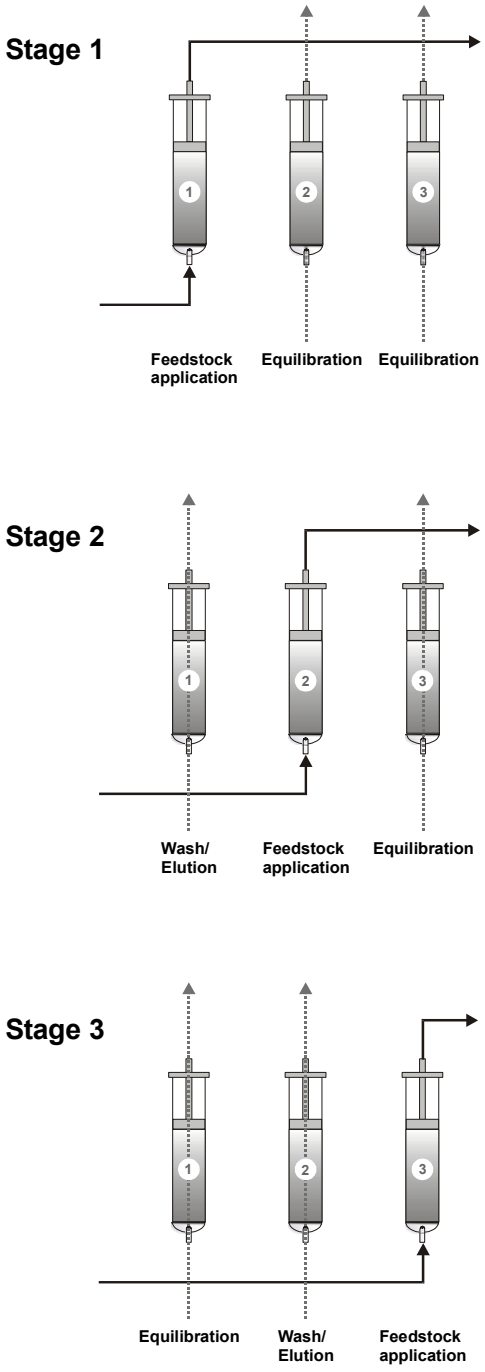

In a system of appropriately down-scaled fluidised beds, feedstock is continuously fed into a fluidised bed previously primed for adsorption. Saturated beds are taken off-line, eluted and reused for adsorption

4 PROCESS INTEGRATION OF CELL DISRUPTION AND FLUIDISED BED ADSORPTION

4.1 Introduction

Adsorption in expanded or fluidised beds is now widely adopted for the direct recovery of protein products from particulate feedstocks. As an integrative protein recovery operation it circumvents process bottlenecks encountered with the solid liquid separation required upstream of fixed bed adsorption, whilst achieving considerable concentration and primary purification of products(Hjorth, 1997). For example it has been demonstrated that the use of fluidised bed adsorption reduced the cell concentration in the eluted fraction by a factor of 10^4 – 10^5 (Hjorth *et al.*, 1995) which is at least one to two orders of magnitude higher than that for industrial centrifuges (10^2 – 10^3, claimed by Datar and Rosen (1996). However, such technology still employs discrete upstream operations of fermentation or cell disruption, and is commonly characterised by potentially detrimental hold-up periods whilst batches of feedstock are accumulated and/or conditioned prior to fluidised bed processing. Hold-up risks product modification, inactivation or degradation by system antagonists such as proteases, carbohydrases and drifting physical conditions of temperature, pH and ionic strength (Kaufmann, 1997). Consequently, a logical physical coupling of fluidised bed adsorption with upstream operations of fermentation or cell disruption might be predicted to gain additional benefits of product yield and quality by virtue of the immediate and direct sequestration of products from process feedstocks at source (Hamilton *et al.*, 2000; Bierau *et al.*, 1999).

Direct product sequestration (DPS) of extracellular molecules from productive bioreactors can be achieved by the operation of a fluidised bed of product-selective adsorbent in an external loop by broth recirculation. It has the potential to minimise product degradation

and increase overall yield by acting as a product sink for proteins regulated by feedback inhibition (Morton and Lyddiatt, 1994a). This was clearly demonstrated by Hamilton *et al.* (1999) by the employment of a manifold of fluidised beds attached to a bioreactor for the primary purification of an extracellular acid protease produced by *Yarrowia lipolytica*. Here, a threefold increase in enzyme productivity and the elimination of product autolysis was achieved. Similar advantages were noted with the DSP of α-amylase from fermentations of *Bacillus amyloliquifaciens* exploiting a manifold of fluidised beds (Burns, 1997). The use of a manifold of contactors, wherein one acts as an external loop whilst others are variously exposed to off-line wash, desorption, and/or re-equilibration, has the advantage of minimising the volume of the external loop. Such a strategy minimises the time spent by producer cells outside the controlled environment of the bioreactor, thereby reducing physiological stress together with the adsorbent inventory required to service a productive fermentation.

During the purification of intracellular microbial enzymes, cell disruption by mechanical or (bio)chemical means is the first step required in the process (refer to Figure 1.1). However, it commonly initiates cellular and molecular degradation processes, analogous to those of natural cell death and lysis, due to the disintegration of intracellular compartments which confine lytic enzymes (Kaufmann, 1997; Middelberg, 1995). In addition, the generation of fine cell debris may promote electrostatic and/or hydrophobic product-debris interactions (see Section 2.3.3.3). Such adverse effects will compromise the yield and molecular fidelity of protein products, particularly when feedstocks are accumulated and processed in time-dependent batch operations. Proteolytic activity may be restrained by the addition of specific inhibitors. However, due to the complexity and diversity of different host organisms such measures are haphazard. Consequently, rapid processing for example by the direct product sequestration at cell disruption should minimise such degradation and enhance

the yield and quality of even the most labile products. Here, instead of accumulating a disruptate in a holding tank, the product remains in its physiological environment, i.e. the intact cell, as long as possible and is exposed to the adsorbent immediately after its release from the cell in the disrupter. Contact times between the target molecule and the disruptate are thus minimal.

Mechanical cell breakage in a bead-mill has many attractive process characteristics including high disruption efficiency, high throughput and biomass loading, good temperature control and unlimited scale-up for most bioprocesses (see Chapter 2). In addition, the operational characteristic of single-pass and continuous operation recommends the bead mill as the ideal feedstock generator for direct sequestration of released products in a fluidised bed.

This chapter summarises experiments which seek to demonstrate the feasibility of the integration of cell disruption by bead milling with product capture by fluidised bed adsorption. In the first place, a study of the primary purification of the enzyme G3PDH from brewers' yeast exploiting Cibacron Blue Macrosorb is reported (see Section 4.3). Here, the practical objective was to method scout global problems of the coupled handling of the two unit operations whilst preserving precious stocks of *Erwinia* cell paste. Subsequently, the integrated primary purification of L-asparaginase from *Erwinia* disruptates exploiting cation exchange adsorbents was investigated (see 4.3.1). This study included the comparison of different scaled-up versions of fluidised bed contactors (UpFront contactor, 5 cm i.d., and BRG contactor, 4.5 cm i.d.) with regard to flow distributor design (RTD analysis, see 4.3.2.1) and frontal analysis (4.3.2.2). The purity of partially purified L-asparaginase by fluidised bed adsorption was compared with samples derived from a conventional production process by SDS PAGE analysis in tandem with activity and total protein assays. In addition, the phenomenon of L-asparaginase adsorption to cell debris (see Section 2.3.3.3) was re-

investigated. Here, the objective was to assess to what extent the immediate exposure of the disruptate to the adsorbent (as in integrated disruption/adsorption) reduces enzyme losses through unwanted adsorption to cell debris by competitively shifting the adsorption equilibrium towards positive capture on fluidised bed adsorbents (see 4.3.2.3).

4.2 Materials and methods

4.2.1 Fluidised bed contactors

Two different contactors were used in the experiments described here. A commercially available contactor (UpFront Chromatography, 5 cm i.d.) and the custom-built BRG contactor (Biochemical Recovery Group, School of Chemical Engineering, University of Birmingham, 4.5 cm i.d.) was employed. A schematic depiction of the contactors is given in Figure 4.1.

The UpFront contactor distributed the feed by a motor-driven stirrer paddle located near the feedstock inlet in the bottom of the column. Effluent left the contactor via a glass tube which was adjustable in height and was sealed airtight in the top lid. In contrast, the BRG contactor comprised a hemispherical inlet port which was clamped to the glass column. This configuration allowed the inclusion of a mesh (e.g. stainless steel, 98 μm) between the inlet and the column for the support of the settled adsorbent bed and distribution of the incoming flow. As an alternative method for flow distribution, a short bed of glass beads could be used filling the hemispherical inlet and the column (2 cm height). The BRG contactor was also fitted with an adjustable top adapter (plunger) in order to minimise headspace.

4.2.2 Immobilisation of Cibacron Blue 3GA on Macrosorb K6AX

Cibacron Blue was immobilised onto Macrosorb K6AX using a method described by Dean and Watson (1979). 100 ml of base matrix was suspended in 100 ml of deionised water.

Figure 4.1. Fluidised bed contactors used for process integration experiments

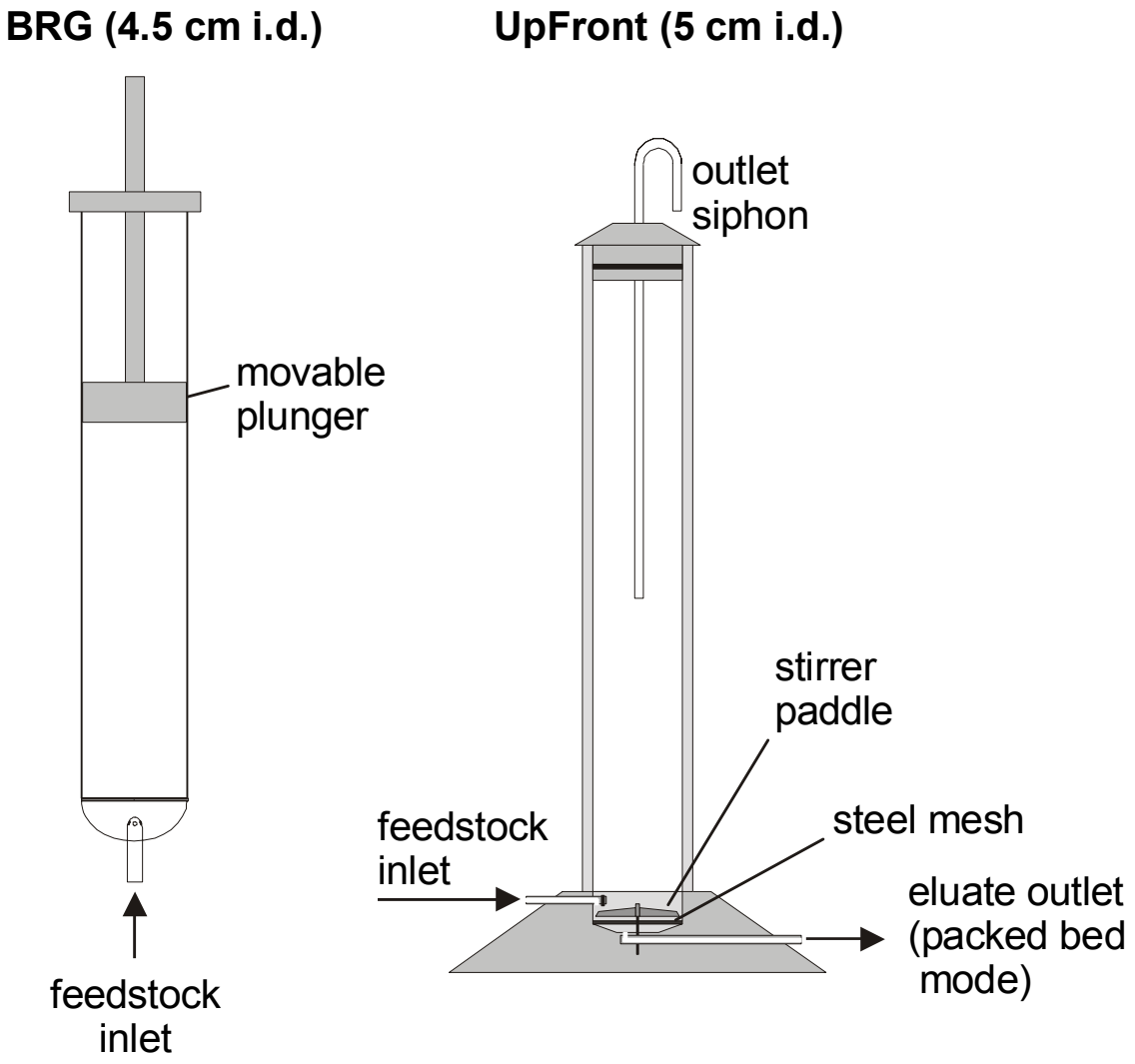

Two different fluidised bed contactors were used, the commercially available UpFront contactor (UpFront Chromatography, 5.0 cm i.d.) and the custom built BRG contactor (Biochemical Recovery Group, School of Chemical Engineering, University of Birmingham, 4.5 cm i.d.). Flow distribution in the UpFront contactor was achieved by a motor-driven stirrer paddle located in the bottom of the column. The hemispherical inlet of the BRG contactor, attached to the column by a clamp, allowed different flow distributor designs, e.g. a stainless steel mesh and/or a bed of glass beads.

3.0 g of Cibacron Blue 3GA was added and the suspension was mixed for 15 min to dissolve the dye powder. 30 g of sodium chloride was added and the suspension was mixed for a further 30 min. Then 120 ml of sodium carbonate (1 M) was added and mixed for 5 min. The mixture was transferred into a round bottom flask which was attached to a rotary mixing unit. The flask was semi-submerged in a water bath at 65 °C and incubated for 24h under rotational mixing. After the incubation, the adsorbent was separated from spent reactants by filtration through a sintered funnel. Unbound dye was washed from the adsorbent with hot and cold deionised water. Weakly bound dye was removed from the adsorbent by a cycle of protein adsorption (BSA) and subsequent chaotropic (KSCN) elution (Gilchrist, 1996). Here, the adsorbent was packed into a chromatography column and 100 ml of BSA (1 mg ml^{-1}) in buffer A (10 mM Tris/HCl, pH 7.5) was loaded onto the adsorbent bed. Elution of the protein, together with weakly bound dye, was achieved by the irrigation of the adsorbent with 100 ml of 3 M potassium thiocyanate (KSCN) in buffer A. The adsorbent was subsequently equilibrated using buffer A.

4.2.3 Integrated cell disruption by bead milling and fluidised bed adsorption of target molecules

4.2.3.1 Primary purification of G3PDH from brewers' yeast

The bead mill was a *DYNO MILL KDL-I* model (Willi A. Bachofen AG, Switzerland, refer to Figure 2.2) consisting of a glass chamber cooled by re-circulating iced water (0 °C) from a reservoir. The chamber was loaded with glass beads (0.2-0.5 mm) to 83% settled volume occupancy. The agitator speed was 3200 rpm corresponding to a peripheral speed of the agitating discs of 10.5 m s^{-1}. Waste brewers' yeast was thawed overnight below 4 °C in buffer A (10 mM Tris/HCl, pH 7.5 containing 1 mM EDTA). The temperature of the

suspension was maintained below 4 °C by storage in an ice bath. In integrated experiments, cell suspension (15 % ww/v herein) was fed to the mill by a peristaltic pump at a flow rate of 4.05 l h^{-1} and the temperature of the disruptate was maintained at the outlet of the chamber between 21 and 22 °C. In order to achieve an experimental steady-state condition with regard to effluent protein and G3PDH concentrations, the first 5 chamber volumes of effluent were discarded before switching the disruptate to the contactor (see 3.2.1, BRG contactor, 4.5 cm i.d., flow distribution by glass beads 3.5 – 4.5 mm and a 98 µm stainless steel mesh) containing the adsorbent (Macrosorb K6AX Cibacron Blue, see 4.2.2, equilibrated and fluidised in buffer A, SBH 15.5 cm). After loading of the disruptate, the adsorbent bed was washed using buffer A until a clear effluent, judged by visual inspection, was achieved. Subsequently, the adsorbent was allowed to settle and elution of bound solutes was achieved under reversed flow in four stages (elution with 0.2 M NaCl, re-equilibration in buffer A, elution with 0.25 M KSCN, adsorbent cleaning in 3 M KSCN).

4.2.3.2 Primary purification of L-asparaginase from *Erwinia*

Cell disruption was performed by bead milling according to methods established earlier (refer to Chapter 2). A Dyno Mill KDL-I (Willi A. Bachofen AG, Switzerland) was employed consisting of a silicon-carbide lined stainless steel chamber (600 ml) cooled by re-circulating iced water (0°C). The chamber was loaded with zirconia beads (0.3 mm) to 83% settled volume occupancy. The agitator speed was 3200 rpm corresponding to a peripheral tip speed of the agitating discs of 10.5 m s^{-1}. Frozen cells were thawed and resuspended in equilibration buffer (buffer A, 20 mM citric acid / tri-sodium citrate, pH 5.5). The cell suspension was adjusted to a pH of 5.5 (20 mM citric acid) and a biomass concentration of 15% wet weight per volume (ww/v). Cell suspension was fed to the mill by a peristaltic pump at a flow rate of 4.05 l h^{-1}. The disruptate was directly fed from the bead mill into the fluidised bed contactor

(BRG 4.5 cm, UpFront 5.0 cm). Prior to the application of feedstock all beds were fluidised at the loading flow velocity. After loading of the disruptate, the adsorbent bed was washed using buffer A (10 SBV). Elution was routinely performed in fluidised bed mode using buffer B (20 mM citric acid / tri-sodium citrate, pH 5.5, 1 M NaCl).

4.2.4 G3PDH activity assay

The enzyme activity was estimated by a method developed by Stallcup (1972) and adapted by Byers (1982) and Gilchrist (1996). The physiological reaction catalysed by G3PDH can be summarised as follows:

(1) D-glyceraldehyde 3-phosphate + NAD^+ + P_i $\longleftrightarrow$ 1,3-diphosphoglycerate + NADH + H^+

However, the assay is based on the arsenolysis reaction introduced by Warburg and Christian (1939) and described by Velick (1955).

(2) D-glyceraldehyde 3-phosphate + NAD^+ + P_i $\xrightarrow{HAsO_4^{2-}}$ 3-phosphoglycerate + NADH + H^+

Reaction (2) is preferred to the physiological reaction (1) due to its irreversible nature since the immediate product 1-arseno-3-phosphoglycerate is rapidly hydrolysed. This allows for a convenient and efficacious assay for G3PDH. The production of NADH was monitored spectrophotometrically (Pharmacia Ultraspec III) at 340 nm using a software package designed for enzyme kinetic studies (Viglen Ltd). An appropriate concentration of G3PDH produced a linear increase of NADH in the assay mixture. This increase was recorded and the slope of the curve was used to calculate enzyme activity of the sample.

Table 4.1 lists the reagent solutions required for the assay. An assay mixture containing 10 µl of enzyme solution, 100 µl of NAD^+, 50 µl of sodium arsenate solution and 790 µl of bicine buffer (pre-warmed, 25 °C) was incubated at 25 °C for 3 minutes and the reaction was

initiated by the addition of 50 µl of the D-G3P solution. The mixture was then immediately transferred into a quartz cuvette and the conversion of NAD+ to NADH (i.e. the increase in absorption at 340 nm) was recorded. Using the slope of the curve in a 30 sec interval (e.g. 15 – 45 sec after initiation) the enzyme activity in the sample could be calculated using the molar extinction coefficient (E) for NADH of 6.3 x 0^3 M^{-1} cm^{-1}. The unit of enzyme activity was designated as the number of µmoles of NADH produced minute at 25 °C per ml of solution. (IU ml^{-1}). The specific activity was defined as the enzyme activity per mg pf total protein (IU mg^{-1}).

Table 4.1. Reagents for the G3PDH assay

Reagent	Ingredients		
Bicine buffer	50	mM	Bicine (N,N-bis 2-hydroxyethyl glycine, Sigma Chemicals, Poole, UK)
	1	M	sodium acetate
	1	1 mM	EDTA
			pH adjusted to 8.5 using 1 M NaOH, buffer was stored at 4 °C
NAD^+	10	mM	NAD^+ (Sigma Chemicals, Poole, UK), concentration was determined spectrophotometrically at 260 nm (E=1.73 x 10^4 M^{-1} cm^{-1} (Haid, 1974), pH adjusted to 4.0, aliquots were stored at –20 °C.
Sodium arsenate	0.5	M	Na_2HAsO_4 (Sigma Chemicals, Poole, UK), pH adjusted to 8.5 (1 M HCl), solution was stored at 4 °C
Substrate (D-G3P)	20	mM	DL-Glyceraldehyde 3-phosphate (DL-G3P, Sigma Chemicals, Poole, UK). The concentration of the D-G3P enantiomeric form of the substrate was determined enzymatically by oxidation in Bicine buffer (pH 8.5) containing 25 mM arsenate and sufficient pure G3PDH to completely oxidise the D-enantiomer in 3 minutes. The substrate solution was then diluted with deionised water to yield a 20 mM solution. Aliquots were stored at – 20 °C.

4.2.5 Gel electrophoresis (SDS-PAGE)

Protein composition profiles of specific samples and fractions were analysed and compared by sodium dodecyl sulphate polyacrylamide gel electrophoresis (SDS-PAGE).

Gradient gels (8 – 18 % acrylamide, 1.5 mm) were cast and run in a vertical slab electrophoresis chamber (Protean II xi, Bio-Rad, California, USA). Low molecular weight markers (LMW, Pharmacia, Uppsala, Sweden: phosphorylase b 94 kD, albumin 67 kD, ovalbumin 43 kD, carbonic anhydrase 30 kD, trypsin inhibitor 20.1 kD, β-lactalbumin 14.4 kD) were included in the gels.

Gradient solutions were prepared according to Table 4.2. Ammonium persulphate solution was added last to initiate the polymerisation. The resolving gel was poured into the chamber using a gradient former. During polymerisation (approximately 30 min) the surface of the gel was covered with a layer of water-saturated butanol. After polymerisation, the surface of the gel was washed with water to remove the butanol. A stacking gel was cast on top of the resolving gel (see Table 4.2). Sample wells in the stacking gel were formed by inserting template combs. Polymerisation of the stacking gel required approximately 1 h.

Table 4.2. Gel composition for SDS-PAGE gradient gels

Component	Resolving gel		Stacking gel
	Gradient solution 1 8% acrylamide	Gradient solution 2 18% acrylamide	
Acrylamide-bisacrylamide (30% w/v acrylamide, 2 % bis-acrylamide)	3.2 ml	7.2 ml	1.2
Resolving gel buffer (Tris/HCl, 3 M, pH 8.8)	1.5 ml	1.5 ml	-
Stacking gel buffer (Tris-HCl, 0.5 M, pH 6.8)	-	-	2.5 ml
SDS (10% w/v)	120 µl	120 µl	100 µl
Deionised water	6.8 ml	2.8 ml	5.65 ml
Sucrose	-	1.8 g	-
TEMED ($N_1N_1N_1'N'$ tetramethyl ethylendiamine)	5 µl	5 µl	10 µl
Ammonium persulphate (30 mg ml^{-1})	280 µl	280 µl	500 µl

The gels were placed into the electrophoresis tank and immersed into running buffer (3.03 g l^{-1} Tris, 14.4 g l^{-1} glycine, 1 g l^{-1} SDS). Protein samples and standard markers were treated by solubilisation and denaturation in reducing buffer (62.5 mM Tris-HCl pH 6.8, 10% v/v glycerol, 2% w/v SDS, 5% v/v β-mercaptoethanol, 0.05% w/v bromphenol blue) and boiled for 5 min. Gels were run at 150 V until the dye front penetrated the stacking gel to the resolving gel. The voltage was then increased to 300 V and the run was terminated when the dye front reached the bottom of the gel.

Gels were stained in staining solution (41.7% v/v deionised water, 41.7% v/v methanol, 16.7% v/v glacial acetic acid, 0.1% w/v Coomassie Blue R-250 1 g) for approximately 1 h. Then the gel was developed in destaining solution (82.5% v/v deionised water, 10% v/v methanol, 7.5% v/v glacial acetic acid until clear protein bands appeared and the background staining was removed. The gel was then immersed into shrinking solution (50% v/v deionised water, 48% v/v methanol, 2% v/v glycerol) over night.

4.2.6 Flow distributor comparison by RTD analysis

RTD analysis was performed employing fluidised bed contactors with different flow distributor configurations. The BRG contactor was either fitted with a stainless steel mesh (98 μm) clamped between the column and its hemispherical inlet, or with beds of glass beads (3.5 – 4.5 mm and 710 – 1180 μm) filling the inlet and the column up to a height of 2 cm (refer to Figure 4.1). In addition, the local stirring by a motor driven paddle in the UpFront contactor was tested. A bed of CM HyperD LS at a constant settled bed height of 15 cm was fluidised in buffer A at two linear flow velocities. RTD analysis was performed as described in Section 3.2.4. The number of theoretical plates was calculated and expressed in terms of theoretical plates per meter of expanded bed (see Figure 4.8).

4.2.7 Diafiltration of CM HyperD LS eluates

Diafiltration of eluates from the fluidised bed was performed in a Millipore Minitan cross-flow system using a 30 KDa MWCO membrane (6 cassettes, 0.06 m^2 per cassette, 10 psi transmembrane pressure). The eluate was diluted tenfold using 20 mM Tris/HCl buffer (pH 8.7) and concentrated to the original volume while the permeate was discarded. The procedure was repeated twice in order to reduce the concentration of remaining NaCl from the elution in the sample.

4.2.8 Batch binding of L-asparaginase on CM HyperD in the presence of cell debris (debris-matrix competition)

Batch binding experiments were performed by incubating 1 ml settled volume of the cation exchanger CM HyperD LS (equilibrated in buffer A) with different volumes (5 / 10 / 15 / 20 / 30 / 40 ml) of freshly generated *Erwinia* disruptate (bead mill feed rate 5 l h^{-1}, 15% original biomass wet w/v at pH 5.5). The reaction tubes were placed on a roller incubator and at given time intervals tubes were removed from the roller and, after the matrix was allowed to settle (approx. 10-15 sec), a small sample (200 µl) of the supernatant, i.e. the particulate disruptate was taken. Cell debris in the sample was eliminated by centrifugation (7600g, 10 min) and the clear supernatant removed, quantified volumetrically, and assayed for asparaginase activity to yield the variation with time of enzyme concentrations in the liquid phase. The cell debris was re-suspended in a 50 mM borate buffer (pH 8.5) in order to desorb L-asparaginase bound to sedimented cell debris (see Section 2.2.8). After a 2 h incubation time, samples were again clarified by centrifugation (7600 g, 10 min), and the supernatant assayed for free L-asparaginase activity. Debris bound L-asparaginase was estimated by a mass balance.

4.3 Results and Discussion

4.3.1 Primary purification of G3PDH by integrated cell disruption and Fluidised Bed Adsorption

The primary purification of the enzyme glyceraldehyde 3-phosphate dehydrogenase (G3PDH) was exploited herein as a preliminary study to method scout and demonstrate the feasibility of the integrated operation of cell disruption by bead milling and immediate product capture by fluidised bed adsorption (see panel A in Figure 4.2 for experimental configuration). G3PDH is a key enzyme in the glycolytic conversion of glucose to pyruvic acid which represents an essential pathway of carbohydrate degradation in most organisms. The wide availability in different species led to its popularity among enzymologists and protein chemists such that its characteristics are well documented (Harris and Waters, 1976). Yeast G3PDH comprises a tetramer of identical subunits with a native molecular weight of 146,000 Dalton. It binds nicotinamide adenine dinucleotide (NAD) as a cofactor which enables the use of the triazene dye Cibacron Blue 3GA as a pseudo-affinity ligand for its purification. Cibacron Blue mimics the structure of NAD and thus interacts specifically with enzymes which associate with such nucleotide cofactors (Boyer and Hsu, 1993). Cibacron Blue was immobilised onto Macrosorb K6AX in order to prepare a fluidisable adsorbent for the purification of G3PDH (see 4.2.2).

Scouting experiments were conducted to establish the efficacy of wet-milling alone in respect of protein release and temperature rises, exploiting a range of biomass concentrations (15 to 50 % ww/v) and feedstock flow rates (4 to 25 l h^{-1}, see Table 4.3). With respect to total protein or G3PDH release the data indicated that total cell disruption was effectively achieved over a wide range of feed rates from 5 to 25 l h^{-1}. Lower feed rates resulted in extended

Figure 4.2. Experimental configuration for the integrated, primary purification of intracellular proteins from unclarified disruptates

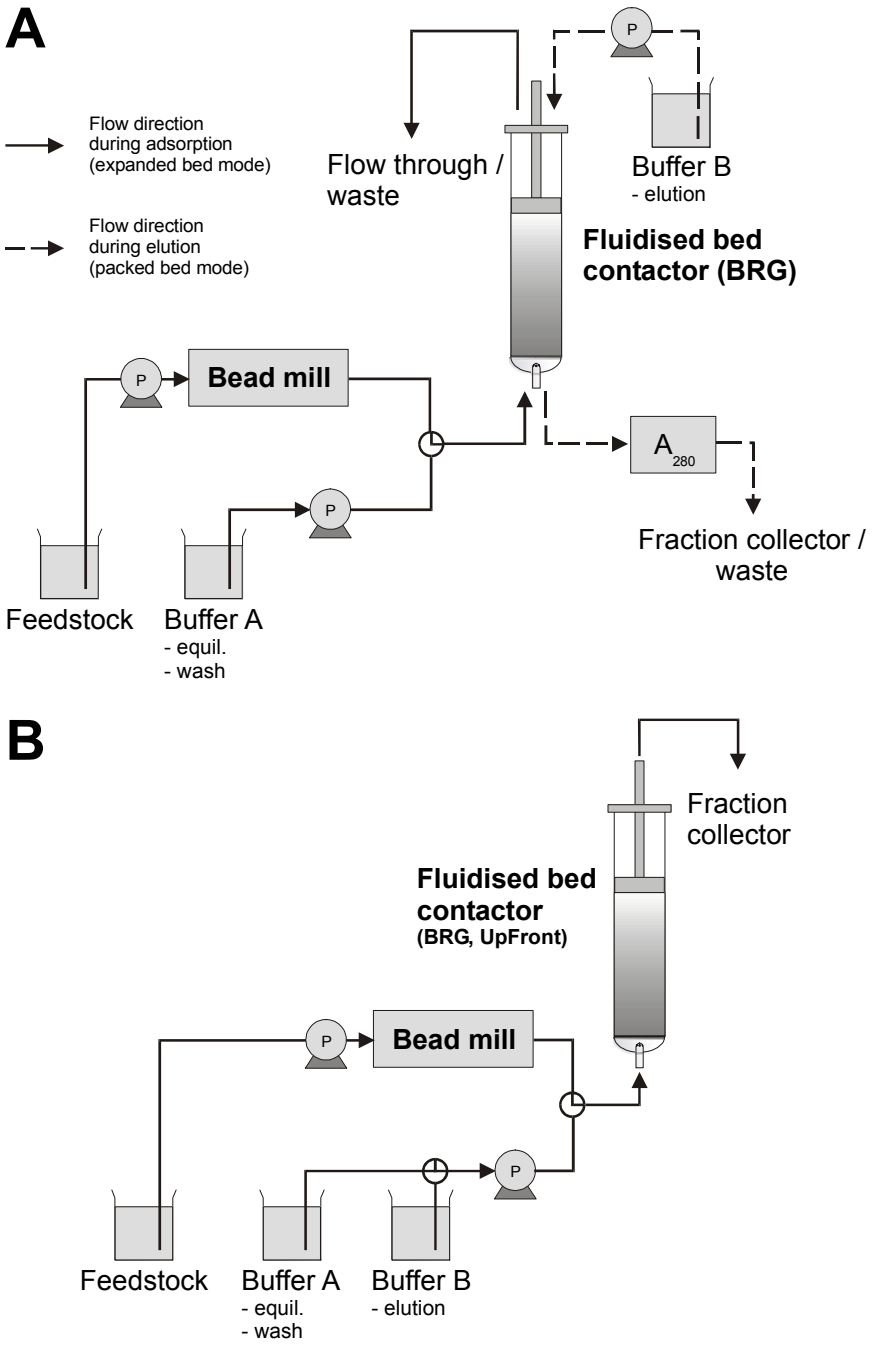

Panel A. Configuration employed for the purification of G3PDH from waste brewers' yeast (see 4.3.1). Elution was performed in packed bed mode under reversed flow. Panel B. Configuration for loading, wash and elution in fluidised bed mode (employed for the purification of L-asparaginase from Erwinia chrysanthemi (see 4.3.2).

residence times and risked increased temperature for unit volumes of processed feedstock. Earlier studies exploiting an acetone pulse as a tracer, indicated that the rate of change of residence time within the milling chamber was greatest at feed rates between 3 and 10 l h^{-1} (refer to Figure 2.3). The outlet temperature at low feed rates, e.g. 5 l h^{-1}, was close to ambient temperature and thus heat denaturation of the labile product was possible. The efficiency of cell disruption apparently increased with biomass concentration of the feedstock as evidenced by product release at 30 and 40% (ww/v) biomass concentration when normalised to that achieved at 50% biomass (see Table 4.3). These findings indicate that bead milling can effectively be carried out at high yeast biomass loads, e.g. 50 % (frozen wet weight/volume), and high feed rates, e.g. 25 l h^{-1} in order to maximise throughput (Zhang, 1998). Such physical characteristics define the specification limit for an integrated fluidised bed contactor.

Table 4.3. Disruption of brewers' yeast by bead milling.

Feedstock	Feed rate (l h^{-1})	Outlet temp. (°C)	Total protein released (mg ml^{-1})	G3PDH released (IU ml^{-1})
50 % biomass	5	23.8	19.4	402
	15	17.1	19.4	437
	25	13.6	18.7	427
40 % biomass	25	12.6	13.8 (17.4)	298 (376)
30 % biomass	25	11.9	8.6 (15.2)	144 (256)
15 % biomass	4.05	21.5	[3.0]	[5.9]

The experiments were carried out in the DYNO MILLl KDL-1 using glass beads (diameter 0.2 - 0.5 mm) at a bead occupancy of 83 % of the chamber volume and an agitator speed of 3200 rpm. The yeast was suspended in buffer A (10 mM Tris/HCl, pH 7.5, and 1 mM EDTA). The inlet feedstock was maintained at a temperature of 2 °C. Values in parentheses are normalised to a 50 % ww/v fresh yeast feedstock to facilitate comparison. Values in square brackets were obtained using yeast stored for 9 months at –20 °C.

However, in this demonstration of principle, the operating parameters of the bead mill had to be matched with the dimensions and the expansion characteristics of the 4.5 cm diameter fluidised bed BRG contactor (see Figure 4.1) available for preliminary experiments. Figure 4.3 depicts the bed expansion of underivatised Macrosorb K6AX when fluidised in buffer A or in the presence of various concentrations of disrupted biomass. The elevated viscosity associated with increased biomass strongly increased the expansion of the bed for a given flow rate. Experimental conditions, i.e. 15 % biomass concentration, feed rate 4 l h^{-1}, were established for the demonstration of process integration with the 4.5 cm contactor.

During adsorption, disruptate was applied to the bed until apparent saturation of the adsorbent capacity for G3PDH had been achieved (see Figure 4.4). The bed was initially expanded (H/H_0=1.8) using buffer A as determined in preliminary experiments (see Figure 4.3). However, during loading, the bed expanded further (H/H_0=2.3) in the face of the elevated viscosity of chilled feedstock. Immediate breakthrough of enzyme activity was evident which might be associated with the channelling clearly visible in the lower segment of the expanded bed on switching the column inlet from buffer to disruptate. This indicated that axial mixing of Macrosorb K6AX, a highly heterogeneous particle (Gilchrist, 1996; Morton and Lyddiatt, 1994b) is greater than for other matrices and promotes poor adsorption behaviour. Tracer studies which comparatively assessed the degree of axial dispersion of various adsorbents revealed considerably higher HETP values for Macrosorb K6AX (refer to Figure 3.5) which was already indicative of a relatively high degree of axial dispersion for this adsorbent at the superficial flow velocity employed. An idealised breakthrough curve is included in Figure 4.4 to indicate the extent of improvement of fluidised bed adsorption required in the integrated process.

Figure 4.3. Bed expansion characteristics of underivatised Macrosorb K6AX

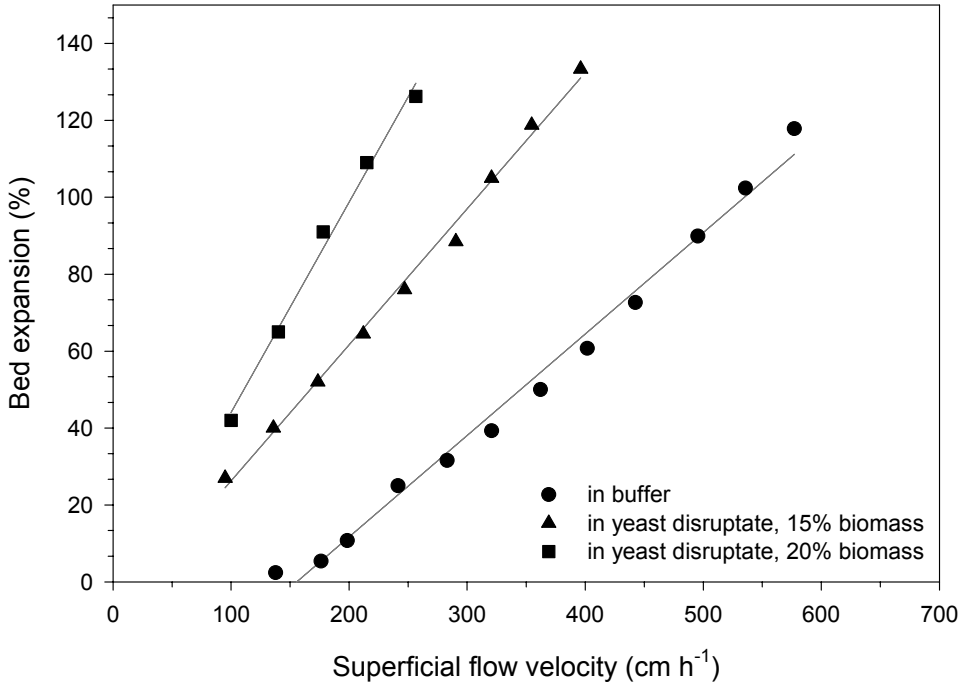

Influence of biomass concentration (disrupted brewers' yeast) on the bed expansion of Macrosorb K6AX. The adsorbent was fluidised in a 4.5 cm BRG contactor at a settled bed height of SBH 15 cm.

Figure 4.4. Expanded bed adsorption of G3PDH from wet-milled yeast onto Macrosorb K6AX-Cibacron Blue 3GA

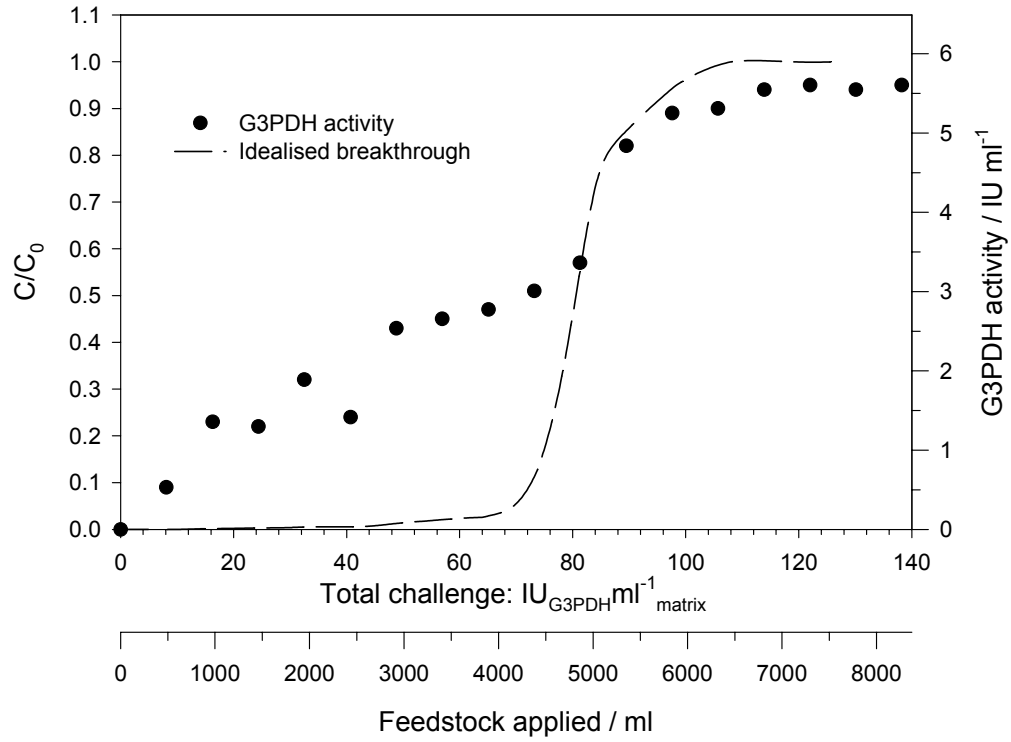

The feedstock contained 15 % brewers' yeast (wet weight per volume, ww/v) and was fed to the bead mill at a rate of 4.05 l h^{-1} which corresponded to a superficial velocity of 255 cm h^{-1} within the contactor operated at a settled bed height 155 mm and (settled bed volume: 247 ml). Disruptate from the mill was directly applied to the fluidised bed contactor. Samples were taken from the outlet of the column and assayed for G3PDH activity.

At the termination of the adsorption stage residual particulate material was washed from the expanded bed with buffer A until a clear effluent was achieved. Enzyme elution was achieved in a four-stage process (see Figure 4.5), performed in packed bed mode under reversed flow (Figure 4.2). Initially, 0.2 M NaCl in buffer A eluted a considerable amount of weakly bound contaminants together with traces of enzyme product which were discarded. Following re-equilibration of the bed in buffer A, the enzyme was desorbed in 0.25 M KSCN in buffer A (a chaotropic elution was adopted since preliminary screening of alternative specific eluents for dehydrogenases such as NADP or NADPH yielded low elution efficiencies (Zhang, 1998). A final treatment using 3M KSCN in buffer A stripped residual material bound to the matrix as a prelude to the re-equilibration and the re-use of the adsorbent. A typical mass balance of G3PDH purification is documented in Table 4.4. Specific activities were higher than those previously recorded from wet-milling and fluidised bed adsorption operated as discrete processes over longer time scales (Zhang, 1998). This was encouraging given the low starting activity of yeast which had been stored at -20 °C for 9 months (< 15 % of fresh material, see Table 4.3).

Table 4.4. Mass balance of G3PDH recovery

Stage	Volume (ml)	Protein (mg)	Enzyme activity (IU)	Specific activity (IU mg^{-1})	Purification factor
Disruptate	7763	23290	45802	2.0	1
Flow through	7763	20823	30808	1.5	-
Elution (peak)	190	602	5241	8.7	4.4

Brewers' yeast (stored at –20 °C for 9 months) was disrupted by bead milling and directly applied to the fluidised bed contactor containing Macrosorb K6AX Cibacron Blue 3GA.

Figure 4.5. Elution of bound solutes from Macrosorb K6AX-Cibacron Blue 3GA in packed bed mode

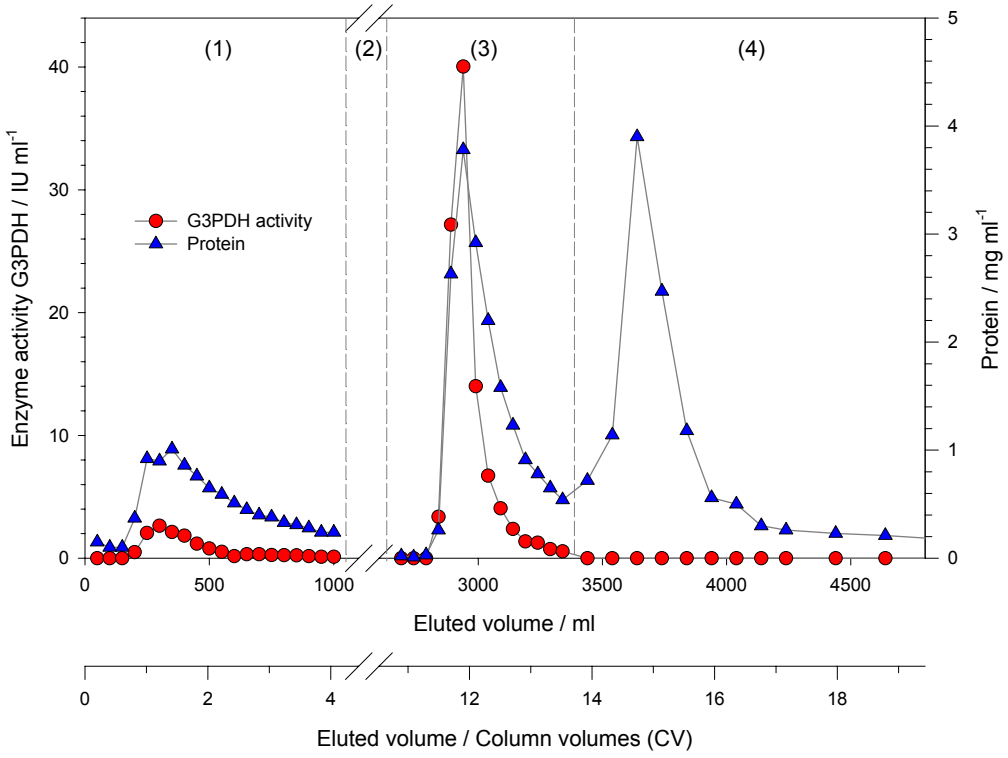

The fluidised bed was loaded as depicted in Figure 4.4. After washing the bed, the adsorbent was allowed to settle and elution was performed in packed bed mode under reversed flow. The following elution procedures were used. (1) 4 column volumes of 0.2 M NaCl in buffer A (10 mM Tris/HCl, pH 7.5 containing 1 mM EDTA) at a superficial velocity of 75 cm h^{-1}. (2) Re-equilibration of the adsorbent by 7 column volumes of buffer A at a superficial velocity of 75 cm h^{-1}. (3) 3 column volumes of 0.25 M KSCN in buffer A at a superficial velocity of 25 cm h^{-1}. (4) 5 column volumes of 3 M KSCN in buffer A at a superficial velocity of 75 cm h^{-1}.

The 0.25 M KSCN treatment resulted in a discrete peak of G3PDH activity coincidental with a broader peak of protein material. Sodium dodecyl sulphate-polyacrylamide gel electrophoresis (SDS-PAGE) indicated the presence of the subunit of the tetrameric G3PDH in all samples taken throughout this protein peak (see Figure 4.6, lanes 7-11) but later fractions (3100-3400 ml, lanes 10 and 11) were inactive. This might reflect different affinities of active and inactive forms of G3PDH for Macrosorb K6AX Cibacron Blue 3GA generated during the disruption process. Alternatively, the enzyme may have been partially inactivated during the elution process due to the extended time of exposure to the chaotrope KSCN. For example, it has been reported that high ionic strength promotes sub-unit dissociation of the enzyme and that only the intact tetramer retains catalytic activity (Harris and Waters, 1976). In order to assess the influence of KSCN on the activity of G3PDH, a sample was taken from the eluted peak (stage 3 of the elution, 0.25 M KSCN, see Figure 4.5) and stored for up to 36 h at 4 °C in an undiluted state (i.e. in 250 mM KSCN in buffer A) as well as diluted tenfold (i.e. in 25 mM KSCN in buffer A). Here, decreases of enzyme activity of 50% and 29% respectively were recorded for the undiluted sample and the 10-fold diluted sample. This indicated that enzyme inactivation occurred due to prolonged exposure to KSCN and was dependent upon the chaotrope concentration. The labile nature of G3PDH was confirmed by the loss of activity seen on prolonged storage of the yeast at -20 °C (see Table 4.3). The time of exposure to high concentrations of KSCN could be shortened by online application of the eluate to a gel filtration column for desalting (Gilchrist, 1996) or direct elution of the G3PDH peak into a buffer reservoir in order to dilute the KSCN. Both options would considerably increase the volume of the eluate.

SDS PAGE analysis depicted the presence of a strong protein band at approximately 43 kDa in all fractions of the elution stages 1 and 3 (lanes 3-11 in Figure 4.6). In the same way as

Figure 4.6. SDS PAGE analysis of elution samples: G3PDH purification from waste brewers' yeast

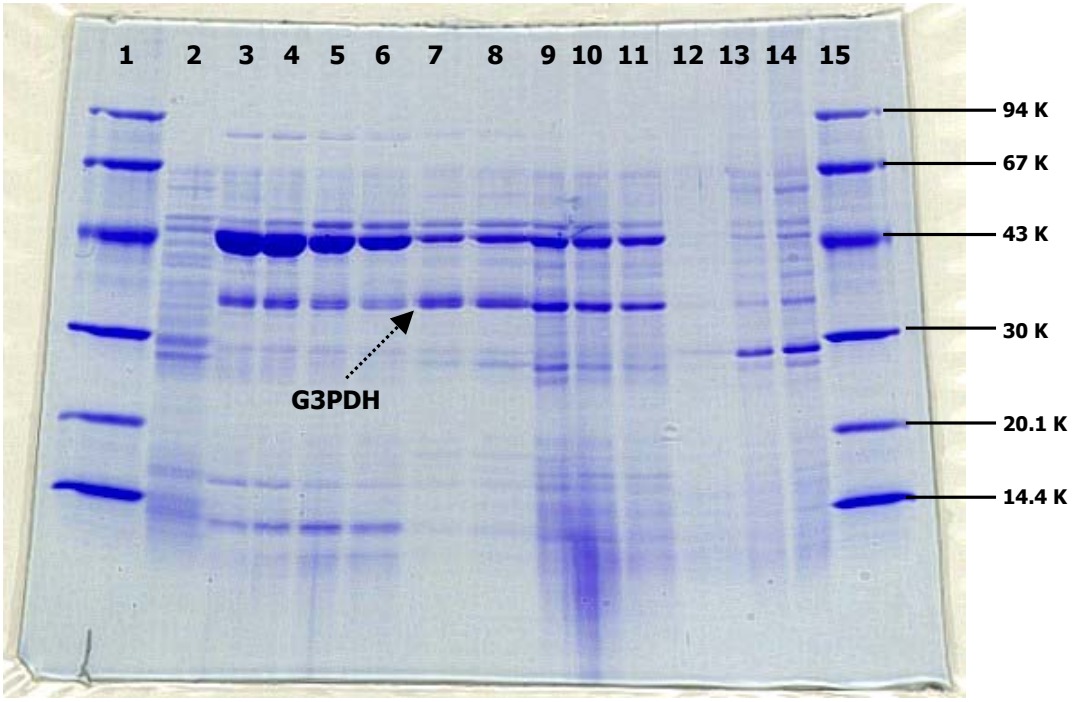

Fractions were taken from various elution stages (see Figure 4.5) and a constant mass of total protein (30 µg) was loaded per lane. The position of the G3PDH monomer band in the gel is indicated by the arrow. Lane 1 and 15, low molecular marker (LMW). Lane 2: yeast disruptate 15% biomass ww/v. Lane 3 – 6: fractions of elution stage 1 (0.2 M NaCl). Lane 7 – 11: fractions of elution stage 3 (0.25 M KSCN). Lane 12 – 14: fractions of elution stage 4 (3 M KSCN).

G3PDH, this protein appeared to be considerably concentrated in comparison with the disruptate (lane 2). This suggested that this component is another (NAD dependent) protein which specifically interacted with Cibacron Blue. Other enzymes which were isolated from disrupted yeast exploiting Cibacron Blue as an affinity ligand are for example aldehyde dehydrogenase (Tamaki *et al.*, 1977), phosglycerate kinase (Kulbe and Schuer, 1979), ATP-AMP phosphotransferase (Ito *et al.*, 2000), fumarate reductase (Muratsubaki *et al.*, 1994) and 6-phosphofructokinase (Chase and Draeger, 1992a; Kopperschlager and Johansson, 1982). However, the protein represented by the 43 kDa band could not be successfully identified by N-terminal sequencing because of an apparently blocked N-terminus (Dr J Fox, Alta Bioscience, The University of Birmingham).

4.3.2 Primary purification of L-asparaginase by integrated cell disruption and Fluidised Bed Adsorption

4.3.2.1 Influence of flow distributor design on the degree of axial dispersion

Two different fluidised bed contactors were used for the integrated recovery of L-asparaginase (see Section 3.2.1). The internal diameters of the contactors were similar (BRG 4.5 cm, UpFront 5.0 cm) but different modes of flow distribution could be employed (refer to Figure 4.1). The BRG contactor could be fitted either with a mesh distributor or a bed of glass beads. However, previous experiments employing a 1 cm BRG contactor with a mesh distributor demonstrated that such a mesh was prone to fouling by precipitates and or cell debris.

The UpFront contactor distinguished itself by its novel flow distributor design. Similar to the 1 cm UpFront contactor (see Figure 3.1), the incoming stream was distributed by local stirring in the bottom of the column. Here, a motor-driven paddle (in contrast to a magnetic

flea) generated a local vortex near the feedstock inlet and thus divided the fluidised bed into a well-mixed zone around the stirrer and a stable fluidised zone above. The rotational velocity of the stirrer could be set on an arbitrary scale from 0 to 10 (maximum rotational velocity). In order to investigate the influence of the rotational velocity of the stirrer upon axial dispersion in a fluidised bed, RTD analysis was used to determine the number of theoretical plates at various rotational velocities (see Figure 4.7). The method employed a dilute acetone solution as a tracer and was described earlier (see Section 3.2.4). At a rotational velocity settings lower than 4 visible channelling appeared in the lower part of the fluidised bed suggesting that the stirrer speed was not sufficient to avoid channelling by distributing the incoming stream. At a rotational velocity setting greater than 3, no discernible channelling occurred. But the vortex generated by the stirrer increased slightly with increasing the rotational velocity of the stirrer. This behaviour was also reflected in the number of theoretical plates depicted in Figure 4.7 which shows a maximum number of theoretical plates at the rotational velocity at which the channelling ceased and the vortex height was at a minimum. However, this behaviour presumably changes with feedstock viscosity and therefore it was judged advisable for further experimentation to choose a rotational velocity at which channelling in the bed is just eliminated. It should be noted that estimates of the number of revolutions per time unit or stirrer tip speed could not be recovered from the arbitrary scale.

A comparison of four different flow distributor configurations is depicted in Figure 4.8. Here, a bed of adsorbent at a constant settled bed height of 15 cm was fluidised and the number of theoretical plates was determined by RTD analysis (see Section 3.2.4). The BRG contactor was fitted with three different configurations which were compared with the novel design of the UpFront contactor (see Section 4.2.6). Here, the influence of the difference in column diameter of the contactors (4.5 and 5.0 cm) was judged to be insignificant.

It can be seen in Figure 4.8 (panel A) that the best performance with regard to axial dispersion was achieved by a bed of glass beads (710 – 1180 μm), and that the other

Figure 4.7. Effect of stirrer speed on axial mixing: UpFront contactor (5 cm i.d.)

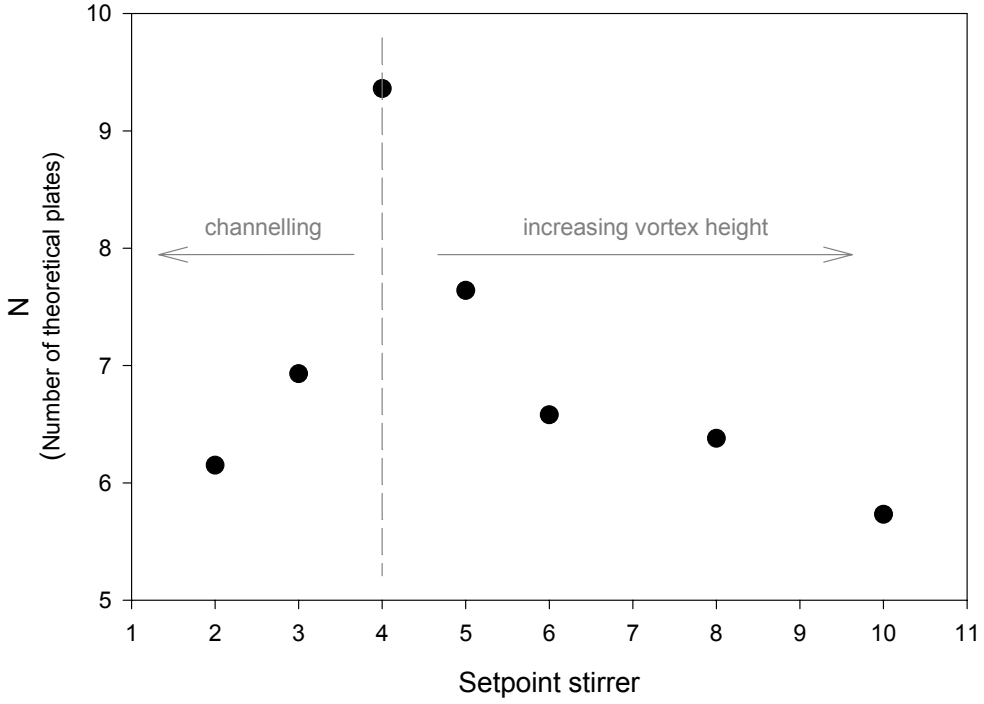

The adsorbent, CM HyperD LS at a settled bed height of 15 cm, was fluidised at a superficial flow velocity of 330 cm h-1 resulting in a degree of bed expansion of 82 %. A dilute acetone solution was introduced into the column as a tracer. The UV absorbance was measured in the exit stream from the column (refer to 3.2.4). The number of theoretical plates was calculated from the negative step input signal.

Figure 4.8. Comparison of flow distributor design on axial dispersion and bed expansion

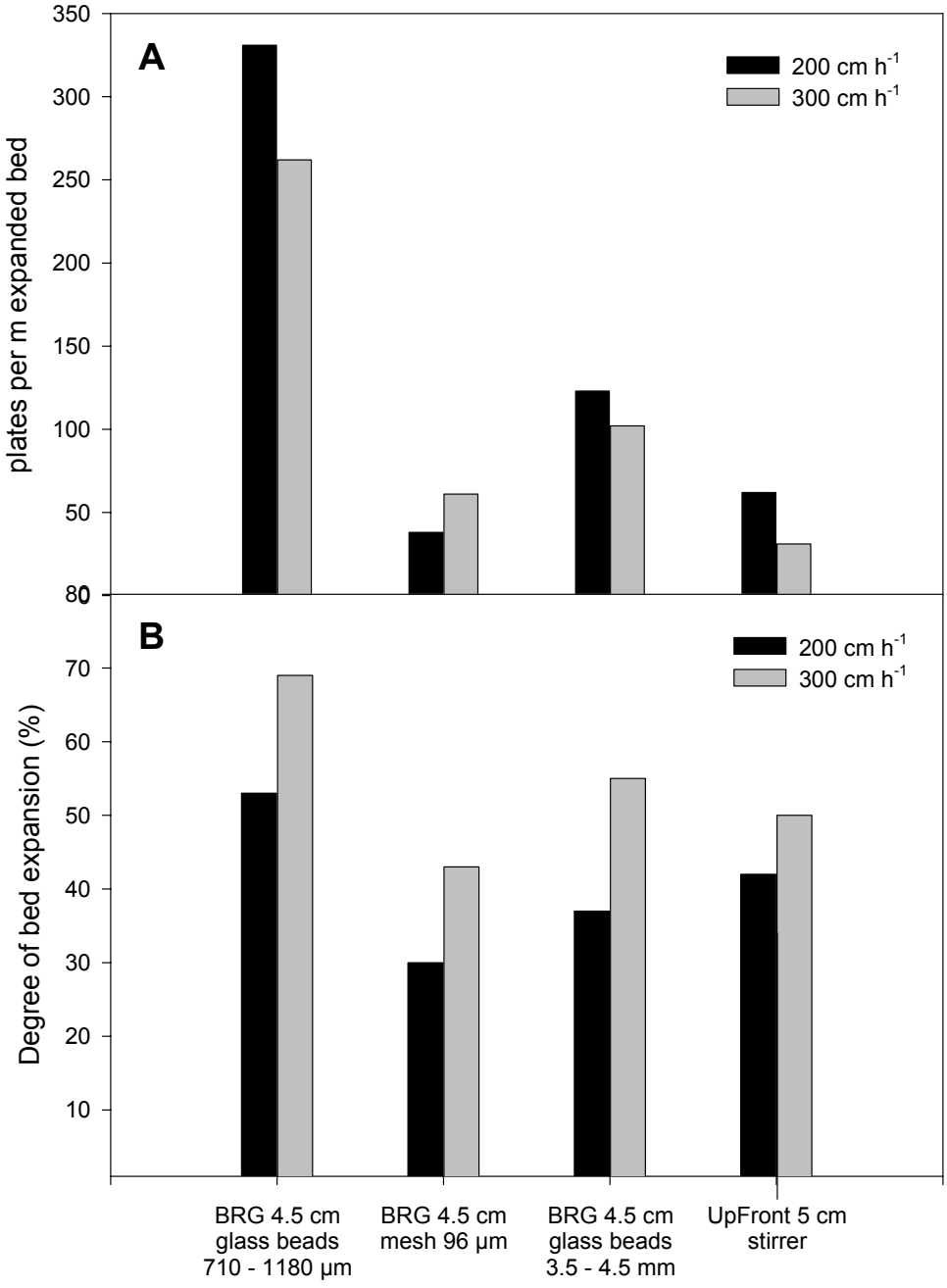

A bed of CM HyperD LS (SBH 15 cm) was fluidised in buffer A employing a BRG contactor (4.5 cm), fitted with various flow distributors, and an UpFront contactor (5.0 cm, stirrer distributor). Axial dispersion was measured by RTD analysis (refer to Section 3.2.4).

configurations yielded considerably lower numbers of theoretical plates at a given SBH and linear flow velocity. The variation in performance found in the BRG contactor apparently correlated to the degree of bed expansion (panel B of Figure 4.8). Here, a low degree of axial dispersion coincided with a high degree of bed expansion which showed that the degree of bed expansion at a given flow velocity may be used as a quick measure of bed stability (Chang *et al.*, 1995; Lan *et al.*, 1999). When the mesh distributor was used, visual inspection revealed a high degree of channelling in the lower part of the bed. This behaviour was reflected by the RTD analysis, i.e. a low number of theoretical plates. The stirring action in the UpFront contactor generated a visible vortex up to approximately a third of the fluidised bed height. This apparently promoted the poor performance with respect to the estimated number of theoretical plates in comparison with the BRG contactor fitted with glass beads (710 – 1180 μm).

4.3.2.2 Adsorption performance during integrated recovery of L-asparaginase – UpFront (5.0 cm) and BRG (4.5 cm) fluidised bed contactor

The experimental conditions established in Chapter 3 for the primary purification of L-asparaginase by CM Hyper D LS were exploited here at a larger scale. In a side-by-side comparison the UpFront and the BRG contactors (see Figure 4.1) were used for the fluidised bed capture of the enzyme directly integrated with cell disruption by bead milling (see panel B in Figure 4.2 for experimental configuration).

Loading of unclarified cell disruptates onto larger-scale columns is depicted in Figure 4.9. In experiments using the UpFront contactor, significant product breakthrough occurred comparatively early during the loading process while loading in a similarly operated BRG contactor was continued over an extended period with only negligible breakthrough. Thus, dynamic capacities achieved in the UpFront contactor were significantly lower. This

Figure 4.9. Integrated cell disruption and fluidised bed adsorption of L-asparaginase on CM HyperD LS from unclarified *Erwinia* disruptates

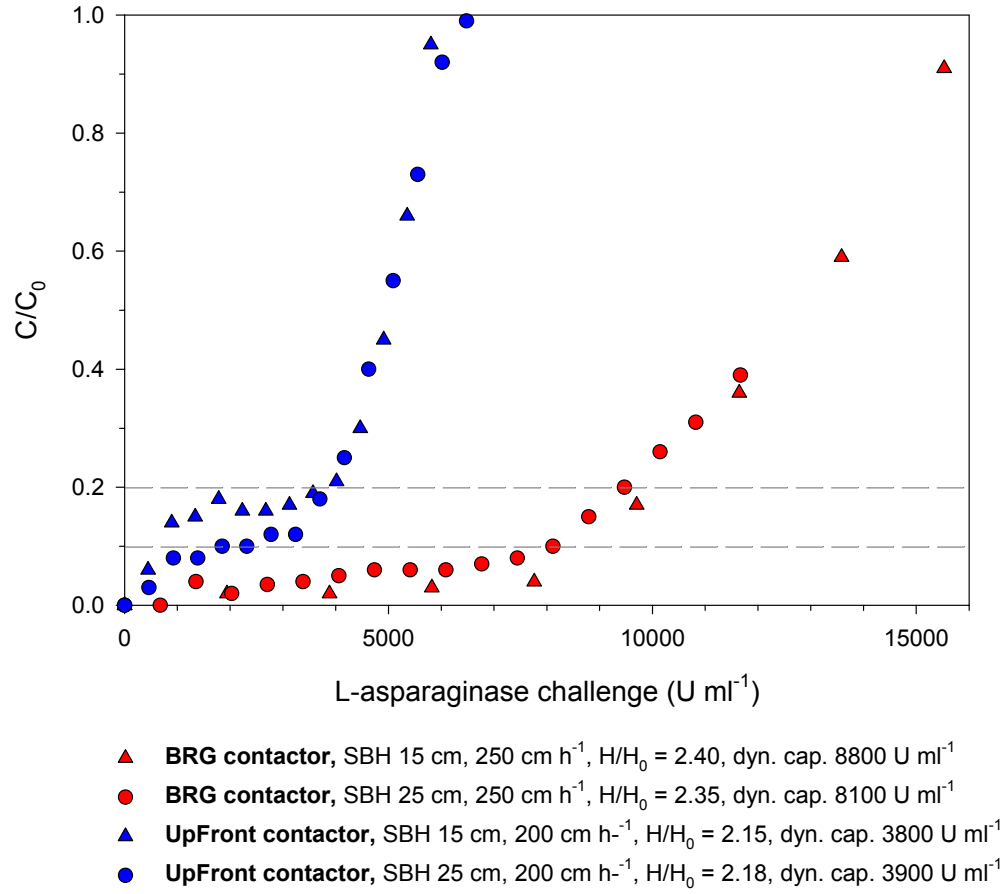

The adsorbent was equilibrated in buffer A and a disruptate generated by the bead mill (15 % ww/v original cells) was directly introduced into the contactors (integration of cell disruption and fluidised bed adsorption, see panel B in Figure 1.1 for configuration). The bead mill feed rate of 4 l h^{-1} corresponded to a superficial flow velocity of 200 cm^{-1} in the UpFront contactor (5.0 cm i.d.) and 250 cm h^{-1} in the BRG contactor (4.5 cm i.d.). The respective settled bed heights of the adsorbent, and the degrees of bed expansion and achieved dynamic capacities (at C/C_0 = 0.1 for the BRG contactor, at C/C_0 = 0.2 for the UpFront contactor) are given with the symbols in the Figure. Stirrer speed in the UpFront contactor was set to 4 (rotational and tip speed unknown).

suggested that the stirrer, providing the distribution of the incoming flow, diminished the adsorption performance of CM HyperD LS when operated in this contactor. The poor adsorption performance was in accordance with the findings of the RTD analysis (depicted in Figure 4.8) where flow distribution by the stirrer in the upscaled UpFront contactor resulted in comparatively low numbers of theoretical plates. In experiments employing disruptate, the vortex generated by the stirrer in the lower part of the bed reached heights of 6 – 7 cm, corresponding to 15 – 19 % of the total expanded height of the fluidised bed (H/H_0 approximately 2.1). However, by way of contrast, the vortex height generated in the small-scale UpFront contactor (1 cm i.d.) was less than 1 cm (3 % of the total bed height) resulting in a packed bed-like performance (refer to Figure 3.10). Experiments conducted by Amersham Pharmacia Biotech AB (1997) demonstrated that the volume of adsorbent particles is not evenly distributed throughout a fluidised bed but is naturally increased in lower parts because of the particle size distribution. In their experiments a bed of STREAMLINE particles was fluidised to 2.5 times its settled bed volume. Here, the bottom 25% of the fluidised bed contained 41% of the adsorbent particles (by volume) whereas in the top 25% of the bed only 12% was present. These results emphasised the influence of the proportion of the well-mixed zone, generated by the stirrer in the UpFront contactor, relative to the expanded bed volume, on the adsorption performance and suggested that for a given settled bed height, the adsorption performance decreases with increasing contactor diameter due to a higher vortex-bed height ratio. However, increasing the settled bed height in the UpFront contactor from 15 to 25 cm only slightly flattened the early product breakthrough but did not significantly enhance the achieved dynamic capacity.

The results obtained in the 4.5 cm BRG contactor are in good agreement to those found at an intermediate scale (2.5 cm BRG contactor, refer to Figure 3.13). Equivalent dynamic

capacities (BRG 4.5 cm: 8100 – 8800 U ml^{-1}, BRG 2.5 cm: 8400 U ml^{-1}) were achieved in both experiments depicted in Figure 4.9, one maintaining the settled bed height used in earlier experimentations in the 2.5 cm contactor (15 cm) and the second one employing a similar height to diameter ratio for both contactors (approx. 6 at 25 cm settled bed height).

Figure 4.10 depicts the elution of L-asparaginase in the larger scale contactors, routinely performed in fluidised bed mode at a superficial flow velocity of 100 cm h^{-1} and Table 4.5 summarises a qualitative assessment of the eluates obtained. As observed for the small-scale experiments (see Figure 3.11 and panel B in Figures 3.13 and 2.4), a wash volume of 5 settled bed volumes (SBV) for both contactors was generally sufficient to reduce the concentration of contaminating proteins in the effluent of the fluidised bed by more than 95%. A sufficiently clear effluent was achieved after 10 SBV. Elution in fluidised bed mode by a step input of buffer B desorbed the enzyme in 2 – 3 SBV in the UpFront contactor. The elution volume in the BRG contactor (4.5 cm i.d.) required 3 – 4 SBV, which was slightly increased when compared with experiments performed in the 2.5 cm BRG contactor (refer to panel B of Figure 3.13). This suggested a higher degree of axial mixing during fluidised bed desorption in the larger contactor. During elution the UpFront contactor exhibited an equivalent performance with regard to elution volume to that achieved in the BRG contactor, which might be attributed to a lower amount of product initially adsorbed to the bed and to a reduced bed voidage under elution conditions (100 cm h^{-1}, at a lower viscosity for the mobile eluting phase). Recovery values and purification factors (see Table 4.5) were in good agreement with results achieved in previous experiments using CM HyperD LS (refer to Table 3.4).

A comparison of the purity of samples collected from key stages of both the conventional commercial process (supplied by Hinton R.J. and Nwoguh, C., CAMR, Porton Down) and the integrated cell disruption/fluidised bed adsorption employing CM HyperD LS

Figure 4.10. Elution of L-asparaginase from CM HyperD LS in fluidised beds.

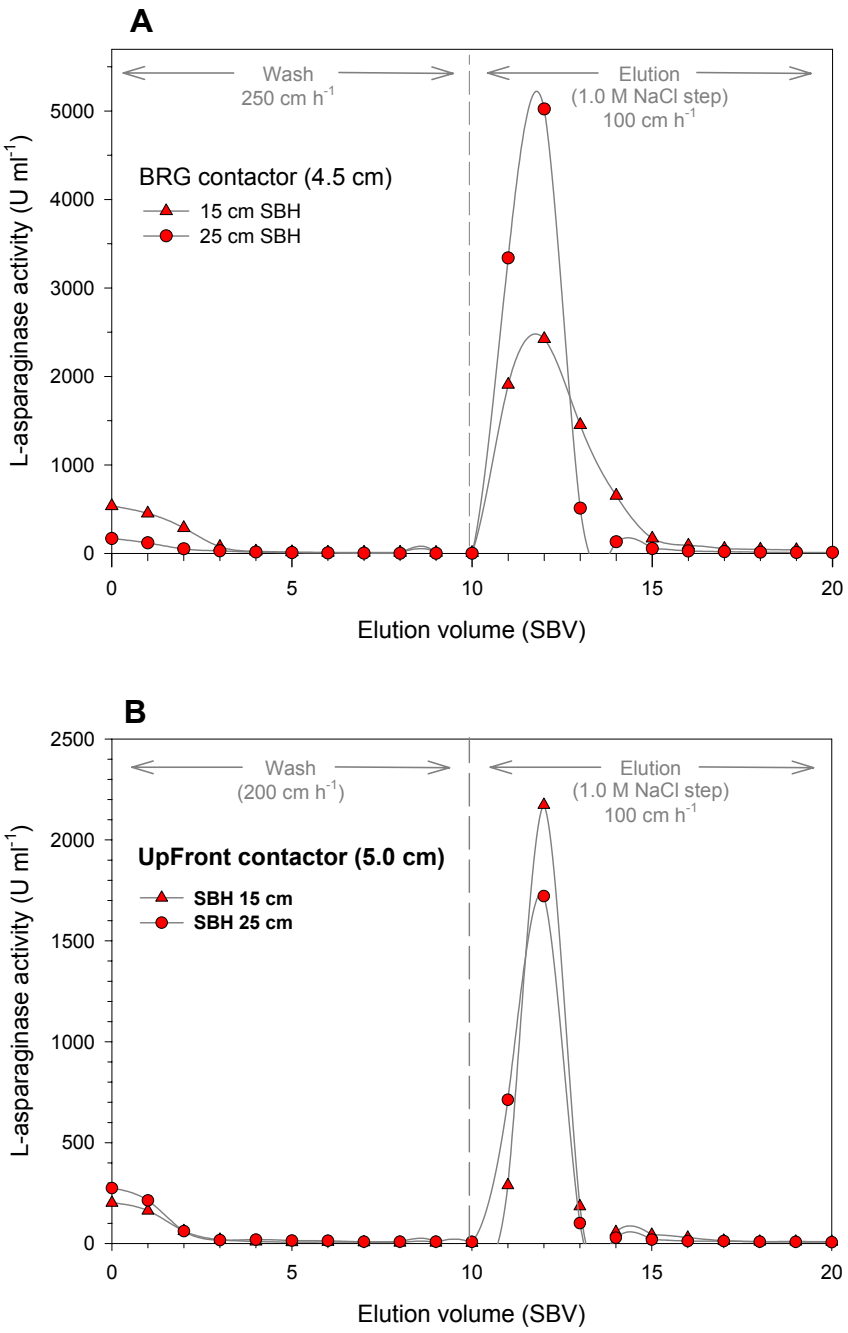

Fluidised beds were loaded as depicted in Figure 4.9. The beds were washed with 10 settled bed volumes (SBV) of buffer A at the loading flow velocity (BRG contactor 250 cm h^{-1}, UpFront contactor 200 cm h^{-1}). Elution was achieved in fluidised bed mode at a linear flow velocity of 100 cm h^{-1} by a step of 1.0 M NaCl in buffer A.

is depicted in Figure 4.11. Also included is an eluate sample obtained from small-scale (1 cm contactor) fluidised bed experiments using SP UpFront. Fluidised bed eluates (CM HyperD in lane 2 , SP UpFront in lane 6) appeared to be more pure from SDS-PAGE analysis than the equivalent interim product of the current purification process (lane 7 and 8) which was also confirmed by a higher specific activitiy (CM HyperD LS at 442 U mg^{-1}, SP UpFront at 421 U mg^{-1}, compared with CAMR CM Cellulose at 328 U mg^{-1}). The comparative yields for these three process routes were respectively 2.9 MU kg^{-1} (CM HyperD LS), 3.0 MU kg^{-1} (SP UpFront), and 1.9 MU kg^{-1} (CAMR CM Cellulose).

Table 4.5. Purification of L-asparaginase by integrated cell disruption and fluidised bed adsorption (CM HyperD LS)

Contactor	SBV (ml)	Feed enzyme activity (U ml^{-1})	Feed total protein (mg ml^{-1})	Feed specific activity (U mg^{-1})	Eluate enzyme activity (U ml^{-1})	Eluate total protein (mg ml^{-1})	Eluate specific activity (U mg^{-1})	Purif. factor	Recovery (%)	Productivity U ml^{-1}_{matrix} min^{-1}
BRG										
15 cm SBH	239	462	5.50	84	1979	5.21	380	4.5	93	56.3
25 cm SBH	398	336	4.73	71	3085	7.40	417	5.8	87	29.1
UpFront										
15 cm SBH	294	168	4.30	39	1281	4.48	286	7.2	89	15.5
25 cm SBH	490	321	5.35	60	1375	5.61	245	4.1	61	10.3

Data given for the eluates represent the pooled fractions of the respective elution peak (depicted in Figures 4.10). The productivity at a given flow velocity was estimated as the amount of enzyme adsorbed at 10% product breakthrough (dynamic capacity at C/C_0 = 0.1, given in Figure 4.9) divided by the settled volume of the adsorbent (SBV) and the total process time (loading to C/C_0 = 0.1 at the respective flow rate; wash of 10 SBV at the respective flow rate; elution of 5 SBV at 100 cm h^{-1}, 100% desorption assumed).

$$\text{Purif. factor} = \frac{\text{eluate specific activity}}{\text{feedstock specific activity}}$$

$$\text{Recovery} = \frac{\text{total enzyme activity in eluate}}{\text{total enzyme adsorbed}}$$

$$\text{total enzyme adsorbed} = \sum \text{flowthrough fraction volume} \cdot (C_0 - C_{\text{fraction}})$$

Figure 4.11. Purity comparison (SDS PAGE) of the conventional purification process and integrated cell disruption/fluidised bed adsorption.

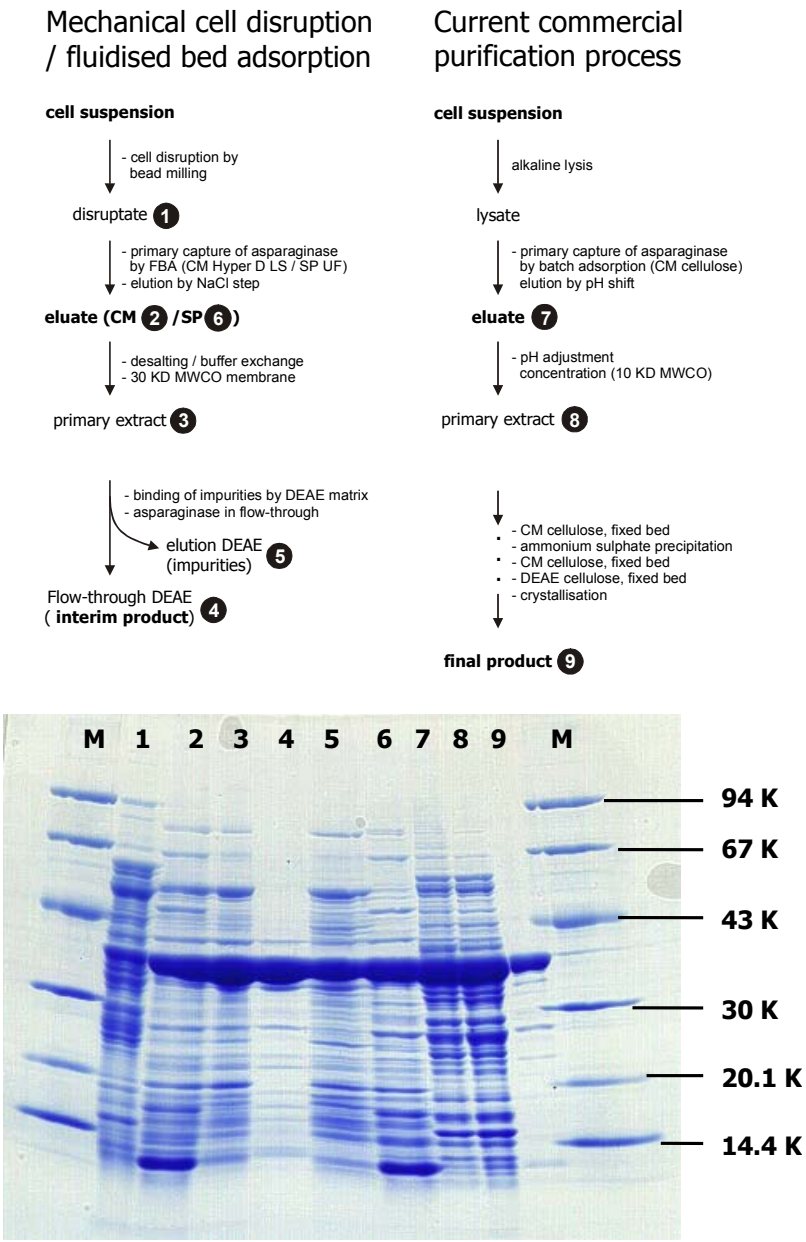

The numbers given in the flow sheet indicate the origin of samples and correspond to their respective lane numbers. Lanes: M - low molecular weight markers; 1 - Erwinia disruptate, 15 % biomass ww/v; 2 - eluate CM HyperD LS, fluidised bed; 3 - desalted eluate (after dia/ultrafiltration, 30 K MWCO membrane); 4 - flow-through, DEAE fixed bed; 5 - elution, DEAE fixed bed; 6 - SP UpFront eluate; 7 - CM cellulose eluate; 8 - CM cellulose eluate, final; 9 - final commercial product. Approximately 50 µg of total protein was loaded per lane.

The product from the two process routes are distinguished by variation in the pattern of impurities. Eluates from fluidised bed adsorption show a strongly stained band of a low molecular weight contaminant (< 14.4 KDa) which is either absent or not pronounced in the CM cellulose eluate (refer to lane 7 and 8 of Figure 4.11). Further processing of the FBA eluate (depicted in lane 2) confirmed that a subsequent diafiltration step using a 30 KDa MWCO membrane (see Section 4.2.7) eliminated most of this material (refer to lane 3 in Figure 4.11). A subsequent subtractive adsorption step exploiting DEAE Trisacryl, selected to mimic an anion exchange step operated further downstream in the current purification process (refer to Figure 4.11), confirmed the practical potential for its separation from the product and the elimination of other contaminants (see lane 4 in Figure 4.11). This chromatographic step was carried out at pH 8.6, the pI of L-asparaginase, in order to facilitate product passage through the adsorbent bed and to retain more acidic contaminants (lane 5 in Figure 4.11). In the preliminary conducted studies here, about 40 % of the applied L-asparaginase also adsorbed to the anion exchanger (refer to lane 5). Clearly, this step needs further optimisation in order to minimise adsorptive losses of L-asparaginase whilst retaining maximum clearance of the 14 KDa impurity. However, the purity of the enzyme product (715 U mg^{-1}) after 3 operational steps of integrated bead milling/FBA, diafiltration and fixed bed adsorption is highly encouraging (CAMR final product 850 U mg^{-1}).

4.3.2.3 Reduced product-debris interaction through competitive adsorption on CM HyperD LS

Preliminary work (see Section 2.3.3.3) has demonstrated that L-asparaginase has a tendency to adsorb to cell debris in a pH and ionic strength dependent manner similar to behaviour seen with a cation exchange matrix (Goward *et al.*, 1992). The fact, that levels of L-asparaginase activity in disruptates could be increased by the addition of salt (e.g. 1M

NaCl) or shifting the pH towards a more basic condition (addition of 50 mM borate buffer) suggested that electrostatic interactions between the enzyme and oppositely charged cell debris were influential upon achievable product yields. However, with regard to process economy, it is of course desirable to minimise such adsorptive losses to debris. Here, a study was performed in order to determine whether the direct and immediate exposure of disruptates to the adsorbent solid phase in an integrated fluidised bed contactor promoted a beneficial competition for L-asparaginase and a concomitant shift in the debris-product adsorption equilibrium. The net effect would be expected to be a reduction in product-debris interactions and/or an actual desorption from debris of already bound product.

The results of this study are depicted in Figure 4.12 (batch binding experiment, see 4.2.8). Cell disruption by bead milling yielded a disruptate containing an initial soluble enzyme activity in the liquid phase of 417 U ml^{-1} (enzyme activity of the clarified disruptate) which corresponds to a cell paste activity of 2.78 MU per kg of biomass. Initial values of debris bound enzyme (estimated by desorption of debris bound L-asparaginase by a pH shift, refer to Section 2.2.8) were estimated at 1.62 MU per kg of biomass which is equivalent to 36% of the total available enzyme (i.e. soluble enzyme in clarified disruptate plus enzyme desorbed from debris). Panel A in Figure 4.12 depicts the decrease in liquid phase concentration of L-asparaginase as a function of incubation time in the presence of freshly milled cells and a cation exchange adsorbent. These curves reflected only the uptake of the enzyme by CM HyperD LS since soluble enzyme in the disruptate (control sample, not in contact with matrix) appeared to remain constant over the time course of the experiment, i.e. no degradation of the enzyme occurred. However, debris bound enzyme in disruptate which was in contact with the cation exchange matrix decreased with incubation time which suggested that L-asparaginase was desorbed from cell debris during the course of the experiment (see

Figure 4.12. Matrix-debris competition in the batch adsorption of L-asparaginase from unclarified *Erwinia* disruptates.

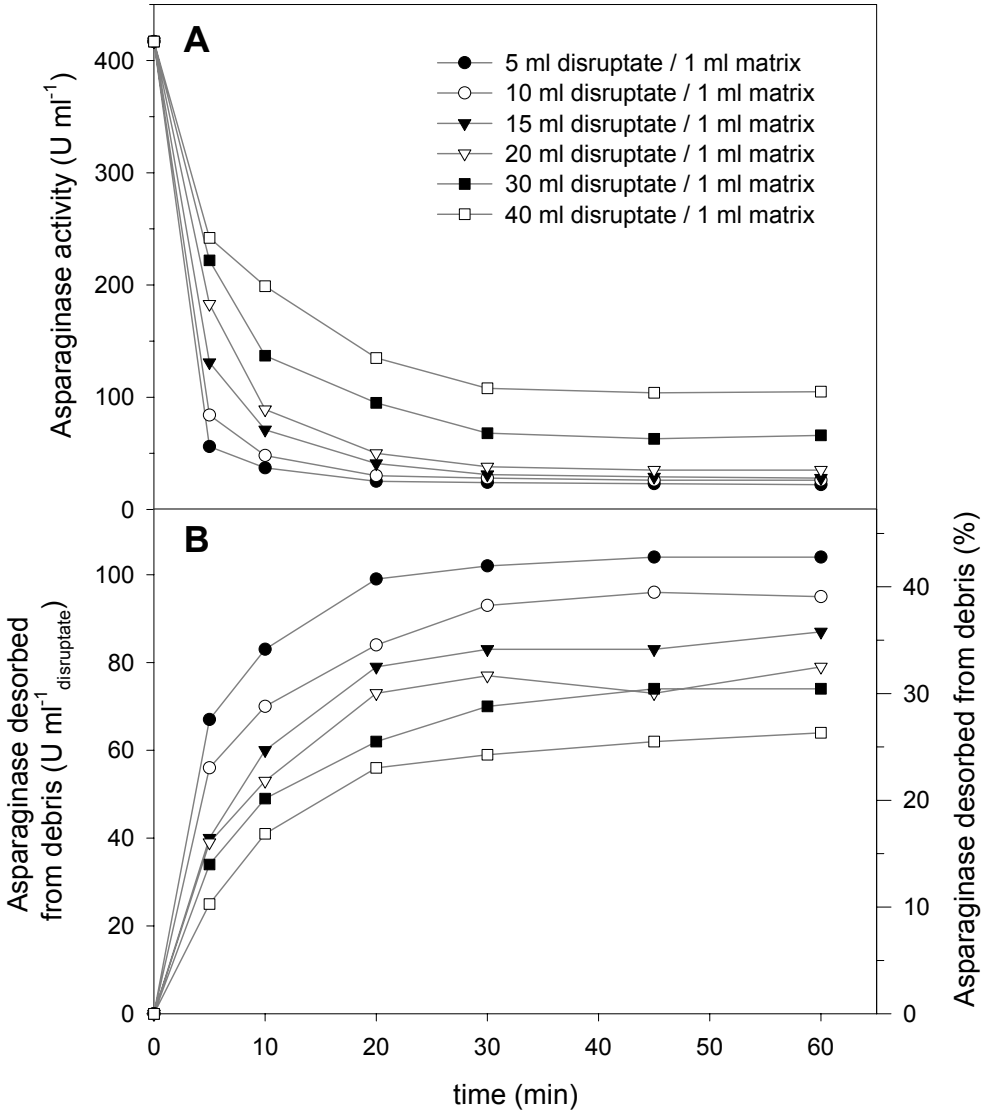

A constant volume of CM HyperD LS (1 ml) was incubated with different volumes of Erwinia disruptate (5 / 10 / 15 / 20 / 30 / 40 ml). L-asparaginase, both in the liquid phase and debris bound was quantified with time. Panel A: uptake of L-asparaginase by CM HyperD LS from unclarified Erwinia disruptates as a function of incubation time. Panel B: release of debris bound L-asparaginase as a function of incubation time.

panel B of Figure 4.12). Furthermore, the amount of enzyme desorbed from debris increased with incremental decreases of the disruptate-matrix ratio. This demonstrated that the exposure of a disruptate to an adsorbent matrix facilitates a competitive reduction of product-debris adsorption. However, although matrix adsorption reduced enzyme levels in the liquid-phase by approximately 95% (panel A in Figure 4.12, 5 ml disruptate per ml of matrix) the amount of debris bound enzyme was only reduced by 43% (panel B, Figure 4.12).

After cell disruption the disruptate was stored for 60 minutes during preparations for the batch binding experiment depicted in Figure 4.12. During this period, the product was exposed to cell debris and some adsorption inevitably took place. It would have been beneficial to expose the disruptate immediately after cell disruption to an adsorbent matrix such that contact times between product and cell debris were minimised and gross product losses by adsorption to debris reduced overall. Such a facilitation has been proposed earlier by the integration of cell disruption by bead milling and the primary product capture by fluidised bed adsorption (Bierau *et al.*, 1999). It would be expected to favour further benefits of decreased product degradation, shortened process times and lower operational costs.

4.4 Interim conclusions

4.4.1 Primary purification of G3PDH by integrated cell disruption and Fluidised Bed Adsorption

The approach to process integration as reported herein for potentially labile enzymes clearly proved that a bioproduct can rapidly be removed from the potentially harmful environment of the cell disruptate by performing cell disruption and primary capture simultaneously. Table 4.6 summarises a stage comparison of a conventional purification scheme for G3PDH and the integrated approach adopted herein. It is evident that there is a

considerable reduction in the number of consecutive unit operations in line with operating time-frame and product losses when the integrated process is compared with the conventional process. Such immediate product sequestration will be particularly important for labile proteins in order to improve both the yield and molecular integrity of the target products.

Table 4.6. Stage definition of conventional purification compared with integrated disruption/purification of G3PDH

Conventional purification of G3PDH from yeast (Byers, 1982)	Integrated disruption / purification
▪ Cell disruption by high pressure homogenisation (2 passes) ▪ Solid-liquid separation (centrifugation) ▪ Fractionation of impurities (50% ammonium sulphate precipitation) ▪ Fractionation of product (80% ammonium sulphate precipitation) ▪ Desalting by gel filtration ▪ Fractionation of product by fixed bed ion-exchange chromatography ▪ Purification of product by affinity chromatography ▪ Product formulation	▪ Cell disruption / selective recovery on Macrosorb Cibacron Blue ▪ Product formulation

Early breakthrough of product during the fluidised bed capture was attributed to the poor fluidisation properties of Macrosorb K6AX. This was evident by visible bed channelling and comparatively high HETP values obtained by RTD studies (refer to Figure 3.5). The fluidisation characteristics could be improved with an increased operational bed height and by the use of an adsorbent having a higher density and a more regular particle geometry. Such measures would reduce the mixing of adsorbent particles and improve overall adsorption

performance as illustrated in the idealised breakthrough curve in Figure 4.4. Composites of silica-dextran, pyrex-agarose, titanic-cellulose and zircon-agar all possess such characteristics (Gilchrist, 1996; Morton and Lyddiatt, 1994a), but were not available in forms suited to the chemical derivatisation required for this study.

Throughput of feedstock in this experiment was limited by the cross-sectional area of the contactor but could be increased by use of a denser matrix requiring higher fluid velocities for equivalent bed expansion. Using an adsorbent of a density of 1.6 g ml^{-1}, Beveridge (1997) has recorded that a superficial flow velocity of 1250 cm h^{-1} was required to generate 100% bed expansion in an equivalent contactor (45 mm diameter). Assuming that a disruptate originating from 15 % initial cell biomass extends the degree of bed expansion by a factor of 2.5 at a superficial flow velocity of 300 cm h^{-1} (see Figure 4.3), then such a high density matrix could be operated at superficial flow velocities of 700 cm h^{-1} in the present contactor representing a three-fold increase of throughput (i.e. milling at 12 l h^{-1}).

A comparatively low purification factor (Table 4.4) suggested that a considerable amount of non-specific adsorption of impurities occurred during primary capture. This is not an uncommon finding, since protein binding to Cibacron Blue is viewed as a combination of several forces including both electrostatic and hydrophobic interactions (Boyer and Hsu, 1989; Boyer and Hsu, 1993; Scopes, 1987).

4.4.2 Primary purification of L-asparaginase by integrated cell disruption and Fluidised Bed Adsorption

The concept of directly integrating conventionally discrete operations of cell disruption by bead milling and the product capture by fluidised bed adsorption previously demonstrated for the purification of G3PDH from yeast was adapted for the purification of L-asparaginase from *Erwinia*. In a side-by-side comparison with the established purification process for this

enzyme, the novel process proved to be more efficient by yielding a purer interim product using either CM HyperD or SP UpFront as an adsorbent (see Figure 4.11). The overall yield of the integrated process (i.e. the amount of enzyme revovered in the eluate relative to the initial biomass activity) bettered the one commonly achieved in the commercial process (52% in the integrated process, 39% in the commercial process, see Table 4.7). Furthermore, operational sequences were considerably compressed without the need of disruptate clarification and/or storage. Here, the total process time (cell disruption / loading, washing and elution) to yield an equivalent primary extract would be less than 2.5 hours when employing an appropriately up-scaled fluidised bed (e.g. column diameter 48 cm, settled bed volume 28 litres), refer to Figure 1.4. This process duration was estimated for an average biomass activity of 3.6 MU kg^{-1} cell paste (corresponding to 540 U ml^{-1} of feedstock at 15% biomass ww/v), an adsorbent dynamic capacity of 8000 U ml^{-1} achieved at a flow velocity of 250 cm h^{-1}, a wash of 10 SBV at 250 cm h^{-1}, and elution in 5 SBV at 100 cm h^{-1}). Taking this considerable reduction in the overall process time into account, the integrated process exhibits a tenfold higher productivity (estimated as the total amount of enzyme recovered in the eluate per kg of cell paste divided by the total process time, see Table 4.7). With the given system configuration operated at pilot-scale, the throughput of biomass was only limited by the dimensions of the fluidised bed contactor since optimal product release was achieved at a bead mill feed rate of 8 l h^{-1} (corresponding to a superficial flow velocity of 500 cm h^{-1} in the column, a twofold increase in comparison with flow velocities used in this study). Process intensification, i.e. increased biomass throughput, could be achieved by increasing the contactor diameter and/or by the use of an adsorbent with enhanced density. Such material, provided that capacity and mass transfer characteristics were appropriate, would facilitate the

use of higher superficial flow velocities and/or higher biomass concentrations in the feedstock.

By employing the 4.5 cm BRG contactor, the fluidised bed capture of L-asparaginase was scaled up from an intermediate level of operation (2.5 cm, see Chapter 3). Maintaining a constant settled bed height or H/d ratio and a constant linear flow velocity yielded consistent results with regard to dynamic capacity, recovery and purification factors. However, operating the 5.0 cm UpFront contactor under similar conditions resulted in early product breakthrough and thus greatly reduced dynamic capacities in comparison to the BRG contactor. Although the 1.0 cm UpFront contactor exhibited an adsorption performance similar to a packed bed (refer to Figure 3.10) the poor performance of the 5.0 cm contactor can be attributed to the mode of flow distribution. Here, the stirrer paddle generated a proportionally larger vortex and thus a considerable fraction of the adsorbent bed behaved like a stirred tank reactor, equivalent to a single adsorption stage, as opposed to a stable fluidised bed which is characterised by multiple adsorption stages. This was reflected both by the RTD analysis, i.e. the number of theoretical plates, and the early product breakthrough under frontal analysis. It may be expected that with a further increase in diameter (column and stirrer), the height of the generated vortex increases which suggests that the disturbance of stable fluidisation by the local stirring has to be compensated by maintaining comparatively high H/d ratios. However, the use of glass beads (710 – 1180 μm) in the BRG contactor proved to be a simple, yet effective means of flow distribution. This design was not prone to blockage and yielded considerably higher numbers of theoretical plates in comparison with fluid distributors exploiting a defined mesh distributor, a bed of larger beads (3.5 – 4.5 mm) or the stirrer design in the UpFront contactor.

It was demonstrated that a partial elimination of debris bound losses could be promoted by the immediate exposure of disruptates to an adsorbent matrix, by establishing a competition between the two solid phases present in the system, i.e. cation exchange adsorbent and debris. The exposure of the disruptate to CM HyperD LS reduced the amount of debris bound enzyme by more than 40%. However, in order to minimise the initial amount of debris bound enzyme, rapid processing was essential and this was achieved by the direct integration of cell disruption and product capture by fluidised bed adsorption. The observation that the release of debris bound enzyme in batch binding experiments was increased at lower volume ratios of disruptate to adsorbent (panel B, Figure 4.12) might indicate that within a fluidised bed L-asparaginase release from debris is enhanced at low degrees of bed voidage, i.e. low degrees of bed expansion.

Table 4.7: Process performance in the primary purification of L-asparaginase

Current commercial process					Integrated bead milling and FBA [*d]				
Stage / process stream	**Elapsed process time [*a] (h)**	**Total enzyme act. [*a] (MU)**	**Enzyme yield (MU kg^{-1})**	**Overall enzyme recovery (%)**	**Stage / process stream**	**Elapsed process time (h)**	**Total enzyme activity (MU)**	**Enzyme yield (MU kg^{-1})**	**Overall enzyme recovery (%)**
Cell suspension Total biomass: 60 kg Total volume: 900 l Biomass conc.: 7 % ww/v Biomass activity: 3.6 MU kg	0	216	3.6	100	**Cell suspension** Total biomass: 60 kg Total volume: 400 l Biomass conc.: 15 % ww/v Biomass activity: 3.6 MU kg	0	216	3.6	100
Unclarified lysate	3	168	2.8	78 [*a]	**Disruptate**		134	2.23	62 [*b]
Clarified lysate	12				**Eluate (from FBA)**	2.5 [*e]	111	1.85	52 [*c]
Eluate (from batch adsorption)	20	84	1.4	39 [*a]					
Productivity: 70,000 U kg$_{biomass}^{-1}$ h^{-1}					**Productivity: 740,000 U kg$_{biomass}^{-1}$ h^{-1}**				

[*a] Data provided by CAMR, Porton Down Salisbury.
[*b] The estimated recovery value for this step is based on the result that enzyme release by bead milling was commonly about 79% of that achieved by alkaline lysis (refer to Table 2.3).
[*c] Average recovery for CM HyperD LS in integrated recovery experiments 83% (refer to Table 4.5).
[*d] In this process example, an appropriately up-scaled fluidised bed of CM HyperD LS is employed, for calculation refer to Section 4.4.2 (column diameter 48 cm, SBV 28l, adsorbent dynamic capacity 8000 units per ml of adsorbent at a loading flow velocity of 250 cm h^{-1})
[*e] This process time reflects the cell disruption with simultaneous loading of the disruptate onto the fluidised bed, a wash of 10 settled bed volumes at 250 cm h^{-1}, and an elution in 3 settled bed volumes at 100 cm h^{-1}.

This table summarises the performance of the two approaches to the primary purification of L-asparaginase from Erwinia chrysanthemi. Recovery data for the current, commercial process was provided by CAMR (Porton Down, Salisbury). The calculation was based on a typical batch size of the current commercial process (60 kg cell paste per campaign, average biomass activity 3.6 MU kg^{-1}). The productivity is given as the total amount enzyme activity recovered per kg of biomass divided by the total process time.

5 CONCLUSIONS AND FURTHER WORK

5.1 Final conclusions

The study presented here was concerned with the redesign of a process for the primary purification of the intracellular enzyme L-asparaginase from *Erwinia chrysanthemi*. The overall aim was to establish a simpler, yet more efficient, means of recovering the enzyme without compromising existing standards of purity and activity. Of particular importance was the omission of bottlenecks present in the current commercial process which diminish process economy and entail losses of enzyme activity.

The current, commercial process employs alkaline lysis for the disintegration of *Erwinia chrysanthemi* and the release of L-asparaginase (refer to Figure 1.4). The lysate is clarified by centrifugation steps and the product is recovered by a batch adsorption step. However, this process is characterised by several disadvantages. Firstly, the initial biomass concentration employed for the lysis is limited since a considerable increase in broth viscosity during the addition of sodium hydroxide aggravates homogeneous mixing of the broth and may therefore promote product damage by extreme local pH values. Secondly, the batch-wise operation of the lysis may result in a loss of enzyme activity due to the exposure of the product to system antagonists, such as proteases and cell debris, while the lysate is accumulated and clarified. Broth clarification is accomplished by centrifugation, which predominantly contributes to the overall process duration (refer to Figure 1.4). Moreover, the addition of alkali and acid during the lysis results in a comparatively high conductivity of the lysate. A dilution is thus required for an efficient adsorption of the product by the cation exchange adsorbent.

For the revision of the process, an integration of cell disruption and fluidised bed adsorption was proposed (refer to Figure 1.4 and 1.5). By employing fluidised bed adsorption, the clarification of the broth would be incorporated with the capture of the product which would result in a considerably shortened overall process time. Here, an efficient cell disruption method capable of continuous, single-pass operation would omit the accumulation of the disruptate prior to the product capture and therefore benefit its yield and molecular fidelity by the minimisation of its contact time with antagonists present in the disruptate.

The experiments presented in Chapter 2 investigated the development of a cell disruption process for *Erwinia chrysanthemi* by bead milling. Although not widely used for the disruption of bacteria, bead milling proved to be an efficient means for the release of L-asparaginase. Here, the product yield per unit of biomass (i.e. resuspended cell paste) was slightly lower in comparison with that achieved by alkaline lysis for the same batch of cell paste (refer to Table 2.3). This may be attributed to a combination of process intensification (up to 15% biomass ww/v for bead milling; refer to Figure 1.4) and back mixing phenomena in the disruption chamber. However, this was judged acceptable in view of the process advantage of continuous, single-pass disruption, but requires further optimisation. An optimum range of feed rates for the milling process, resulting in maximum product release whilst minimising product-debris interactions, was established (8 – 10 l h^{-1}, refer to Figure 2.5). It was found that at a low range of feed rates (< 8 l h^{-1}) product-debris interactions were increased and thus influential on achievable product yields (refer to Figure 2.5 and Figure 2.9). These results suggested that disruption at low feed rates, i.e. at prolonged liquid residence times within the disruption chamber, promoted product debris interactions as a result of an increased specific surface area due to the increased micronisation of cell fragments. It was demonstrated that product-debris interactions were of an electrostatic nature

and decreased with increasing ionic strength and disruptate pH (see Figure 2.8). A measurable adsorption of purified L-asparaginase from buffer solutions to glass and zirconia grinding beads could be found (see Figure 2.7). However, such interactions will be clearly reduced in a competitive environment, e.g. when the grinding beads are in contact with a complex mixture of biological molecules during the continuous disruption of a cell suspension.

Experiments summarised in Chapter 3 investigated the development of a fluidised bed process for the initial fractionation of L-asparaginase from unclarified *Erwinia* disruptates generated by bead milling. Candidate adsorbents were physically characterised, i.e. their bed expansion and axial dispersion characteristics were studied. Two cation exchange adsorbents, CM HyperD LS and SP UpFront, were selected for fluidised bed experiments using *Erwinia* disruptates. In a side-by-side comparison, their adsorption characteristics, i.e. uptake rate and equilibrium capacity, were assessed in batch binding experiments. Frontal analysis was employed to study the effect of superficial flow velocity and settled bed height on the dynamic capacity of the adsorbents.

Bed expansion studies demonstrated that fluidisation of CM HyperD LS and SP Upfront in a 15% biomass (ww/v) containing feedstock increased their bed expansion at given flow velocities approximately by a factor of three in comparison with fluidisation in buffer (see Figure 3.4). Increased particle density considerably reduced bed expansion at given flow velocities which facilitated the use of higher flow velocities. During frontal analysis experiments employing CM HyperD LS (1.41 g ml^{-1}) in a 15% biomass containing feedstock at a superficial flow velocity of 300 cm h^{-1}, adsorbent particles elutriated from the fluidised bed suggesting that, with respect to the given feedstock viscosity, an upper limit for operations using this adsorbent was approached. Owing to its enhanced particle density of 2.35 g ml^{-1}, SP UpFront exhibited a significantly lower bed expansion in comparison with

CM HyperD LS and could be operated at 400 cm h^{-1} in 15% biomass without any entrainment of adsorbent particles. However, increasing the biomass concentration to 22% (ww/v) diminished the stable fluidisation of SP UpFront even at low flow velocities (200 cm h^{-1}) and promoted channelling which resulted in early product breakthrough (refer to Figure 3.14 panel A).

It was found that product-debris interactions were considerably reduced at a disruptate pH of 6.0 in comparison with a pH of 5.0 (refer to Figure 2.8). However, both adsorbents, CM HyperD LS and SP UpFront, exhibited a considerable reduction in equilibrium capacity for L-asparaginase when pH values of 6.0 were approached (see Figure 3.6). Thus, an intermediate pH of 5.5 was adopted for the fluidised bed capture of L-asparaginase as a trade-off between adsorbent capacity and product-debris adsorption.

CM HyperD LS and SP UpFront represented two structurally distinct solid phases (refer to Figure 3.7). The former comprises a highly porous, rigid skeleton filled with a hyper-diffusive hydrogel containing the ion-exchange groups. The pellicular SP UpFront comprises a non-porous solid, stainless steel core coated with a porous agarose layer. It was estimated that the inert core amounted to 22% of the total bead volume (i.e. a 100 μm composite bead comprising 60 μm steel core). Owing to their distinct solid phase structures, both adsorbents exhibited different adsorption characteristics. Batch binding experiments revealed a threefold higher equilibrium capacity for CM HyperD LS which could be attributed only to a degree to a greater internal particle volume. Here, the higher ligand concentration of CM HyperD LS appeared to have contributed to this result. The pellicular SP UpFront, on the other hand, distinguished itself by a higher adsorption rate attributable to reduced diffusion paths in the macroporous layer. Despite different uptake rates, both adsorbents exhibited an equivalent proportional decrease in dynamic capacity with increasing flow velocity (see Figure 3.15).

The higher uptake rates of SP UpFront did not result in a better performance, presumably due to considerably shorter liquid residence times in SP UpFront fluidised beds as a result of the reduced bed expansion. Under equivalent conditions with regard to fluid residence times, e.g. in a fixed bed, it would be expected that the dynamic capacity of an adsorbent with a higher adsorption rate would be less affected by an increase in flow velocity.

Frontal analysis performed at different settled bed heights revealed that dynamic capacities were comparatively low at 7 cm SBH (refer to Figure 3.16). Increasing the SBH to 15 cm resulted in considerably improved dynamic capacities. A further increase of the SBH to 22 cm improved the dynamic capacities only slightly. The increase in dynamic capacity found with increasing SBH appeared to be due to a combination of a prolonged residence time of a fluid front within the fluidised bed and the dampening of flow irregularities at the bottom of the bed promoted by uneven flow distribution. Both for CM HyperD and for SP UpFront, a settled bed height of 15 cm or greater resulted in a good utilisation of the adsorbent capacity.

The contrasting characteristics of the two adsorbents, high static and dynamic capacity (CM HyperD LS) as opposed to enhanced particle density in combination with high uptake rates (SP UpFront) may be exploited for particular applications. High capacity enhances process economy by a reduced adsorbent inventory. On the other hand, increased particle density in combination with high uptake rates enable efficient product capture at high linear flow velocities. Such properties would be ideal for applications such as the *in-situ* product removal where a fluidised bed is connected as an external loop to a productive fermenter (Hamilton *et al.*, 1999). Here, high flow velocities in the external loop would minimise the time for the producer cells to be outside the controlled environment of the bioreactor. The concept of a manifold of fluidised beds (see Figure 3.18) as exploited by (Hamilton *et al.*, 1999) would also be applicable to the processing of a disruptate generated by a continuous,

single pass process such as bead milling (refer to Chapter 2). Advantages of such a system of multiple, down-scaled fluidised beds would be a reduced adsorbent inventory, short feedstock residence times and thus short cycles of adsorption, washing, desorption and re-conditioning.

Chapter 4 summarised experiments concerned with the integration of cell disruption by bead milling and product capture by fluidised bed adsorption. Here, the feasibility of the concept of performing cell disruption and product capture simultaneously was demonstrated for the purification of the glyceraldehyde 3-phosphate dehydrogenase (G3PDH) from *Saccharomyces cerevisiae* and L-asparaginase from *Erwinia chrysanthemi.* From a stage comparison of conventional purification routes of the respective enzymes with the integrated approach (G3PDH: refer to Table 4.6, L-asparaginase: refer to Figure 1.4) it is evident that there is a considerable reduction in the number of consecutive unit operations in line with operating time-frames and concomitant product losses (in particular due to the elimination of disruptate accumulation and discrete solid-liquid separation steps). Since proteins are generally stabilised when adsorbed onto a solid support (Melrose, 1971), it is advantageous to place an adsorptive step as far upstream as possible. As a consequence, the immediate and direct sequestration of products from cell disruptates, as proposed by the integration of bead milling and fluidised bed adsorption in the same time frame, particularly benefits the purification of potentially labile proteins. This is largely because the hold-up periods, whilst batches of feedstock are accumulated and/or conditioned prior to fluidised bed processing, are minimised.

Disruptates of *Erwinia chrysanthemi* were generally characterised by a considerable amount of debris bound enzyme (e.g. 25% of the total available enzyme, refer to Section 2.3.3.3). This fraction of enzyme would not be accessible for recovery when disruptates were to be clarified prior to the product capture. Since these interactions were of an electrostatic

nature, they are not system-specific but represent a generic problem in the downstream processing of basic proteins by cation exchange processes. Employing a batch adsorption experiment it was demonstrated that the exposure of an unclarified *Erwinia* disruptate to a cation-exchange adsorbent reduced the amount of debris-bound L-asparaginase by approximately 40% (see Figure 4.12). Here, a competition between the two solid phases (i.e. the cation exchanger and cell debris) appeared to shift the product-debris adsorption equilibrium towards positive product capture on the ion exchanger. The immediate exposure of the disruptate to an adsorbent matrix in a fluidised bed, directly connected to a bead mill, might therefore reduce the initial amount of debris-bound product by minimising the incubation time of the product with cell debris. This process is schematically depicted in Figure 5.1.

It has been demonstrated earlier that fluidised bed adsorption is a scaleable operation (Barnfield-Frej *et al.*, 1997). In the same way, bead mills are commercially available from laboratory to industrial scale (Kula and Schütte, 1987; Middelberg, 1995). Thus, integrated bead milling and fluidised bed adsorption is a scalable and generic approach to the efficient recovery of intracellular proteins.

Figure 5.1. Stages during the primary purification of L-asparaginase.

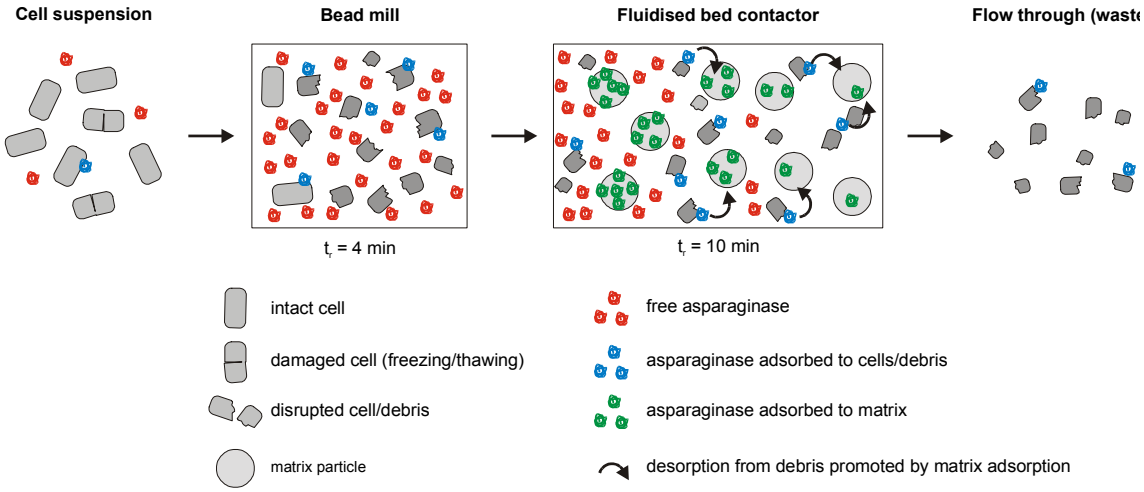

L-asparaginase in solution is present in the cell suspension prior to cell disruption presumably due to freezing and thawing of the cells. Bead milling releases intracellular L-asparaginase and generates fine cell debris which adsorbs enzyme in solution. Immediate exposure of the disruptate to an adsorbent matrix in a fluidised bed minimises the contact time of the product and debris and promotes desorption of debris bound product.

5.2 Future work

The primary purification of L-asparaginase could be further enhanced by (i) optimised product release (i.e. disruption conditions which minimise product-debris interactions), (ii) the maximisation of biomass throughput using high density adsorbents, and (iii) an alternative method of product capture (e.g. mixed mode or affinity adsorbents). In addition, the potential of the direct product sequestration at cell disruption should be validated for the purification of a particular labile product.

Optimisation of operating conditions for the disruption of *Erwinia chrysanthemi*

The reduction of debris-bound L-asparaginase following cell disruption requires further investigation. Under the operating conditions adopted for bead milling (refer to Section 4.2.3), a considerable amount of debris-bound product was observed (refer to Section 2.3.3.3) which could in part be desorbed by the exposure of the disruptate to an adsorbent matrix (refer to Section 4.3.2.3). However, it would be beneficial to minimise the amount of debris bound product formed. It was demonstrated that product-debris interactions were minimal at a disruptate pH of 6.0. However, under such conditions, the capacity of ion exchange adsorbents was diminished (refer to Section 3.3.2). Thus, the adoption of a disruptate pH greater than 6.0 would minimise adsorptive product losses, but on the other hand require an alternative method of product capture (e.g. affinity or mixed mode adsorbents, see below).

Maximisation of biomass throughput by high-density adsorbents

Due to its higher density in comparison with other well-established, commercially available adsorbents, such as the STREAMLINE range (1.15 g ml^{-1}, Amersham Pharmacia), CM HyperD LS (1.4 g ml^{-1}, Biosepra/Life Technologies) appeared to be better suited for the primary purification of L-asparaginase. However, viscosity driven elutriation still limited its

operational window with regard to fluidisation velocity (refer to Section 3.3.5). Pellicular, adsorbents with enhanced densities, such as the prototype SP UpFront (2.35 g ml^{-1}, UpFront Chromatography), demonstrated that high-density adsorbents facilitate stable fluidisation at increased loading flow velocities. However, a considerably lower static and dynamic capacity was found for SP UpFront in side-by-side comparison with CM HyperD. This can only to a limited degree be attributed to a reduced internal bead volume and thus needs further investigation. In this regard, an equivalent ligand concentration per available unit of internal bead volume would yield a more valid comparison.

It has been demonstrated that cell disruption in bead mills can be efficiently achieved at high biomass concentrations (e.g. 50% yeast ww/v, refer to Section 4.3.1). However, in the integrated purification of L-asparaginase from *Erwinia*, the initial biomass concentration in the feedstock was limited. For example, a biomass concentration of 22% ww/v promoted channelling and bed instability when employing SP UpFront at a loading flow velocity of 200 cm h^{-1}, refer to Section 3.3.5). Here, a high-density adsorbent could improve the bed stability at high feedstock viscosities, i.e. high biomass concentrations.

Further application for high-density adsorbents with appropriate mass transfer characteristics lies in in-situ product removal, e.g. by fluidised beds as an external loop attached to a productive fermenter, as reported by Hamilton et al. (1999). Here, high flow velocities would minimise the residence time of the culture broth outside the controlled environment of the bioreactor. In such a system, enhanced particle density might also reduce the entrainment of adsorbent particles caused by perturbations of the fluidised bed, e.g. by air bubbles transferred from a bioreactor into the fluidised bed. Another attractive application for high-density adsorbents would be the integration of a manifold of fluidised beds with a continuously operating cell disrupter. Instead of processing a given batch of biomass with a

large, single fluidised bed, a manifold of appropriately down-scaled fluidised beds could reduce the adsorbent inventory by the re-use of smaller beds within a purification campaign (refer to Figure 3.18).

Alternative modes of product capture in the purification of L-asparaginase

It was demonstrated that product debris interactions were minimal at pH values greater than 6.0. However, product capture at such pH ranges was compromised by diminished adsorbent capacities. Thus, adsorbents which offer effective adsorption of L-asparaginase whilst being less sensitive to disruptate pH and /or ionic strength (e.g. affinity or mixed mode adsorbents) would improve the product yield by minimising adsorptive losses to cell debris. For example, Hamilton et al. (2000) reported the development of a mixed mode adsorbent which facilitated the in-situ product removal of an extracellular acid protease from cultures of *Yarrowia lipolytica* at pH values close to the pI of the enzyme where ion exchange adsorbents would prove inappropriate.

Verification of the potential for the integration of cell disruption and FBA

The potential of the integrated process as presented in Chapter 4 should be verified by its application to the purification of a particularly labile product. For example, Grodberg and Dunn (1988) reported a case where a recombinant RNA polymerase, expressed and accumulated in Escherichia coli, was found to be very susceptible to cleavage by at least one outer membrane endoprotease following cell lysis. The inclusion of a variety of standard protease inhibitors during purification failed to prevent cleavage of the enzyme. Employing such a production system, the impact of immediate product sequestration (DPS) on product degradation could be ascertained.

REFERENCES

AFEYAN, N. B., N. F. GORDON, I. MAZSAROFF, L. VARADY, S. P. FULTON, Y. B. YANG, AND F. REGNIER. 1990. Flow-through particles for the High Performance Liquid Chromatographic separation of biomolecules: perfusion chromatography. Journal of Chromatography 519: 1-29.

AGERKVIST, I. AND S.-O. ENFORS. 1990. Characterisation of *E.coli* cell disintegrates from a bead mill and high pressure homogenisers. Biotechnology and Bioengineering 36: 1083-1089.

AL-DIBOUNI, M. R. AND J. GARSIDE. 1979. Particle mixing and classification in liquid fluidised beds. Trans.Instn.Chem.Engrs. 57: 94-103.

AMERSHAM PHARMACIA BIOTECH AB 1997. Expanded Bed Adsorption: principles and methods. S-751 82 Uppsala, Sweden.

ASENJO, J. A. AND I. PATRICK 1990. Large-scale protein purification. In E. L. V. Harris and S. Angal [eds.], Protein purification applications 1-28. Oxford University Press, Oxford.

BARNFIELD-FREJ, A.-K., R. HJORTH, AND A. HAMMARSTROM. 1994. Pilot-scale recovery of recombinant annexin-V from unclarified *Escherichia coli* homogenate using expanded bed adsorption. Biotechnology and Bioengineering 44: 922-929.

BARNFIELD-FREJ, A.-K., H. J. JOHANSSON, S. JOHANSSON, AND P. LEIJON. 1997. Expanded bed adsorption at production scale: Scale-up verification, process example and sanitization of column and adsorbent. Bioprocess Engineering 16: 57-63.

BARTHELS, C. R., G. KLEINMANN, N. J. KORZON, AND D. B. IRISH. 1958. A novel ion-exchange method for the isolation of streptomycin. Chemical Engineering Progress 54: 49-52.

BASCOUL, A., J. P. COUDERC, AND H. DELMAS. 1993. Movement of solid particles in liquid fluidised beds. Chemical Engineering Journal and The Biochemical Engineering Journal 51: 135-150.

BASCOUL, A., H. DELMAS, AND J. P. COUDERC. 1988. Hydrodynamic characterisation of liquid solid fluidisation-influence of the distributor. Chemical Engineering Journal and The Biochemical Engineering Journal 37: 11-24.

BELTER, P. A., F. L. CUNNINGHAM, AND J. W. CHEN. 1973. Development of a recovery process for novobiocin. Biotechnology and Bioengineering 15: 533-549.

BERTHOLD, W. AND R. KEMPKEN. 1994. Interaction of cell culture with downstream purification: a case study. Cytotechnology 15: 229-242.

BEVERIDGE, K. Characterisation of novel fluidised bed contactors. 1997. The University of Birmingham. MSc Thesis.

BIERAU, H., Z. ZHANG, AND A. LYDDIATT. 1999. Direct process integration of cell disruption and fluidised bed adsorption for the recovery of intracellular proteins . Journal of Chemical Technology and Biotechnology 74: 208-212.

BONNERJEA, J., S. OH, M. HOARE, AND P. DUNNILL. 1986. Protein purification: the right step at the right time. Bio/Technology 4: 954-958.

BOSCHETTI, E. 1994. Advanced sorbents for preparative protein separation purposes. Journal of Chromatography A 658: 207-236.

BOYER, P. M. AND J. T. HSU. 1989. Biotechnology Techniques 4: 61.

BOYER, P. M. AND J. T. HSU. 1993. Protein purification by dye-ligand chromatography. Adv.Biochem.Eng Biotechnol. 49: 1-44.

BRADFORD, M. M. 1976. A rapid and sesitiv method for the quantitation of microgram quantities of protein utilising the priciple of protein-dye binding. Analytical Biochemistry 72: 248-254.

BRISTOW, A. F. 1990. Purification of proteins for therapeutic use. In E. L. V. Harris and S. Angal [eds.], Protein purification applications 29-44. Oxford University Press, Oxforf.

BRUCE, L. J., S. GHOSE, AND H. A. CHASE. 1998. The effect of column verticality on separation efficiency in expanded bed adsorption. Bioseparation 8: 69-75.

BUJIS, A. AND J. A. WESSELINGH. 1980. Batch fluidised ion-exchange column for streams containing suspended particles. Journal of Chromatography 201: 319-327.

BURNS, M. A. AND D. J. GRAVES. 1985. Continuous affinity-chromatography using a magnetically stabilised fluidised-bed. Biotechnology Progress 1: 95-103.

BURNS, M. T. Process development for the direct recovery of a hydrophobic protein from bacterial fermentation broth. 1997. University of Birmingham. PhD Thesis.

BURTON, S. C. AND D. R. K. HARDING. 1997. Preparation of chromatographic matrices by free radical addition ligand attachment to allyl groups. Journal of Chromatography A 796: 273-282.

BYERS, L. D. 1982. Glyceraldehyde-3-phosphate dehydrogenase from yeast. Methods in Enzymology 89: 326-335.

CAMMACK, K. A., D. I. MARLBOROUGH, AND D. S. MILLER. 1972. Physical properties and subunit structure of L-asparaginase isolated from *Erwinia carotova*. Biochem.J. 126: 361-379.

CHANG, Y. K. AND H. A. CHASE. 1996b. Development of operating-conditions for protein-purification using expanded bed techniques - The effect of the degree of bed expansion on adsorption behaviour. Biotechnology and Bioengineering 49: 512-526.

CHANG, Y. K. AND H. A. CHASE. 1996a. Ion-exchange purification of G6PDH from unclarified yeast-cell homogenates using expanded bed adsorption. Biotechnology and Bioengineering 49: 204-216.

CHANG, Y. K., G. E. MCCREATH, AND H. A. CHASE. 1995. Development of an expanded bed technique for an affinity purification of G6PDH from unclarified yeast-cell homogenates. Biotechnology and Bioengineering 48: 355-366.

CHASE, H. A. 1994. Purification of proteins by adsorption chromatography in expanded beds. Trends in Biotechnology 12: 296-303.

CHASE, H. A. AND N. M. DRAEGER. 1992a. Affinity purification of proteins using expanded beds. Journal of Chromatography 597: 129-145.

CHASE, H. A. AND N. M. DRAEGER. 1992b. Expanded bed adsorption of proteins using ion-exchangers. Separation Science Technology 27: 2021-2039.

CHISTI, Y. AND M. MOO-YOUNG. 1986. Disruption of microbial cells for intracellular products. Enzyme and Microbial Technology 8: 194-204.

CLARKSON, A. I., P. LEFEVRE, AND N. J. TITCHENER-HOOKER. 1993. A study of process interactions between cell disruption and debris clarification stages in the recovery of yeast intracellular products. Biotechnol.Prog. 9: 462-467.

DASARI, G., I. PRINCE, AND M. T. W. HEARN. 1993. High-perfomance liquid chromatography of amino acids, peptides and proteins. CXXIV. Physical characterisation of fluidised-bed behaviour of chromatographic packing materials. Journal of Chromatography 631: 115-124.

DATAR, R. V., T. CARTWRIGHT, AND C. G. ROSEN. 1993. Process economics of animal cell and bacterial fermentations: a case study analysis of tissue plasminogen activator. Biotechnology (N.Y.) 11: 349-357.

DATAR, R. V. AND C. G. ROSEN 1996. Cell and cell debris removal: centrifugation and crossflow filtration. In G. Stephanopoulos [ed.], Bioprocessing 472. VCH, Weinheim.

DE LUCA, L., D. HELLENBROICH, N. J. TITCHENER-HOOKER, AND H. A. CHASE. 1994. A study of the expansion characteristics and transient behaviour of expanded beds of adsorbent particles suitable for bioseparations. Bioseparation 4: 311-318.

DEAN, C. R. AND O. P. WARD. 1992. The use of EDTA or polymyxin with lysozyme for the recovery of intracellular products from *Escherichia coli*. Biotechnology Techniques 6: 133-138.

DEAN, P. D. G. AND D. H. WATSON. 1979. Protein purification using immobilised triazine dyes. Journal of Chromatography 165 (3): 301 - 319.

DRAEGER, N. M. AND H. A. CHASE. 1990. Protein purification using liquid fluidized beds. Advances of Separation processes 161-172. Institution of Chemical Engineers, Rugby, England.

DRAEGER, N. M. AND H. A. CHASE. 1991. Liquid fluidised bed adsorption of proteins in the presence of cells. Bioseparation 2: 67-80.

ENGLER, C. R. 1985. Disruption of microbial cells. In M. Moo-Young [ed.], Comprehensive Biotechnology, vol. 2, 305-324. Pergamon Press, Oxford.

ENGLER, C. R. AND C. W. ROBINSON. 1981. Effects of organism type and growth conditions on cell disruption by impingement. Biotechnology Letters 3: 83-88.

ERICKSON, J. C., J. D. FINCH, AND D. C. GREENE 1994. Direct capture of recombinant proteins from animal cell culture media using a fluidised bed adsorber. In B. Griffiths, R. E. Spier, and W. Berthold [eds.], Animal Cell Technology: Products for today, prospects for tomorrow 557-560. Butterworth & Heinemann, Oxford.

FÄRENMARK, J., J. GUSTAVSSON, I. LAGERLUND, AND L. SANDBERG. 1999. Characterisation of STREAMLINE^{TM} Phenyl. Bioseparation 8: 139-144.

FERNANDEZ, M. A. AND G. CARTA. 1996. Characterization of protein adsorption by composite silica-polyacrylamide gel anion exchangers .1. Equilibrium and mass transfer in agitated contactors. Journal of Chromatography A 746: 169-183.

FEUSER, J., J. WALTER, M. R. KULA, AND J. THOMMES. 1999. Cell/adsorbent interactions in expanded bed adsorption of proteins. Bioseparation 8: 99-109.

FINETTE, G. M. S., Q. M. MAO, AND M. T. W. HEARN. 1996. Studies on the expansion charcteristics of fluidised beds with silica-based adsorbents used in protein purification. Journal of Chromatography A 743: 57-73.

FISH, N. M. AND M. D. LILLY. 1984. The interactions between fermentation and protein recovery. Bio/Technology 623-627.

FLEET, G. H. 1991. Cell walls. In A. H. Rose and J. S. Harrison [eds.], The yeasts: yeast organelles, vol. 4, 199-277. Academic press, London.

GAILLIOT, F. P., C. GLEASON, J. J. WILSON, AND J. ZWARICK. 1990. Fluidised bed adsorption for whole broth extraction. Biotechnology Progress 6: 370-375.

GIBSON, N. B. AND A. LYDDIATT. 1990. Economic fabrication and utilisation of agar composites in bioselective recovery in fixed and fluidised beds. In D. L. Pyle [ed.], Separations for Biotechnology 2 152-161. Elsevier Science Publishers.

GIBSON, N. B. AND A. LYDDIATT. 1993. Cellulose composites in liquid fluidised bed adsorption and recovery of proteins. In J. F. Kennedy, G. O. Phillips, and P. A. Williams [eds.], Cellulosics - materials for selective separations and other technologies 55-62. Ellis-Horwood.

GILBERT, H. J., R. BLAZEK, H. M. S. BULLMAN, AND N. P. MINTON. 1986. Cloning and expression of the *Erwinia chrysanthemi* asparaginase gene in *Escherichia coli* and *Erwinia carotova*. Journal of General Microbiology 132: 151-160.

GILCHRIST, G. R. Direct fluidised bed adsorption of protein products from complex particulate feedstocks. 1996. The University of Birmingham. PhD Thesis.

GILCHRIST, G. R., M. T. BURNS, AND A. LYDDIATT 1994. Solid phases for protein adsorption in liquid fluidised beds: comparison of commercial and custom-assembled particles. In D. L. Pyle [ed.], Separations for Biotechnology 3 186-192. Elsevier Applied Science, London and New York.

GOWARD, C. R., G. B. STEVENS, I. J. COLLINS, I. R. WILKINSON, AND M. D. SCAWEN. 1989. Use of Macrosorb kieselguhr composite and CM-Sepharose Fast Flow for the large-scale purification of L-asparaginase from *Erwinia chrysanthemi*. Enzyme and Microbioal Technology 11: 810-814.

GOWARD, C. R., G. B. STEVENS, R. TATTERSALL, AND T. ATKINSON. 1992. Rapid large-scale preparation of recombinant *Erwinia chrysanthemi* L-asparaginase. Bioseparation 2: 335-341.

GÖKLEN, K. E., M. THIEN, S. AYLER, S. SMITH, E. FISHER, M. CHARTRAIN, P. SALMAN, J. WILSON, A. ANDREWS, AND B. BUCKLAND. 1994. Development of crossflow filtration processes for the commercial-scale isolation of a bacterial lipase. Bioprocess Engineering 11: 49-56.

GRAY, P. P., P. DUNNILL, AND M. D. LILLY 1972. The continuous-flow isolation of enzymes. In G. Terui [ed.], Fermentation Technology Today 347-351. Society of Fermentation Technology, Japan.

GRIFFITH, C. M., J. MORRIS, M. ROBICHAUD, M. J. ANNEN, A. V. MCCORMICK, AND M. C. FLICKINGER. 1997. Fluidization characteristics of and protein adsorption on fluoride- modified porous zirconium oxide particles. Journal of Chromatography A 776: 179-195.

GRODBERG, J. AND J. J. DUNN. 1988. ompT encodes the *Escherichia coli* outer mebrane protease that cleaves T7 RNA polymerase during purification. Journal of Bacteriology 170: 1245-1253.

HAID, E. 1974. In H. U. Bergmeyer [ed.], Methods of enzymatic analysis 546. Academic Press, New York.

HAMILTON, G. E., F. LUECHAU, S. C. BURTON, AND A. LYDDIATT. 2000. Development of a mixed mode adsorption process for the direct product sequestration of an extracellular protease from microbial batch cultures. Journal of Biotechnology 79: 103-115.

HAMILTON, G. E., P. H. MORTON, T. W. YOUNG, AND A. LYDDIATT. 1999. Process intensification by direct product sequestration from batch fermentations: Application of a fluidised bed, multi-bed external loop contactor. Biotechnology and Bioengineering 64: 310-321.

HANSSON, M., S. STAHL, R. HJORTH, M. UHLEN, AND T. MOKS. 1994. Single-step recovery of a secreted recombinant protein by expanded bed adsorption. Bio/Technology 12: 285-288.

HARRIS, E. L. V. 1989. Protein purification methods: a practical approach. IRL Press, Oxford.

HARRIS, J. I. AND M. WATERS 1976. Glyceraldehyde-3-phosphate dehydrogenase. In P. D. Boyer [ed.], The Enzymes, vol. XIII, 1-49. Academic press, New York.

HARRISON, S. T. L. 1991. Bacterial cell disruption: a key unit operation in the recovery of intracellular products. Biotechnology Advances 9: 217-240.

HJORTH, R. 1997. Expanded-bed adsorption in industrial bioprocessing: Recent developments. Trends in Biotechnology 15: 230-235.

HJORTH, R. 1999. Expanded bed adsorption: elution in expanded mode. Bioseparation 8: 1-9.

HJORTH, R., S. KÄMPE, AND M. CARLSSON. 1995. Analysis of some operating parameters of novel adsorbents for recovery of proteins in expanded beds. Bioseparation 5: 217-223.

HÖLTJE, J.-V. AND B. GLAUNER. 1990. Structure and metabolism of the murein sacculus. Inst.Pasteur Res.Microbiol. 141: 75-103.

HUBBUCH, J., D. B. MATTHIESEN, T. J. HOBLEY, AND O. R. T. THOMAS. 2000. High-gradient magnetic separation versus expanded bed adsorption: a first principle comparison. Bioseparation submitted for publication.

HUDDLESTON, J. G., S. O'BRIEN, H. PICARD, AND A. LYDDIATT 1992. The recovery in aqueous two-phase systems of intracellular protein products from wet-milled brewers' yeast. In D. H. Logsdail and M. J. Slater [eds.], Solvent extractions in the process industries, vol. 2, 1048-1055. Elsevier Applied Science.

HUGHES, D. E., J. W. T. WIMPENNY, AND D. LLOYD 1971. The disintegration of micro-organisms. In J. R. Norris and D. W. Ribbons [eds.], Methods in Microbiology, vol. 5B, 1-54. Academic, New York.

ITO, Y., A. G. TAMASELLI, AND L. H. NODA. 1980. ATP:AMPphosphotransferase from bakers' yeast. Purification and properties. European Journal of Biochemistry 105: 85 - 92.

JOHNSON, B. J. AND M. H. HECHT. 1994. Recombinant proteins can be isolated from *E. coli* cells by repeated cycles of freezing and thawing. Bio/Technology 12: 1357-1360.

KARAU, A., J. BENKEN, J. THÖMMES, AND M.-R. KULA. 1997. The influence of particle size distribution and operating conditions on the adsorption performance in fluidised beds. Biotechnology and Bioengineering 55: 54-63.

KAUFMANN, A. AND Y. D. STIERHOFF. 1993. New outer membrane-associated protease of *Escherichia coli* K-12. Journal of Bacteriology 176: 359-367.

KAUFMANN, M. 1997. Unstable proteins: how to subject them to chromatographic separations for purification procedures . Journal of Chromatography B 699: 347-369.

KOPPERSCHLAGER, G. AND G. JOHANSSON. 1982. Affinity partitioning with polymer-bound Cibacron blue F3G-A for rapid, large-scale purification of phosphofructokinase from Baker's yeast. Anal.Biochem. 124: 117-124.

KRONER, K. H., H. SCHÜTTE, H. HUSTEDT, AND M.-R. KULA. 1984. Cross-flow filtration in the downstream processing of enzymes. Process Biochemistry 19: 67-74.

KULA, M.-R. 1990. Trends and future prospects of aqueous two-phase extraction. Bioseparation 1: 181-189.

KULA, M.-R. AND H. SCHÜTTE. 1987. Purification of proteins and the disruption of microbial cells. Biotechnology Progress 3: 31-42.

KULBE, K. D. AND R. SCHUER. 1979. Large-scale preparation of phosphoglycerate kinase from Saccharomyces cerevisiae using Cibacron Blue-Sepharose 4B pseudoaffinity chromatography. Anal.Biochem. 93: 46-51.

KUNII, D. AND O. LEVENSPIEL 1969. Fluidisation Engineering. John Wiley & Sons, New York.

LAN, J. C.-W., G. E. HAMILTON, AND A. LYDDIATT. 1999. Physical and biochemical characterization of a simple intermediate between fluidized and expanded bed contactors. Bioseparation 8: 43-51.

LANGLOTZ, P. AND K. H. KRONER. 1992. Surface-modified membranes as a matrix for protein purification. J.Chromatogr. 591: 107-113.

LEE, S. M. 1989. The primary stages of protein recovery. Journal of Biotechnology 11: 103-118.

LEE, S. M., M. H. WROBLE, AND J. T. ROSS. 1989. L-Asparaginase from *Erwinia carotova* - An improved recovery process using affinity chromatography. Applied Biochemistry and Biotechnology 22: 1-11.

LEVENSPIEL, O. 1972. Chemical Reaction Engineering. Wiley & Sons, New York.

LIHME, A., E. ZAFIRAKOS, M. B. HANSEN, AND M. OLANDER. 1998. Simplified and more robust EBA processes by elution in expanded bed mode. Bioseparation 8: 93-97.

LIMON-LASON, J., M. HOARE, C. B. ORSBORN, D. J. DOYLE, AND P. DUNNILL. 1979. Reactor properties of a high-speed bead mill for microbial cell rupture. Biotechnology and Bioengineering XXI: 745-774.

MCCREATH, G. E., H. A. CHASE, AND C. R. LOWE. 1994. Novel affinity separations based on perfluorocarbon emulsions - Use of a perfluorocarbon affinity emulsion for the direct extraction of Glucose-6-phosphate dehydrogenase from baker's yeast. Journal of Chromatography 659: 275-287.

MCCREATH, G. E., H. A. CHASE, R. O. OWEN, AND C. R. LOWE. 1995. Expanded bed affinity chromatography of dehydrogenase from baker's yeast using dye ligand perflourocarbon supports. Biotechnology and Bioengineering 48: 341-354.

MELROSE, G. J. H. 1971. Rev.pure and appl.Chem. 21: 83.

MIDDELBERG, A. P. J. 1995. Process-scale disruption of microorganisms. Biotechnology Advances 13: 491-551.

MILBURN, P. T. AND P. DUNNILL. 1994. The release of virus-like particles from recombinant *Saccharomyces cerevisiae*: Effect of freezing and thawing on homogenisation and bead milling. Biotechnology and Bioengineering 44: 736-744.

MORRIS, J. E., C. G. TOLPPI, P. W. CARR, AND M. C. FLICKINGER. 1994. Protein separations using HPLC and fluidised-bed zirconia supports. Abstratcs of papers of the American Chemical Society 207.

MORTON, P. AND A. LYDDIATT. 1994a. Direct integration of protein recovery with productive fermentations. In D. L. Pyle [ed.], Separations for Biotechnology 3 329-335. Royal Society of Chemistry.

MORTON, P. AND A. LYDDIATT. 1994b. Direct integration of protein recovery with productive fermentations - a role for liquid fluidised-bed adsorption in bio-extractive bona-fide transformations. Journal of Chemical Technology and Biotechnology 59: 106-107.

MORTON, P. H. AND A. LYDDIATT 1992. Direct recovery of protein products from whole fermentation broths: a role for ion exchange adsorption in fluidised beds. In M. J. Slater [ed.], Ion Exchanger Advances 237-244. Elsevier Applied Science.

MURATSUBAKI, H., K. ENOMOTO, Y. ICHIJOH, T. TEZUKA, AND T. KATSUME. 1994. Rapid purification of yeast cytoplasmic fumarate reductase by affinity chromatography on blue sepharose CL-6B. Prep.Biochem. 24: 289-296.

NIKAIDO, H. 1973. Biosynthesis of and assembly of lipopolysaccharide and outer membrane layer of the Gram negative cell wall. In L. Levine [ed.], Bacterial Membranes and Walls 131-208. Marcel Dekker Inc., New York.

PALSSON, E., P. E. GUSTAVSSON, AND P. O. LARSSON. 2000a. Pellicular expanded bed matrix suitable for high flow rates. J.Chromatogr.A 878: 17-25.

PALSSON, E., M. P. NANDAKUMAR, B. MATTIASON, AND P. O. LARSSON. 2000b. Miniaturised expanded-bed column with low dispersion suitable for fast flow-ELISA analyses. Biotechnology Letters 22: 245-250.

PISABARRO, A. G., M. A. DE PEDRO, AND D. VASQUEZ. 1985. Structural modifications in the peptidoglycan of *Eschericia coli* associated with changes in the state of growth of the culture. Journal of Bacteriology 161: 238-242.

REHÁCEK, J. AND J. SCHAEFER. 1977. Continuous disintegration of microorganisms in a new laboratory apparatus. Biotechnology and Bioengineering 19: 1523-1534.

RITO-PALOMARES, M. AND A. LYDDIATT. 1996. Impact of cell disruption and polymer recycling upon aqueous two-phase processes for protein recovery. Journal of Chromatography B 680: 81-89.

ROE, S. D. 1987. Whole broth extractions of enzymes from fermentation broths using commercially available adsorbents. In M. S. Verrral and M. J. Hudson [eds.], Separations for Biotechnology 210. Ellis Horwood, Chichester.

SCHÜTTE, H., K. H. KRONER, H. HUSTEDT, AND M.-R. KULA. 1983. Experiences with a 20 litre industrial bead mill for the disruption of microorganisms. Enzyme and Microbioal Technology 5: 143-148.

SCOPES, R. K. 1987. Dye ligands and multifunctional adsorbents: an empirical approach to affinity chromatography Analytical Biochemistry 165 (2): 235 - 246.

SHULER, M. L. AND F. KARGI 1992. Bioprocess Engineering: Basic Concepts. Prentice Hall, Englewood Cliffs, N.J.

SKIDMORE, G. L., B. J. HORSTMANN, AND H. A. CHASE. 1990. Modelling single-component proteinadsorption to the cation exchanger S Sepharose FF. Journal of Chromatography 498: 113-128.

SPALDING, B. J. 1991. Downstream processing: key to shlashing production costs 100 fold. Bio/Technology 9: 229-234.

STALLCUP, W. B. 1972. A rapid purification procedure for glyceraldehyde 3-phosphate dehydrogenase from bakers yeast. Journal of Biological Chemistry 247 (19): 6277 - 6279.

TAMAKI, N., M. NAKAMURA, K. KIMURA, AND T. HAMA. 1977. Purification and properties of aldehyde dehydrogenase from Saccharomyces cerevisiae. J.Biochem.(Tokyo) 82: 73-79.

THIELE, D., P. COTTRELLE, F. IBORRA, J. M. BUHLER, A. SENTENAC, AND P. FROMAGEOT. 1985. Elongation factor 1 alpha from Saccharomyces cerevisiae. Rapid large-scale purification and molecular characterization. Journal of Biological Chemistry 260: 3084-3089.

THÖMMES, J. 1997. Fluidised bed adsorption as a primary recovery step in protein purification. Advances in Biochemical Engineering/Biotechnology 58: 185-230.

THÖMMES, J., A. BADER, M. HALFAR, A. KARAU, AND M.-R. KULA. 1995c. Isolation of monoclonal antibodies from cell containing hybridoma broth using a protein A coated adsorbent in expanded beds. Journal of Chromatography A 752: 111-122.

THÖMMES, J., M. HALFAR, S. LENZ, AND M.-R. KULA. 1995b. Purification of monoclonal antibodies from whole hybridoma fermentation broth by fluidised-bed adsorption. Biotechnology and Bioengineering 45: 205-211.

THÖMMES, J., M. WEIHER, A. KARAU, AND M.-R. KULA. 1995a. Hydrodynamics and performance in fluidised bed adsorption. Biotechnology and Bioengineering 48: 367-374.

VAN DER MEER, A. P., C. M. R. J. P. BLANCHARD, AND J. A. WESSELINGH. 1984. Mixing of particles in liquid fluidised beds. Chemical Engineering Research & Design 62: 214-222.

VANREIS, R., L. C. LEONARD, C. C. HSU, AND S. E. BUILDER. 1991. Industrial scale harvest of proteins from mammalian cell culture by tangential flow filtration. Biotechnology and Bioengineering 38: 413-422.

VELICK, S. F. 1955. Methods in Enzymology 1: 401.

VOGELS, G. AND M.-R. KULA. 1991. Combination of enzymatic and/or thermal pretreatment with mechanical cell disintegration. Chemical Engineering Science 47: 123-131.

WADE, H. E. AND D. A. RUTTER. 1970. Asparaginase-treatment for leukemia. Science Journal 6: 62-66.

WARBURG, O. AND W. CHRISTIAN. 1939. Biochem.Z. 303: 40.

WEAVER, L. E. AND G. CARTA. 1996. Protein adsorption on cation exchangers: Comparison of macroporous and gel-composite media. Biotechnology Progress 12: 342-355.

WELLS, C. M. AND A. LYDDIATT 1987. Liquid fluidised bed adsorption. In M. S. Verrral and M. J. Hudson [eds.], Separations for Biotechnology 217-224. Ellis-Horwood, Chichester.

WHEELWRIGHT, S. M. 1987. Designing downstream processes for large-scale protein purification. Bio/Technology 5: 789-793.

WHITE, M.D. AND MARCUS, D. 1988. Disintegration of Microorganisms. In A. Mizrahi [ed.], Downstream Processes: Equipment and Techniques, vol. 8, 53-90. Alan R. Liss Inc., New York.

WRIGHT, P. R., F. J. MUZZIO, AND B. J. GLASSER. 1998. Batch uptake of lysozyme: Effect of solution viscosity and mass transfer on adsorption . Biotechnology Progress 14: 913-921.

WRIGHT, P. R., F. J. MUZZIO, AND B. J. GLASSER. 1999. Effect of resin characteristics on fluidized bed adsorption of proteins. Biotechnology Progress 15: 932-940.

WRISTON, J. C. 1985. Asparaginase. Methods in Enzymology 113: 608-618.

ZAFIRAKOS, E. AND A. LIHME. 1999. EBA columns with a distribution system based on local stirring. Bioseparation 8: 85-91.

ZHANG, Z. Magnetically stabilised fluidised bed adsorption: practical benefit in the recovery of proteins from particulate feedstocks. 1998. University of Birmingham. PhD Thesis.

ZHU, J., A. LYDDIATT, A. W. PACEK, AND A. W. NIENOW 1997. Fabrication and characterisation of agar/zircon sand composite adsorbents for protein recovery in liquid fluidised beds. In A. W. Nienow [ed.], Bioreactor/Process Fluid Dynamics 103-114. BHR Group/Mechanical Engineering Publications.